Drexel UNIVERSITY

GRADUATE THESIS/DISSERTATION APPROVAL FORM AND SIGNATURE PAGE

Instructions: This form must be completed by all master's and doctoral students with a thesis or dissertation requirement. Please type or print clearly as this form MUST be included as page 1 of your thesis or dissertation via electronic submission to ProQuest. All theses and dissertations must be formatted according to the University and department/program requirements. **Reminder:** It is the responsibility of the student to submit any/all edits requested by the Examining Committee to the Faculty Mentor or Supervising Professor for final approval and signature via the Graduate Program Completion Form.

Type: ☐ Master's Thesis ☑ PhD/Doctoral Thesis or Dissertation

Thesis or Dissertation Title: In Vivo Performance of the Femoral Head-Neck Taper Connection and Development of an Electrochemical Framework for Quantitative Corrosion Investigations

Author's Name: Genymphas B. Higgs

Month and Year: April 2020

The signatures below certify that this thesis / (dissertation) (circle one) is complete and approved by the Examining Committee.

Committee Chairperson's Name:

Paul W. Brandt-Rauf, ScD, MD, DrPH

Title: Distinguished University Professor and Dean

Department: School of Biomedical Engineering, Science and Health Systems

Institution (*if other than Drexel University*):

Signature: _Paul Brandt_

Committee Member's Name: Kenneth A. Barbee, PhD

Title: Professor, Senior Associate Dean, and Associate Dean for Research

Department: School of Biomedical Engineering, Science and Health Systems

Institution (*if other than Drexel University*):

Signature: _Kenneth A. Barbee_
Digitally signed by Kenneth A. Barbee
DN: cn=Kenneth A. Barbee, o=Drexel University, ou=School of Biomedical Engineering, email=barbee@drexel.edu, c=US
Date: 2020.04.01 21:30:18 -04'00'

Committee Member's Name: Joseph J. Sarver, PhD

Title: Teaching Professor

Department: School of Biomedical Engineering, Science & Health Systems

Institution (*if other than Drexel University*):

Signature:

Committee Member's Name: Steven M. Kurtz, PhD

Title: Research Professor

Department: School of Biomedical Engineering, Science and Health Systems

Institution (*if other than Drexel University*):

Signature: _Steven Kurtz_
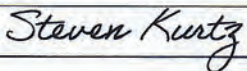
Committee Member's Name: Alison A. Evans, ScD

Title: Associate Professor

Department: Dornsife School of Public Health - Epidemiology and Statistics

Institution (*if other than Drexel University*):

Signature: Alison A Evans, ScD
Digitally signed by Alison A Evans, ScD
DN: cn=Alison A Evans, ScD, o=Drexel University, ou=Department of Epidemiology and Biostatistics, email=aae29@drexel.edu, c=US
Date: 2020.04.01 15:08:51 -04'00'

Committee Member's Name:

Title:

Department:

Institution (*if other than Drexel University*):

Signature:

In Vivo Performance of the Femoral Head-Neck Taper Connection and Development of an Electrochemical Framework for Quantitative Corrosion Investigations

A Thesis

Submitted to the Faculty

of

Drexel University

By

Genymphas B. Higgs

in partial fulfillment of the

requirements for the degree

of

Doctor of Philosophy

June 2019

© Copyright 2020

Genymphas B. Higgs. All Rights Reserved.

<u>Dedications</u>

This dissertation is dedicated to my parents, brothers and sister.

<u>Acknowledgments</u>

I must first thank my parents, Glenn and Christine, and siblings, Gadareth, Gadryn, and Chrisellyn, for kindly obliging my inquisitive nature. By suffering through the many "experiments" I endeavored to conduct as a child, you facilitated a familial environment that nurtured the skills and thought processes that proved indispensible for the completion of this work.

To my advisor, Dr. Steven Kurtz, thank you for the astute mentorship that you've provided since inviting me into your research group as an undergraduate student. You've urged me to set ambitious goals and continually presented me with unique challenges, while also providing the resources and flexibility to derive solutions independently.

To the members of the Implant Research Center, both past and present, thank you for normalizing an atmosphere that encourages camaraderie and collaboration, but also drives personal growth. In particular, I must recognize Daniel MacDonald, Josa Hanzlik, Christina Arnholt, and Alexander Padayatil, who have been particularly instrumental in supporting some of the experiments detailed in this dissertation.

I would especially like to thank Dr. Jeremy Gilbert at Clemson University for his considerable guidance, initiated at the inception of this research. I owe you a debt of gratitude for allowing me to conduct a significant portion of this work within your lab, and I am incredibly appreciative of our rigorous and inspirational discussions. I would also like to thank Dr. William Mihalko and Julie Lowell of the Campbell Clinic, for not only providing cadaveric specimens,

Table of Contents

List of Tables

List of Figures

Abstract

IN VIVO PERFORMANCE OF THE FEMORAL HEAD-NECK TAPER CONNECTION AND DEVELOPMENT OF AN ELECTROCHEMICAL FRAMEWORK FOR QUANTITATIVE CORROSION INVESTIGATIONS

Genymphas B. Higgs

Corrosion at the modular head-neck connection in total hip arthroplasty has been shown to have deleterious biological consequences, and recent clinical observations have postulated that it may compromise the integrity of the taper connection. This dissertation summarizes the patient demographics, clinical details, and design variables of hip implants that were examined to understand their impact on the *in vivo* performance of taper junctions. Furthermore, it describes electrochemical assessment methods that were developed to quantitatively evaluate the effects of corrosion phenomena.

In vivo taper performance was assessed using femoral components retrieved from revision surgery and from cadaveric donors. Preliminary time-to-event analyses were conducted on a collection of 5,821 retrieved joint prostheses, identifying risks factors for infection consistent with the findings of administrative databases and implant registries. The role of an activated immune system on corrosion at the head-neck taper was then explored with a subset of these explants. The results did not indicate more severe corrosion for devices revised with infection, but suggested greater corrosion severity for devices that were implanted in male patients and during primary arthroplasty procedures. Multivariable analysis of clinical and design variables did not identify an

association between corrosion and the size of the modular taper, but found increased corrosion for heavier patients, longer implantation times, greater femoral head offsets and tapers with a lower flexural rigidity. Mechanical assessment of taper connection strength demonstrated that more severely corroded stem trunnions were associated with stronger taper connections. Additionally, greater corrosion was observed on retrievals from revision surgery than on those from cadaveric donors.

In consideration of the electrochemical nature of corrosion processes, a new framework was devised to overcome limitations of visual corrosion assessments. Analysis using electrochemical impedance spectroscopy identified decreased impedance and increased constant phase element (CPE) capacitance as the strongest predictors of increased corrosion severity. Additionally, lower values for impedance phase angle, CPE-exponent and polarization resistance were associated with increased corrosion. From microscopic and metallographic inspection, it was found that components with subsurface damage features had significantly higher capacitance and lower impedance values than those only exhibiting surface corrosion damage features. Given that the surface area of an electrode is inversely proportional to its impedance and directly proportional to its capacitance, electrochemical analyses may provide an opportunity to identify penetrative corrosion features without destructive metallographic evaluation.

Introduction

Total Hip Arthroplasty (THA)

Total hip arthroplasty (THA) has been deemed one of the most effective surgical interventions of the 20th century, and over a million procedures are performed worldwide each year[1,2]. Approximately 505,000 total hip replacements (THRs) are implanted annually in the United States, with a prevalence that is estimated to be 1.49% of the population at sixty years, 3.25% at seventy years, 5.26% at eighty years, and 5.87% at ninety years of age[3,4]. Additionally, it is projected that primary THA will grow 71% in the next decade, highlighting the need to ensure the continued success and longevity of these procedures[5]. An ongoing problem with this surgical intervention is the potential need for an implant-prompted revision surgery. Revision procedures are generally longer and more complex, with 40% higher estimated costs than primary arthroplasties, even in the absence of major complications[4]. It has been postulated that a 1% reduction in cumulative revision risk could reduce Medicare expenditure by almost $1 billion over a 10 year period[6]. Devices may be revised for a variety of reasons, including periprosthetic joint infection (PJI), instability, aseptic loosening and periprosthetic fracture[7,8]. Although a combination of patient, surgeon, component, and intra-operative factors can impact how a device performs in situ, understanding the *in vivo* changes to implants remains a target of arthroplasty research. By-products from implanted arthroplasty devices have been implicated in a number of revision-related phenomena, including osteolysis, soft tissue necrosis, and pseudotumor formation[9-12].

Today's THA procedures are largely based on the work of Sir John Charnley, an orthopedic surgeon who has been considered the father of modern total hip devices[13,14]. His low friction design, as implanted in 1960, consisted of three elements; a polytetrafluoroethylene (PTFE) acetabular component, acrylic bone cement, and a stainless steel femoral stem (Figure 1A)[13]. While this early prosthesis was successful, a number of failure modes eventually presented as recurring issues. Although the PTFE bearing surface was favorable for its low-friction properties, it produced toxic wear particles that resulted in severe bone lysis and adverse tissue reactions that prompted an eventual revision surgery[15-17]. Particles of bone cement were also implicated in "particle disease" and failure of the cement mantle became widely reported as a cause for implant loosening[17,18]. The monobloc femoral stem was another limitation of the Charnley design, as it restricted the surgeon's ability to accommodate the anatomical variations that exist among THA patients[19]. In practice, optimizing native soft-tissue balance and limb length along with femoral offset and version proved challenging with a single femoral component[20].

In an effort to mitigate the challenges brought about by these limitations, changes were implemented into total hip replacements (THRs) in the decades following their introduction. In contemporary THRs, PTFE has been largely replaced by ultra-high-molecular weight polyethylene (UHMWPE) given the latter's more favorable wear properties and biocompatibility[21-23]. While metal-on-UHMWPE articulation has been considered the preferred bearing surface for conventional THA, ceramic-on-UHMWPE, ceramic-on-ceramic, and metal-on-metal couples are used in THA and hip resurfacing surgery[24]. Additionally, alloys

comprising cobalt, chromium, and molybdenum (CoCrMo), as well as titanium, aluminum, and vanadium (Ti6Al4V) were introduced in the 1970's and have since had widespread use[25]. Furthermore, design features such as roughened surfaces, porous coatings, and osteoconductive treatments have been introduced into femoral and acetabular components to encourage bony ingrowth and obviate the need for bone cement[26,27]. Irrespective of bearing surface or fixation method, modularity between the femoral head and femoral stem has become ubiquitous in contemporary THRs[28]. The advent of modular components has allowed surgeons to match an individual patient's anatomy more effectively with a reduced inventory[29,30]. Additionally, selective revision of individual modular components permits well-functioning fixed components to be retained, reducing operation time and patient risk[31,32].

Modular Head-Neck Tapers in THA

Today's orthopedic implant designs may feature a variety of modular elements, including head-neck junctions, neck-stem junctions, anterior-posterior pads, modular collars, maximal shoulders, stem sleeves and modular acetabular components (Figure 1B)[33,34]. This thesis is focused on the modular head-neck junction: a self-locking taper connection between the male trunnion of the femoral stem and female bore of the femoral head[35]. This taper connection shares design elements of the Morse taper, developed by Stephen Morse as a way to replace drill bits quickly and easily in his twist drill invention of 1864[36]. The trunnion-based modular design was introduced with a metal femoral head in 1971 by Bernhard Weber, and later adapted for ceramic femoral heads in 1974 by Heinz Mittelmeier[33,36].
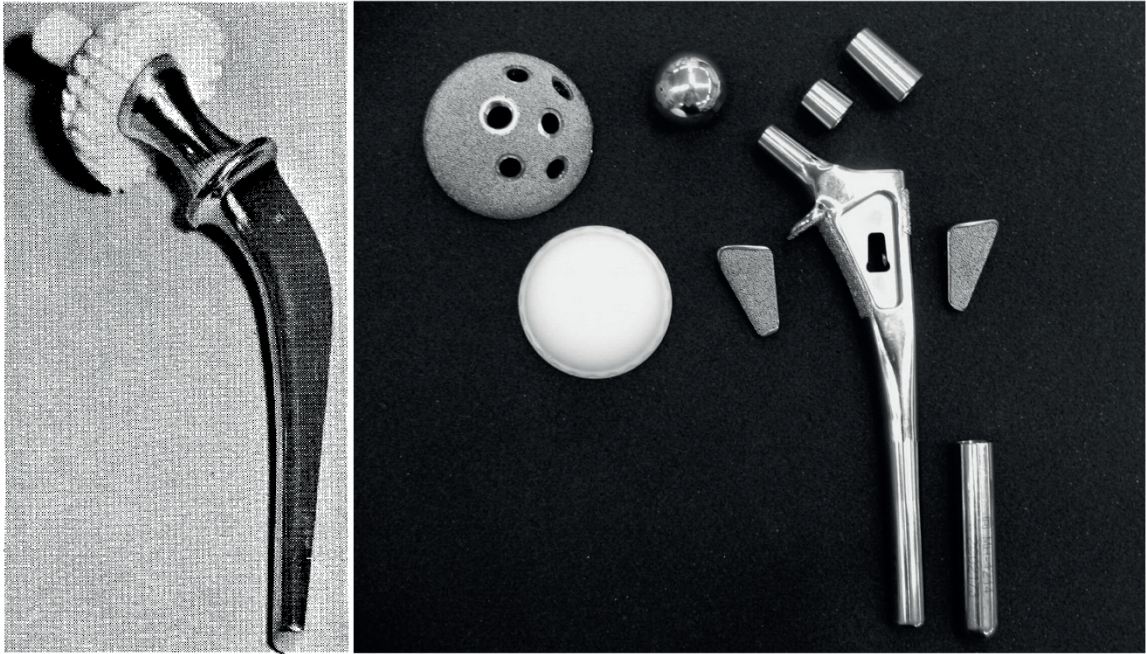
Figure 1. The "low friction arthroplasty" system designed by Sir John Charnley in 1960 comprising a single femoral component and PTFE acetabular component (A). Richards Modular Hip System THA system featuring multiple modular components (B). Reprinted from The Lancet, 277, John Charnley, Arthroplasty of The Hip: A New Operation, 1129-1132, (1961), with permission from Elsevier (A). Reprinted from The Journal of Arthroplasty, Hiroshi Suehara et al., Clinical and Radiographic Results for the Richards Modular Hip System Prosthesis in Total Hip Arthroplasty Average 10-Year Follow-Up, 369-374, (2010), with permission from Elsevier (B).

The stability of this connection is dictated by the engagement mechanics of a self-locking taper. As the femoral head is impacted onto the femoral stem, the conical stem trunnion presses into the walls of the bore, generating pressure and frictional stress which act to keep the components fixed together[36] (Figure 2).
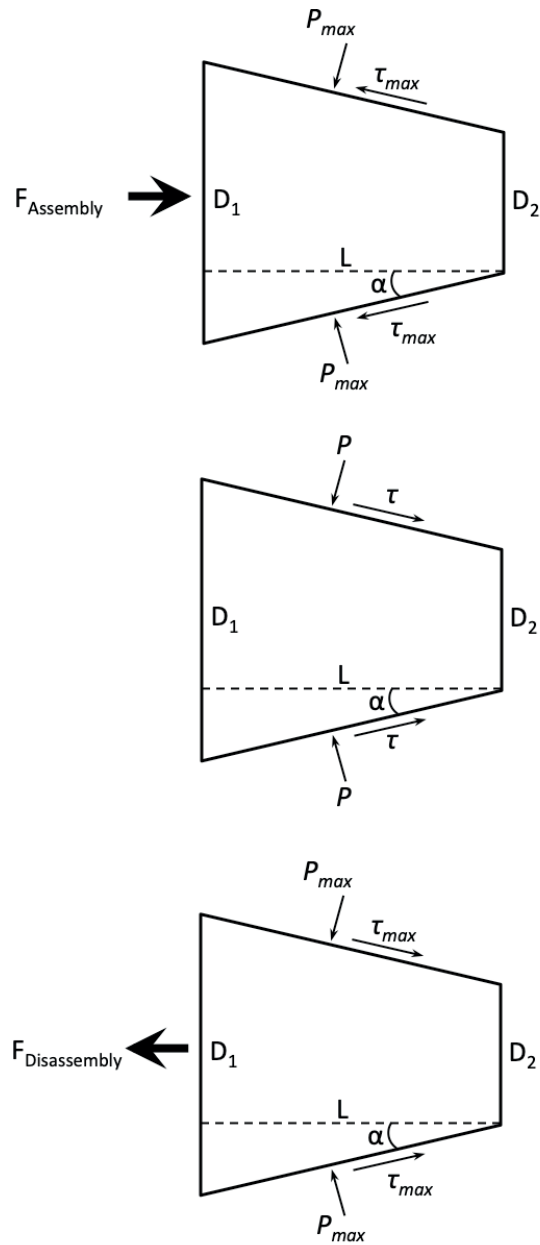
Figure 2. Schematic of the idealized engagement mechanics for a self-locking taper connection, which assumes uniform pressure and uniform contact. During impaction (A), the generated pressure and frictional shear stress oppose the assembly force. When the impaction force is removed from the system (B), the direction of the shear stress reverses and counteracts the residual pressure to keep the taper locked. During disassembly (C), the external force acts along with the pressure to overcome the shear stress and thus, the taper separates.

This idealized static equilibrium analysis assumes constant axial compressive force as well as uniform pressure and perfect contact. As the taper becomes engaged, the assembly force ($F_{Assembly}$) is balanced by axial components of the resulting frictional shear stress (τ) and pressure (P), which have maximum values during impaction. With consideration that frictional shear stress develops from the normal pressure and coefficient of friction (μ)[37], the relationship between these variables can be mathematically summarized as:

$$F_{Assembly} = (\tau \cos \alpha + P \sin \alpha)A = PA(\mu\cos \alpha + \sin \alpha) \qquad \text{\textit{Equation 1}}$$

where α is half the cone angle of the device taper and A is the area of contact, which is determined by D1, D2, and L. When $F_{Assembly}$ is removed, the connection is maintained by a balance between τ and P: the taper remains locked if $\tau \cos \alpha > P \sin \alpha$, a condition more favorable for tapers designed with a greater coefficient of friction and smaller taper angle. The external force required to separate the taper ($F_{Disassembly}$) must therefore satisfy the following relationship:

$$F_{Disassembly} = (\tau \cos \alpha - P \sin \alpha)A = PA(\mu\cos \alpha - \sin \alpha) \qquad \text{\textit{Equation 2}}$$

Taking Equation 1 and Equation 2, the ratio between the assembly and disassembly forces can be presented as:

$$\frac{F_{Disassembly}}{F_{Assembly}} = \frac{(\mu\cos \alpha - \sin \alpha)}{(\mu\cos \alpha + \sin \alpha)} \qquad \text{\textit{Equation 3}}$$

which reveals a relationship that is dictated by μ and α. The coefficient of friction is largely dependent on the materials involved. Fessler *et al.* found values of μ = 0.2 for alumina ceramic heads and μ = 0.15 for CoCrMo heads, when paired with either a CoCrMo or Ti6Al4V stem[38]. For stainless steel couples, μ = 0.13 was observed. Macdonald and colleagues reported μ = 0.19 and μ = 0.17 for zirconia femoral heads, against CoCrMo and Ti6Al4V trunnions, respectively[39]. The taper angle is intrinsic to the design of the head and stem. Nassif *et al.* and Kao *et al.* have reported values between 3.9 and 5.6, corresponding to α values between 1.95 and 2.8[40,41]. Using values of μ = 0.2 and α = 2.67, Gilbert *et al.* demonstrated a ratio of 0.62 for the disassembly to assembly force, and concluded a relevant comparison with experimental values[42]. Rehmer *et al.* found that for a ceramic head with α = 2.88 on a titanium trunnion, the disassembly force was 51–78% of the assembly force, depending on the number of impactions and the material of the impactor used[43].

While useful for a rudimentary understanding of taper stability, the idealized scenario presented above is limited. In practice, *A* is generally smaller than the value that would be calculated under the assumption of uniform contact. Irregularities projecting from the taper surface will dictate asperity-asperity interactions, which result in small non-contacting crevices within the engagement area[42]. Intentional taper angle mismatch may also be used as a feature to control the area of contact. Connections involving a ceramic head have been designed to engage further into the bore ($\alpha_{bore} > \alpha_{trunnion}$) to avoid having pressures act along the thinner distal rim, which would increase the risk for

fracture[44]. The area of contact may be further defined by incorporating ridges or microgrooves into the trunnion, which flatten during impaction and serve as sites of localized contact[31,45]. The aforementioned idealized model does not account for plastic deformation, which also occurs in the case of smooth trunnions, and is dictated by features such as the elastic moduli and tolerances of the head and stem. Additionally, microgrooved trunnions have been experimentally shown to have 53% higher μ values than smooth trunnions in Ti6Al4V couples[46]. In addition to design limitations, the idealized static analysis does not account for variations in the assembly conditions. As there is little standardization in impaction procedure, surgeons have been reported to employ varying numbers of impaction strikes, using a variety of materials, and with a range of impaction forces[43,47-49]. Furthermore, the state of the taper surface can interfere with engagement mechanics, as blood, fat, and bone contaminants have been shown to weaken the strength of the connection by reducing the friction coefficient[50]. Conversely, Krull *et al.* reported stronger connection strengths for tapers contaminated with saline; it was suggested that the lower frictional shear stress facilitated further taper seating, which was followed by sufficient expulsion of the intra-taper fluid[51].

In general, *in vivo* separation of the head-stem taper is a rare complication of THA[52]. The majority of such case reports capture post-traumatic events or disassembly during closed reduction attempts for a dislocated THR[53-60]. Recently, there have been clinical reports on spontaneous decoupling of the head-stem taper, believed to be the result of corrosion-induced material loss within the taper, resulting in taper failure[61-65]. Gross trunnion failure (GTF), has been

associated with characteristic wear patterns on the trunnion, described as having a "bird beak", "trumpet", or "toothpick" appearance, along with circumferential wear tracks at the head bore surface, consistent with spinning on the stem trunnion[66]. Additionally, these separations generally occur as late term complications, and Martin *et al.* reported that an incubation period of 5.4 years was required before material loss on the stem taper could be visibly discerned[67]. These observations have led to the conclusion that the female head bore is widened by material loss due to corrosion, resulting in subsidence of the head on the stem trunnion, until the proximal tip of the trunnion comes into contact with the femoral head, thus "bottoming out"[66]. Failure of the taper interlock allows the head to spin on the stem trunnion in response to torques generated during joint motion, resulting in abrasive wear of the taper and eventual dissociation. In 2016 a voluntary recall was initiated by a major orthopedic manufacturer over concerns that some femoral head production lots could be at risk for taper instability[68,69]. However, these events have also been reported for devices from other manufacturers[61,70], and thus whether this phenomenon represents a persistent challenge of modular head-neck complications or is limited to a subset of implants is unclear. Nonetheless, the posited effect of corrosion occurs in tandem with growing concerns over corrosion-related complications in THA.

Metallic Biomaterials in THA

As previously mentioned, metals used for THRs chiefly comprise cobalt-chromium, stainless steel, and titanium alloys. In general, these materials feature high toughness, tensile strength, fatigue strength, and corrosion resistance[71]. Additionally, titanium-based alloys also exhibit favorable osseointegrative

properties and have a Young's modulus that is closer to native bone, resulting in less stress shielding and osteoporosis than in cases with cobalt-chromium and stainless steel alloys [22,23]. However, as titanium alloys have low shear strength, they can have high wear rates when used as bearing materials[24]. To this end, cobalt-chromium or stainless steel bearing surfaces are generally used in contemporary THRs, though these materials may also be used in other components of the implant. All the aforementioned alloys have reasonable biocompatibility due to their ability to spontaneously form passive oxide films, which serve as a barrier between the base alloys and the surrounding biological environment[25]. Nevertheless, cobalt, chromium, and nickel ions (from stainless steel alloys) have been shown to have cytotoxic and carcinogenic effects[26]. Additionally, wear debris and particles from titanium alloys have been implicated in osteolysis and implant loosening[27].

THR designs featuring a metal femoral head articulating on a metal acetabular liner were once popular option for THA. These metal-on-metal (MOM) devices eventually fell out of favor with the orthopedic community because of their high frictional torque which resulted in a high incidence of early component loosening[28]. Interest in the viability of this bearing couple was renewed in the 1990's following concerns about the osteolytic nature of debris from UHMWPE liners, coupled with cases of MOM survivorship exceeding 25 years. With advances in manufacturing technologies, second generation MOM devices were produced with new designs and stricter tolerances, allowing for a theoretically lower wearing implant and improved *in vivo* longevity[29]. Although laboratory and preclinical trials were promising, clinical reports of adverse soft tissue

reactions following MOM THA raised concerns about this bearing couple. Initially, metal ions and particulate debris from the bearing surface were believed to be the etiological agents of adverse local tissue reactions (ALTRs) such as pseudotumors and tissue necrosis. However, in a retrieval study involving MOM THRs, devices that were revised for ALTRs were reported to have relatively low rates of articular wear, but had considerable damage at the taper connection between the femoral head and stem[80]. Furthermore, clinical studies have shown that ALTRs can also occur in metal-on-UHMWPE and even ceramic-on-UHWPE bearings with a corroded modular junction[81-83]. In addition to having cytotoxic and apoptotic effects locally, corrosion products from CoCrMo alloys have been shown to disseminate to remote organs via lymphatic and hematogenous transport[84-86].

Passivation Behavior of Orthopedic Alloys

Orthopaedic alloys spontaneously form a stable nanometer-thin oxide film, and are therefore referred to as self-passivating. These alloys feature metals that are susceptible to an increase in their valence state, readily changing from atomic element to ion. Generic forms of the equations governing this electrochemical process are as follows:

$$M \rightarrow M^{n+} + ne^-$$

Equation 4

$$nM + H_2O \rightarrow M_nO_m + 2mH^+ + ne^-$$
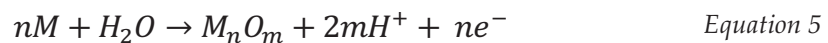
Equation 5

where M represents an unspecified self-passivating metal. These reactions are thermodynamically favorable, resulting in a release of energy that is dictated by the position of M in the electrochemical series. Equation 5 demonstrates that under aqueous conditions, an oxide will form. While this oxide can create a stable film that serves as a physical barrier to impede further corrosion reactions, it is intrinsically an electrochemically dynamic structure. Cabrera and Mott's theory on the oxidation of metals dictate that high electric fields will develop, which drive electromigration of cations and anions to grow the oxide[57]. Electrons from the base metal tunnel through the oxide and undergo affinity-based interactions with oxygen at the oxide-solution interface. This results in a deficit of electrons at the metal-oxide interface (and an accumulation of electrons at the oxide-solution interface), which can drive metal cations through the oxide. Conversely, the electric field encourages anions to migrate from the oxide-solution interface, and the combination of cations with anions results in oxide growth. The build-up of charges on either side of the oxide encourages a capacitive-like behavior across the interface, but the charge differential will encourage the migration of electrons and ions. Thus, the interface can be considered to have both capacitive (due to the separation of charges) and resistive (due to the oxide barrier that impedes, but does not completely prevent electromigration) elements, acting in parallel. This behavior can be modeled using a Randle's circuit depicted in Figure 3.
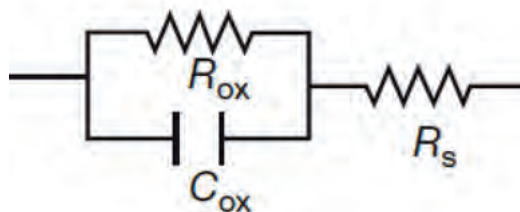
Figure 3. Schematic of a Randle's circuit, which can be used to model the capacitive and resistive nature of the passive oxide film

Where ROX represents the resistive behavior of the interface, COX captures the capacitive element, and RS is the resistance of the solution. This concept will form the basis of the electrochemical corrosion assessments developed in this thesis.

Mechanically Assisted Crevice Corrosion

The current understanding of modular junction implant damage is based on a mechanically assisted crevice corrosion mechanism (MACC)[88-91]. When implants are loaded micromotion between the two metals and interfacial stresses can result in oxide film fracture[91,92]. This exposes the underlying metal to an oxygen rich aqueous environment, resulting in oxidation and repassivation of the base metal[90,93]. As demonstrated in Equation 4, this process increases the concentration of electrons and free metal ions. These excess metal ions can react with chlorides, for which they have a very high affinity, and form metal chlorides that subsequently react with water to form metal hydroxide and hydrochloric acid[90]. Furthermore, it can be deduced from Equation 5 that this process decreases the concentration of free oxygen and lowers the pH within the modular junction crevice. With cyclic mechanical loading, continuous metal oxide fracture and repassivation occurs, resulting in further decrease of the free oxygen

concentration and pH within the crevice. The metal oxide is thermodynamically unstable in acidic conditions[94], and thus the protective nature of the passive layer is compromised. In this environment, the base metal is subject to accelerated corrosion.

In Vivo Taper Corrosion Damage

Although the complex corrosion processes have been summarized as MACC, other underlying modes of corrosion have been observed on retrieved head-neck modular tapers. Investigations of modular junction corrosion have identified several damage modes that include etching, fretting, intergranular corrosion, pitting, film formation, and selective leaching and imprinting (in which the stem trunnion topography is transferred to the head bore)[90,95-98]. The variety of corrosion processes may have differential effects on taper performance. Damage modes such as intergranular and phase boundary corrosion, are characterized by large areas of material dissolution which may weaken the taper interface as others have hypothesized. However, in a summary of corrosion damage modes among 364 retrievals, Hall *et al.* also identified material transfer from the Ti6Al4V stem to the CoCrMo head[99]. This indicates an adhesion mechanism between the two surfaces, which may effectively bolster the strength of the taper interface. An additional complexity is that different damage modes often overlap within the same area. Thus, the ability to reliably distinguish the unique types of corrosion damage within the taper interface can help to comprehensively understand the implications of the phenomenon.

Notwithstanding its electrochemical basis, clinical taper corrosion has been predominantly assessed by visual inspection of explants retrieved from revision surgery. Corrosion processes result in debris visible to the naked eye, which has allowed for qualitative evaluation. Corrosion within the taper may present with discoloration, blackened debris, and/or white haziness[90]. Prior to this current work, a semi-quantitative scoring system of 1-4 was developed in collaboration with the senior author from Goldberg's seminal study on the phenomenon[95,100]; a score of 1 indicates minimal fretting or corrosion, and 4 indicates severe damage[78]. With the understanding that taper corrosion can result in material loss, Kocagoz *et al.* later developed a method to quantify material loss using stylus contact profilometry and cone fitting algorithms[101]. Volumetric loss estimates have also been attained using a coordinate measurement machine[102] and with a chromatically encoded confocal measurement device[40]. The latter is predicated on external surface scans and therefore requires the investigator to first create a negative mold of the female head bore using a high-resolution replication polymer[40].

Although they lack quantitative insights into the corrosion processes occurring within the taper, visual corrosion scores and material loss evaluations have been useful in helping to elucidate some of the implant design variables that impact taper corrosion clinically. The increase in reports of corrosion has been linked to the use of larger femoral heads, which were introduced into THA to increase patient range of motion and lower the rates of dislocation[103]. Larger head sizes experience a greater torque at the taper interface, which may increase micromotion and result in mechanical disruption of the passive film[5]. Using

visual corrosion assessment of 74 retrieved femoral heads, Dyrkacz *et al.* confirmed increased corrosion for 36 mm heads compared to 28 mm heads[104]. Greater torques may also be generated in THRs with an increased femoral head offset, which can be used for soft-tissue balancing and to avoid leg-length discrepancies. In a previous retrieval study, our research group identified increased visual corrosion scores at the head taper for THRs with larger medio-lateral offsets, calculated using a radiographic biomechanical analysis technique[78]. The design of the femoral stem has also been implicated by Goldberg *et al.*, who reported greater head-neck corrosion damage scores for stem trunnions with a lower flexural rigidity[95]. Furthermore, modern femoral stems may feature smaller trunnions to decrease the risk of acetabular impingement, a design feature theorized to favor corrosion because of increased local stresses[105,106]. In an assessment of 40 retrieved heads, Nassif *et al.* did not find taper design to have an effect on taper corrosion but reported increased fretting damage for thicker tapers with longer contact lengths[40]. Additionally, the incorporation of microgrooves into stem trunnions has been purported to increase the risk of corrosion due to altered contact stresses leading to increased trunnion wear[107]. In a matched cohort study of 120 retrievals however, our research group did not identify a difference in taper volumetric wear measurements between smooth and microgrooved trunnions[108]. Alloy material has also been suggested to have an effect on corrosion, with the assumption that mixed alloy couples (CoCrMo head/Ti6Al4V stem) may participate in galvanic corrosion[31,95]. The contribution of galvanic corrosion to MACC has been contested however, given the lack of experimental galvanic interactions between alloys of titanium and cobalt-chromium[109,110].

Clinical variables, such as patient body mass index (BMI), taper assembly condition, and length of time in situ have been proposed as potential contributors to *in vivo* corrosion. Additionally, Gilbert *et al.* has postulated that the phagocytic cells of the skeletal system (including osteoclasts, macrophages, foreign body giant cells and polymorphonuclear leukocytes) may induce corrosion of CoCrMo alloys via secretion of reactive oxygen species (ROS) such as hydrogen peroxide (H2O2) and hydrochloric acid (HCl)[98]. This theory of inflammatory cell-induced corrosion (ICIC) was proposed after observing corrosion damage on surgically retrieved CoCrMo components, consistent with cell-derived morphologies. Additionally, biological material and cellular remnants were found to be attached to the corroded regions. These observations have since been suggested to be the result of electrocautery damage, as the discharge of electrical energy through implants may induce localized surface damage[111-113]. Nevertheless, Kubacki *et al.* have argued that the observed damage on retrievals is not comprehensively explained by electrosurgical damage[113], and an independent retrieval study identified extensive evidence of cells seated within the contact area of the head taper[99]. Experimentally, Liu *et al.* demonstrated the feasibility of ICIC using simulated inflammatory conditions and Fenton chemistry[114]. ROS at concentrations representative of that released by cells, were shown to create a highly aggressive environment that raised the oxidizing power of the solution (significantly altering cathodic behavior of the substrate). This resulted in decreased passivity of the oxide film (making the oxide more defective and less stable), which facilitated corrosion on the CoCrMo surfaces, evidenced by the increased corrosion current and more positive open-

circuit potential. Nevertheless, the role of an activated immune system on taper corrosion has yet to be demonstrated clinically[115].

In this research, *in vivo* corrosion phenomena were evaluated using a collection of modular head-neck components retrieved from arthroplasty patients. First, the ICIC theory was tested by considering PJI as a proxy for an activated immune system to assess whether devices revised for infection were associated with more severe visual corrosion at the head-neck taper. Next, the effect of clinical and design variables hypothesized to contribute to taper corrosion were examined, with multifactorial control to elucidate the clinical effect of taper size on corrosion severity. Furthermore, the proposed contribution of corrosion on the spontaneous dissociation of the taper junction was assessed experimentally by evaluating the effect of *in vivo* corrosion on the strength of head-neck tapers connections, using retrievals from revision surgery and cadaveric donors. The theory of self-passivation for metallic biomaterials was then leveraged to develop a quantitative measurement of taper corrosion severity using electrochemical impedance spectroscopy. Finally, this electrochemical framework was used to characterize corrosion damage modes and identify subsurface damage features nondestructively.

References

1.   Learmonth ID, Young C, Rorabeck C. The operation of the century: total hip replacement. *The Lancet.* 2007;370(9597):1508-1519.

2.   Pivec R, Johnson AJ, Mears SC, Mont MA. Hip arthroplasty. *The Lancet.* 2012;380(9855):1768-1777.

3.   Kremers HM, Larson DR, Crowson CS, et al. Prevalence of total hip and knee replacement in the United States. *The Journal of bone and joint surgery American volume.* 2015;97(17):1386.

4.   Lam V, Teutsch S, Fielding J. Hip and knee replacements: a neglected potential savings opportunity. *Jama.* 2018;319(10):977-978.

5.   Sloan M, Premkumar A, Sheth NP. Projected volume of primary total joint arthroplasty in the US, 2014 to 2030. *JBJS.* 2018;100(17):1455-1460.

6.   Ackerman SJ, Knight T, Wahl PM. Projected Medicare Savings Associated With Lowering the Risk of Total Hip Arthroplasty Revision: An Administrative Claims Data Analysis. *Orthopedics.* 2018;42(1):e86-e92.

7.   Singh J, Politis A, Loucks L, Hedden DR, Bohm ER. Trends in revision hip and knee arthroplasty observations after implementation of a regional joint replacement registry. *Canadian Journal of Surgery.* 2016;59(5):304.

8.   Karam JA, Tokarski AT, Ciccotti M, Austin MS, Deirmengian GK. Revision total hip arthroplasty in younger patients: indications, reasons for failure, and survivorship. *Physician and Sportsmedicine.* 2012;40(4):96-101.

9.   Langton D, Sidaginamale R, Lord J, Nargol A, Joyce T. Taper junction failure in large-diameter metal-on-metal bearings. *Bone and Joint Research.* 2012;1(4):56-63.

10.   Chana R, Esposito C, Campbell P, Walter W, Walter W. Mixing and matching causing taper wear Corrosion associated with pseudotumour formation. *Journal of Bone & Joint Surgery, British Volume.* 2012;94(2):281-286.

11.   Meyer H, Mueller T, Goldau G, Chamaon K, Ruetschi M, Lohmann CH. Corrosion at the cone/taper interface leads to failure of large-diameter metal-on-metal total hip arthroplasties. *Clinical Orthopaedics and Related Research®.* 2012;470(11):3101-3108.

12.   Ren P-G, Irani A, Huang Z, Ma T, Biswal S, Goodman SB. Continuous infusion of UHMWPE particles induces increased bone macrophages and osteolysis. *Clinical Orthopaedics and Related Research®.* 2011;469(1):113-122.

13.   Charnley J. Arthroplasty of the hip: a new operation. *The Lancet.* 1961;277(7187):1129-1132.

14.   Toledo-Pereyra LH. John Charnley—Father of Modern Total Hip Replacement. *Journal of Investigative Surgery.* 2004;17(6):299-301.

15. Charnley J. Arthroplasty of the Hip: A New Operation*. *Clinical Orthopaedics and Related Research (1976-2007).* 1973;95:4-8.

16. Charnley J. Low friction principle. *Low friction arthroplasty of the hip*: Springer; 1979:3-15.

17. Harris WH. Osteolysis and particle disease in hip replacement: a review. *Acta Orthopaedica Scandinavica.* 1994;65(1):113-123.

18. Stauffer R. Ten-year follow-up study of total hip replacement. *The Journal of bone and joint surgery American volume.* 1982;64(7):983-990.

19. Banerjee S, Cherian JJ, Elmallah RK, Pierce TP, Jauregui JJ, Mont MA. Robot-assisted total hip arthroplasty. *Expert review of medical devices.* 2016;13(1):47-56.

20. Srinivasan A, Jung E, Levine BR. Modularity of the femoral component in total hip arthroplasty. *JAAOS-Journal of the American Academy of Orthopaedic Surgeons.* 2012;20(4):214-222.

21. Kurtz SM. The origins of UHMWPE in total hip arthroplasty. *UHMWPE Biomaterials Handbook*: Elsevier; 2016:33-44.

22. Le Fanu J. *The rise and fall of modern medicine.* Hachette UK; 2011.

23. Marwin S. Ultra-High-Molecular-Weight Polyethylene (UHMWPE) in Total Joint Arthroplasty. *Bulletin of the NYU Hospital for Joint Diseases.* 2018;76(1):38-46.

24. Lachiewicz PF, Kleeman LT, Seyler T. Bearing surfaces for total hip arthroplasty. *JAAOS-Journal of the American Academy of Orthopaedic Surgeons.* 2018;26(2):45-57.

25. Gomez PF, Morcuende JA. A historical and economic perspective on Sir John Charnley, Chas F. Thackray Limited, and the early arthroplasty industry. *The Iowa orthopaedic journal.* 2005;25:30.

26. Mai KT, Verioti CA, Casey K, Slesarenko Y, Romeo L, Colwell JC. Cementless femoral fixation in total hip arthroplasty. *American journal of orthopedics (Belle Mead, NJ).* 2010;39(3):126-130.

27. Geesink RG. Osteoconductive coatings for total joint arthroplasty. *Clinical Orthopaedics and Related Research (1976-2007).* 2002;395:53-65.

28. Callaghan JJ, Rosenberg AG, Rubash HE, Clohisy J, Beaulé PE, Della Valle CJ. *The adult hip: hip arthroplasty surgery.* Wolters Kluwer Health Adis (ESP); 2015.

29. Tan SC, Teeter MG, Del Balso C, Howard JL, Lanting BA. Effect of Taper Design on Trunnionosis in Metal on Polyethylene Total Hip Arthroplasty. *The Journal of arthroplasty.* 2015.

30. Cook SD, Barrack RL, Baffes GC, et al. Wear and corrosion of modular interfaces in total hip replacements. *Clinical orthopaedics and related research.* 1994(298):80-88.

31. Hussenbocus S, Kosuge D, Solomon LB, Howie D, Oskouei R. Head-Neck Taper Corrosion in Hip Arthroplasty. *BioMed research international.* 2015;2015.

32. Plummer DR, Berger RA, Paprosky WG, Sporer SM, Jacobs JJ, Della Valle CJ. Diagnosis and management of adverse local tissue reactions secondary to corrosion at the head-neck junction in patients with metal on polyethylene bearings. *The Journal of arthroplasty.* 2016;31(1):264-268.

33. Krishnan H, Krishnan S, Blunn G, Skinner J, Hart A. Modular neck femoral stems. *The bone & joint journal.* 2013;95(8):1011-1021.

34. McTighe T. Cementless Modular Stems. *JISRF Update, April.* 2002.

35. Friedman RJ, Black J, Galante JO, Jacobs JJ, Skinner HB. Current concepts in orthopaedic biomaterials and implant fixation. *JBJS.* 1993;75(7):1086-1109.

36. Hernigou P, Queinnec S, Lachaniette CHF. One hundred and fifty years of history of the Morse taper: from Stephen A. Morse in 1864 to complications related to modularity in hip arthroplasty. *International orthopaedics.* 2013;37(10):2081-2088.

37. Wright RN. *Wire technology: process engineering and metallurgy.* Butterworth-Heinemann; 2016.

38. Fessler H, Fricker D. Friction in femoral prosthesis and photoelastic model cone taper joints. *Proceedings of the Institution of Mechanical Engineers, Part H: Journal of Engineering in Medicine.* 1989;203(1):1-14.

39. Macdonald W, Aspenberg A, Jacobsson C, Carlsson L. Friction in orthopaedic zirconia taper assemblies. *Proceedings of the Institution of Mechanical Engineers, Part H: Journal of Engineering in Medicine.* 2000;214(6):685-692.

40. Nassif NA, Nawabi DH, Stoner K, Elpers M, Wright T, Padgett DE. Taper design affects failure of large-head metal-on-metal total hip replacements. *Clinical Orthopaedics and Related Research®.* 2014;472(2):564-571.

41. Kao Y-YJ, Koch CN, Wright TM, Padgett DE. Flexural rigidity, taper angle, and contact length affect fretting of the femoral stem trunnion in total hip arthroplasty. *The Journal of arthroplasty.* 2016;31(9):254-258.

42. Gilbert J, Mali S, Sivan S. Corrosion of modular tapers in total joint replacements: a critical assessment of design, materials, surface structure, mechanics, electrochemistry, and biology. *Modularity and Tapers in Total Joint Replacement Devices*: ASTM International; 2015.

43. Rehmer A, Bishop NE, Morlock MM. Influence of assembly procedure and material combination on the strength of the taper connection at the head–neck junction of modular hip endoprostheses. *Clinical Biomechanics.* 2012;27(1):77-83.

44. Witt F, Gührs J, Morlock MM, Bishop NE. Quantification of the contact area at the head-stem taper interface of modular hip prostheses. *PloS one.* 2015;10(8):e0135517.

45. Dransfield K, Racasan R, Williamson J, Bills P. Changes in the morphology of microgrooved stem tapers with differing assembly conditions. *Biotribology.* 2019;18:100096.

46. Bitter T, Khan I, Marriott T, Schreurs B, Verdonschot N, Janssen D. Experimental Measurement of the Static Coefficient of Friction at the Ti–Ti Taper Connection in Total Hip Arthroplasty. *Journal of biomechanical engineering.* 2016;138(3):034505.

47. Pennock AT, Schmidt AH, Bourgeault CA. Morse-type tapers: factors that may influence taper strength during total hip arthroplasty. *The Journal of arthroplasty.* 2002;17(6):773-778.

48. Heiney JP, Battula S, Vrabec GA, et al. Impact magnitudes applied by surgeons and their importance when applying the femoral head onto the Morse taper for total hip arthroplasty. *Archives of orthopaedic and trauma surgery.* 2009;129(6):793-796.

49. McGrory BJ, Ng E. No consensus for femoral head impaction technique in surgeon education materials from orthopedic implant manufacturers. *The Journal of arthroplasty.* 2018;33(6):1749-1751. e1741.

50. Lavernia CJ, Baerga L, Barrack RL, et al. The effects of blood and fat on Morse taper disassembly forces. *Am J Orthop (Belle Mead NJ).* 2009;38(4):187-190.

51. Krull A, Morlock MM, Bishop NE. The influence of contamination and cleaning on the strength of modular head taper fixation in total hip arthroplasty. *The Journal of arthroplasty.* 2017;32(10):3200-3205.

52. Shiga T, Mori M, Hayashida T, Fujiwara Y, Ogura T. Disassembly of a modular femoral component after femoral head prosthetic replacement. *The Journal of arthroplasty.* 2010;25(4):659. e617-659. e619.

53. Parker SJ, Khan W, Mellor S. Late nontraumatic dissociation of the femoral head and trunnion in a total hip arthroplasty. *Case reports in orthopedics.* 2015;2015.

54. Namba RS, Van der Reis WL. Femoral head and neck dissociation after a total hip arthroplasty with a constrained acetabular liner. *Orthopedics.* 2000;23(5):489-491.

55. Woolson S, Pottorff G. Disassembly of a modular femoral prosthesis after dislocation of the femoral component. A case report. *JBJS.* 1990;72(4):624-625.

56. Pellicci PM, Haas S. Disassembly of a modular femoral component during closed reduction of the dislocated femoral component. A case report. *JBJS.* 1990;72(4):619-620.

57. Star MJ, Colwell JC, Walker R. Dissociation of modular hip arthroplasty components after dislocation. A report of three cases at differing dissociation levels. *Clinical orthopaedics and related research.* 1992(278):111-115.

58. Parvej Ahmed DK. Late disassembly of femoral head and neck of a modular primary total hip arthroplasty. *Journal of orthopaedic case reports.* 2015;5(1):8.

59. Chu C-M, Wang S-J, Lin L-C. Dissociation of modular total hip arthroplasty at the femoral head–neck interface after loosening of the acetabular shell following hip dislocation. *The Journal of arthroplasty.* 2001;16(6):806-809.

60. Moores TS, Blackwell JR, Chatterton BD, Eisenstein N. Disassociation at the head–trunnion interface: an unseen complication of modular hip hemiarthroplasty. *Case Reports.* 2013;2013:bcr2013200387.

61. Banerjee S, Cherian JJ, Bono JV, et al. Gross trunnion failure after primary total hip arthroplasty. *The Journal of arthroplasty.* 2015;30(4):641-648.

62. Talmo CT, Sharp KG, Malinowska M, Bono JV, Ward DM, Lareau J. Spontaneous modular femoral head dissociation complicating total hip arthroplasty. *Orthopedics.* 2014;37(6):e592-e595.

63. Urish KL, Hamlin BR, Plakseychuk AY, et al. Trunnion failure of the recalled low friction ion treatment cobalt chromium alloy femoral head. *The Journal of arthroplasty.* 2017;32(9):2857-2863.

64. Ko LM, Chen AF, Deirmengian GK, Hozack WJ, Sharkey PF. Catastrophic femoral head-stem trunnion dissociation secondary to corrosion. *JBJS.* 2016;98(16):1400-1404.

65. Runner RP, Bellamy JL, Roberson JR. Gross trunnion failure of a cobalt-chromium femoral head on a titanium stem at midterm follow-up: a report of 3 cases. *JBJS case connector.* 2016;6(4):e96.

66. Morlock MM, Dickinson EC, Günther K-P, Bünte D, Polster V. Head taper corrosion causing head bottoming out and consecutive gross stem taper failure in total hip arthroplasty. *The journal of arthroplasty.* 2018;33(11):3581-3590.

67. Martin AJ, Jenkins DR, Van Citters DW. Role of corrosion in taper failure and head disassociation in total hip arthroplasty of a single design. *Journal of Orthopaedic Research®.* 2018;36(11):2996-3003.

68. Urish KL, Hamlin BR, Plakseychuk AY, et al. Trunnion Failure of the Recalled Low Friction Ion Treatment Cobalt Chromium Alloy Femoral Head. *The Journal of Arthroplasty.* 2017.

69. Urish KL, Hamlin BR, Plakseychuk AY, Levison TJ, Kurtz S, DiGioia AM. Letter to the Editor on "Trunnion Failure of the Recalled Low Friction Ion Treatment Cobalt Chromium Alloy Femoral Head". *The Journal of arthroplasty.* 2019;34(1):190.

70. Bolarinwa SA, Martino JM, Moskal JT, Wolfe MW, Shuler TE. Gross trunnion failure after a metal-on-polyethylene total hip arthroplasty leading to dissociation at the femoral head-trunnion interface. *Arthroplasty today.* 2019;5(1):5-10.

71. Nasab MB, Hassan MR, Sahari BB. Metallic biomaterials of knee and hip-a review. *Trends Biomater Artif Organs.* 2010;24(1):69-82.

72. Rani VD, Vinoth-Kumar L, Anitha V, Manzoor K, Deepthy M, Shantikumar VN. Osteointegration of titanium implant is sensitive to specific nanostructure morphology. *Acta biomaterialia.* 2012;8(5):1976-1989.

73. Kujala S, Ryhänen J, Danilov A, Tuukkanen J. Effect of porosity on the osteointegration and bone ingrowth of a weight-bearing nickel–titanium bone graft substitute. *Biomaterials.* 2003;24(25):4691-4697.

74. Swaminathan V, Gilbert JL. Fretting corrosion of CoCrMo and Ti6Al4V interfaces. *Biomaterials.* 2012;33(22):5487-5503.

75. Gotman I. Characteristics of metals used in implants. *Journal of endourology.* 1997;11(6):383-389.

76. McGregor D, Baan R, Partensky C, Rice J, Wilbourn J. Evaluation of the carcinogenic risks to humans associated with surgical implants and other foreign bodies—a report of an IARC Monographs Programme Meeting. *European journal of cancer.* 2000;36(3):307-313.

77. Lombardi JA, Mallory T, Vaughn B, Drouillard P. Aseptic loosening in total hip arthroplasty secondary to osteolysis induced by wear debris from titanium-alloy modular femoral heads. *The Journal of bone and joint surgery American volume.* 1989;71(9):1337-1342.

78. Higgs G, Hanzlik J, MacDonald D, et al. Method of characterizing fretting and corrosion at the various taper connections of retrieved modular components from metal-on-metal total hip arthroplasty. *Metal-on-metal total hip replacement devices*: ASTM International; 2013.

79. Amstutz HC, Grigoris P. Metal on metal bearings in hip arthroplasty. *Clinical Orthopaedics and Related Research (1976-2007).* 1996;329:S11-S34.

80. Langton DJ, Jameson SS, Joyce TJ, et al. Accelerating failure rate of the ASR total hip replacement. *J Bone Joint Surg Br.* 2011;93(8):1011-1016.

81. Cooper HJ, Della Valle CJ, Berger RA, et al. Corrosion at the head-neck taper as a cause for adverse local tissue reactions after total hip arthroplasty. *The Journal of bone and joint surgery American volume.* 2012;94(18):1655.

82. Lindgren J, Brismar B, Wikstrom A. Adverse reaction to metal release from a modular metal-on-polyethylene hip prosthesis. *The Journal of bone and joint surgery British volume.* 2011;93(10):1427-1430.

83. Scully WF, Teeny SM. Pseudotumor associated with metal-on-polyethylene total hip arthroplasty. *Orthopedics.* 2013;36(5):e666-e670.

84. Hall D, Pourzal R, Della Valle C, Galante J, Jacobs J, Urban R. Corrosion of modular junctions in femoral and acetabular components for hip arthroplasty and its local and systemic effects. *Modularity and Tapers in Total Joint Replacement Devices*: ASTM International; 2015.

85. Catelas I, Petit A, Zukor DJ, Huk OL. Cytotoxic and apoptotic effects of cobalt and chromium ions on J774 macrophages–Implication of caspase-3 in the apoptotic pathway. *Journal of Materials Science: Materials in Medicine.* 2001;12(10-12):949-953.

86. Kwon Y-M, Xia Z, Glyn-Jones S, Beard D, Gill HS, Murray DW. Dose-dependent cytotoxicity of clinically relevant cobalt nanoparticles and ions on macrophages in vitro. *Biomedical materials.* 2009;4(2):025018.

87. Cabrera N, Mott N. REP PROG PHYS. *Rep Prog Phys.* 1948;12:163.

88. Jacobs J, Cooper H, Urban R, Wixson R, Della Valle C. What do we know about taper corrosion in total hip arthroplasty? *The Journal of arthroplasty.* 2014;29(4):668-669.

89. Gilbert JL, Jacobs JJ. The mechanical and electrochemical processes associated with taper fretting crevice corrosion: a review. *Modularity of Orthopedic Implants.* 1997;1301:45.

90. Gilbert JL, Buckley CA, Jacobs JJ. In vivo corrosion of modular hip prosthesis components in mixed and similar metal combinations. The effect of crevice, stress, motion, and alloy coupling. *Journal of biomedical materials research.* 1993;27(12):1533-1544.

91. Jacobs JJ, Gilbert JL, Urban RM. Current Concepts Review-Corrosion of Metal Orthopaedic Implants. *The Journal of Bone & Joint Surgery.* 1998;80(2):268-282.

92. Hallab NJ, Messina C, Skipor A, Jacobs JJ. Differences in the fretting corrosion of metal–metal and ceramic–metal modular junctions of total hip replacements. *Journal of Orthopaedic Research.* 2004;22(2):250-259.

93. Hoeppner D, Chandrasekaran V. Fretting in orthopaedic implants: a review. *Wear.* 1994;173(1):189-197.

94. West JM. Basic corrosion and oxidation. 1986.

95. Goldberg JR, Gilbert JL, Jacobs JJ, Bauer TW, Paprosky W, Leurgans S. A multicenter retrieval study of the taper interfaces of modular hip prostheses. *Clinical orthopaedics and related research.* 2002;401:149-161.

96. Bishop N, Witt F, Pourzal R, et al. Wear patterns of taper connections in retrieved large diameter metal-on-metal bearings. *Journal of Orthopaedic Research.* 2013;31(7):1116-1122.

97. Van Citters D, Martin A, Currier J, Park S-H, Edidin A. Factors related to imprinting corrosion in modular head-neck junctions. *Modularity and Tapers in Total Joint Replacement Devices*: ASTM International; 2015.

98. Gilbert JL, Sivan S, Liu Y, Kocagöz SB, Arnholt CM, Kurtz SM. Direct in vivo inflammatory cell‐induced corrosion of CoCrMo alloy orthopedic implant surfaces. *Journal of Biomedical Materials Research Part A.* 2015;103(1):211-223.

99. Hall DJ, Pourzal R, Lundberg HJ, Mathew MT, Jacobs JJ, Urban RM. Mechanical, chemical and biological damage modes within head‐neck

tapers of CoCrMo and Ti6Al4V contemporary hip replacements. *Journal of Biomedical Materials Research Part B: Applied Biomaterials.* 2018;106(5):1672-1685.

100. Higgs GB, MacDonald DW, Gilbert JL, Rimnac CM, Kurtz SM, Committee IRCW. Does taper size have an effect on taper damage in retrieved metal-on-polyethylene total hip devices? *The Journal of arthroplasty.* 2016;31(9):277-281.

101. Kocagoz SB, Underwood RJ, MacDonald DW, Gilbert JL, Kurtz SM. Ceramic Heads Decrease Metal Release Caused by Head-taper Fretting and Corrosion. *Clinical Orthopaedics and Related Research®.* 2016;474(4):985-994.

102. Huot Carlson JC, Van Citters DW, Currier JH, Bryant AM, Mayor MB, Collier JP. Femoral stem fracture and in vivo corrosion of retrieved modular femoral hips. *The Journal of arthroplasty.* 2012;27(7):1389-1396. e1381.

103. Malkani AL, Ong KL, Lau E, Kurtz SM, Justice BJ, Manley MT. Early-and late-term dislocation risk after primary hip arthroplasty in the Medicare population. *The Journal of arthroplasty.* 2010;25(6):21-25.

104. Dyrkacz RM, Brandt J-M, Ojo OA, Turgeon TR, Wyss UP. The influence of head size on corrosion and fretting behaviour at the head-neck interface of artificial hip joints. *The Journal of arthroplasty.* 2013;28(6):1036-1040.

105. Cales B, Stefani Y. Risks and advantages in standardization of bores and cones for heads in modular hip prostheses. *Journal of biomedical materials research.* 1998;43(1):62-68.

106. Ihekweazu UN, Lyman S, Chiu Y-f, Vaynberg I, Westrich G. Modern trunnion designs do not affect clinically significant patient-reported outcomes. *HIP International.* 2019:1120700019864317.

107. Panagiotidou A, Meswania J, Hua J, Muirhead‐Allwood S, Hart A, Blunn G. Enhanced wear and corrosion in modular tapers in total hip replacement is associated with the contact area and surface topography. *Journal of Orthopaedic Research.* 2013;31(12):2032-2039.

108. Arnholt CM, MacDonald DW, Underwood RJ, et al. Do stem taper microgrooves influence taper corrosion in total hip arthroplasty? A matched cohort retrieval study. *The Journal of arthroplasty.* 2017;32(4):1363-1373.

109. Lucas L, Buchanan R, Lemons J. Investigations on the galvanic corrosion of multialloy total hip prostheses. *Journal of biomedical materials research.* 1981;15(5):731-747.

110. Mears D. The use of dissimilar metals in surgery. *Journal of biomedical materials research.* 1975;9(4):133-148.

111. Campbell P, Yuan N, Luck J, Courpron P, Park S. Re-examining the concept of inflammatory cell-induced corrosion. Paper presented at: Orthopaedic Proceedings2017.

112. Aldinger P, Pawar V. Similarities between reported inflammatory cell-induced corrosion features and electrocautery damage. Paper presented at: Orthopaedic Proceedings2017.

113. Kubacki GW, Sivan S, Gilbert JL. Electrosurgery induced damage to Ti-6Al-4V and CoCrMo alloy surfaces in orthopedic implants in vivo and in vitro. *The Journal of arthroplasty.* 2017;32(11):3533-3538.

114. Liu Y, Gilbert JL. The effect of simulated inflammatory conditions and Fenton chemistry on the electrochemistry of CoCrMo alloy. *Journal of Biomedical Materials Research Part B: Applied Biomaterials.* 2018;106(1):209-220.

115. Pourzal R, Lundberg HJ, Hall DJ, Jacobs JJ. What factors drive taper corrosion? *The Journal of arthroplasty.* 2018;33(9):2707-2711.

I. Risk Factors for Peri-Prosthetic Joint Infection and Modular Head-Neck Corrosion in a Retrieval Population

1.1 Abstract

Database and registry research in orthopedics allow for population-level insight into clinical outcomes, but they lack the physical information on device performance and material behavior that retrieval analysis can provide. While it has been proposed that inflammatory cell secretions from an activated immune system may contribute to *in vivo* corrosion of orthopedic alloys, this relationship has not been investigated clinically. This study identifies the potential of population health analytics for retrieval investigations with an exploration into the role that an activated immune system may play in corrosion. Time-to-event analyses was performed on 3097 retrieved hip implants and 2724 retrieved knee implants to assess risk factors for peri-prosthetic infection (PJI), and the effect of PJI on the severity of taper corrosion was tested. From the univariate cause-specific proportional hazards regression analysis, increased age ($p<0.001$), male sex ($p<0.001$), non-white race ($p=0.04$), BMI ($p<0.001$), previous revision surgery ($p<0.001$), TKR implants ($p<0.001$), and academic revision hospital ($p=0.001$) were found to increase the hazard of revision due to infection. A multivariable log-logistic parametric model with frailty for individual revising hospitals identified increased age ($p<0.001$), male sex ($p<0.001$), BMI ($p=0.012$), previous revision ($p<0.001$), and academic revision hospital ($p<0.047$) as risk factors for infection. From the corrosion analysis, the effect of PJI was not significant ($p=0.645$) in the context of gender and index surgery. These results highlight the

potential role of epidemiological techniques in large-scale retrieval analysis to augment the findings of national database studies. Our findings from taper damage assessment did not identify a significant effect of PJI on corrosion.

1.2 Introduction

Total hip arthroplasty (THA) is the gold standard for advanced osteoarthritis of the hip, with over 500,000 procedures performed annually in the United States [1]. A limitation of this procedure however, is the eventual need for a revision surgery due to implant-related complications. While the leading causes of revision are infection, dislocation and loosening, corrosion products resulting from the modular components of these total hips replacements (THRs) have been identified as a cause for premature revision[2,3]. Recently, it has been proposed that this corrosion may result from an activated biological environment[4]. It is well understood that the body will mount an immune response in the presence of a foreign body, thus the surgical intervention itself will engage the immune system, which can then be exacerbated by a number of *in vivo* events. In an effort to degrade foreign bodies, activated phagocytic immune cells release reactive oxygen species along with digestive enzymes, and it was shown experimentally that these secretions may corrode CoCrMo substrates[5,6]. Additionally, it has been concluded that some of the corrosion damage observed on retrieved hip and knee components was consistent with that induced by cells[4,7]. In their summary, Gilbert *et al.* highlighted that it is unclear whether these observations represent a new phenomenon, or is an occurrence that has evaded researchers and medical device manufacturers for some time[7].

In practice, understanding the *in vivo* performance of implants remains a challenge, as the clinical experience of drugs and medical devices may not be adequately predicted by pre-clinical evaluation. Recent legislation has tried to address this limitation by encouraging the use of real world data (RWD) for post-approval evaluation of drugs and to support new indications for their use[8]. These data provide practical information on the usage as well as risks and benefits of a medical intervention, outside of the randomized clinical trial framework. Sources of RWD recognized by the United States Food and Drug Administration (FDA) include patient registries, which are organized systems that use observational study methods to collect uniform data and evaluate specified outcomes for a population. While such registries may be useful for population-level insights into the clinical history of medical devices, they the lack information on *in vivo* performance and material behavior that retrieval analysis can provide. Retrieval analysis, which involves studying the failure mechanisms of implants that have been obtained during a revision surgery or at autopsy, has provided important insights that have led to key improvements in orthopedic device performance and longevity[9,10].

Retrieval studies are resource-intensive, and therefore are often conducted using relatively small sample sizes, which not only limits statistical power, but also raises concerns about how well the study sample represents the larger arthroplasty population. At the beginning of the 21st century, our research group established a multicenter retrieval program to examine the *in vivo* behavior of joint prostheses by performing an integrated analysis of clinical, patient, and implant details associated with these surgical procedures. As this program now

has more than 8000 devices from across the United States, we sought to explore the use of epidemiological techniques within the retrieval database. The purpose of this study was to compare the clinical history of these explants with that of the larger arthroplasty population by using time-to-event analysis, with the goal of confirming the risk factors for peri-prosthetic joint infection (PJI) that have been previously reported using national databases. We also considered PJI as a proxy for an activated immune system to test the hypothesis that increased immune activity is associated with greater corrosion damage at the modular taper junction.

1.3 Methods

<u>Clinical Data</u>

As a part of a multi-institutional implant surveillance program currently comprising 13 revision centers across seven states in the United States, 4284 total hip replacements (THRs) and 4032 total knee replacements (TKRs) have been consecutively retrieved between 1992 and 2019 during the general routine of revision surgery. In compliance with non-human subject research determination by the internal review board of Drexel University, clinical personnel at the revision hospitals provided the research team with a de-identified summary of clinical information associated with the explanted components. These summaries were used to identify cases of PJI (as diagnosed during the course of revision surgery) as well as to obtain details on patient and surgical covariates. Risk factors for PJI were identified by performing time-to-event analysis with retrievals having clinical summaries available at the time of this study, comprising 3147 THRs and 2798 TKRs.

Hip Taper Damage Evaluation

Retrieval evaluation was conducted on a subset of 530 THRs. These components were disinfected by two soaks in a 1:10 ratio of disinfectant (Discide; AliMed, Dedham, MA) to water for 25 minutes, followed by two ultrasonications in de-ionized water for 30 minutes. A soft nylon brush was used to help remove biological films and loose debris. After cleaning, modular interfaces were inspected both by the naked eye and under a stereomicroscope equipped with a digital camera (Leica DFC490; Leica Microsystems, Wetzlar, Germany), for signs of fretting and corrosion. Fretting, defined by Szolwinski *et al.* as a contact damage process resulting from micromotions of interfacing metals, was identified as scratching perpendicular to machining lines on the taper, and/or wearing away of the machining lines.[11] Corrosion was identified as white haziness (indicative of intergranular crevice corrosion), discoloration, and/or blackened debris[12]. An ordinal metric for taper damage was developed by modifying a previously described 4-point scoring system, in collaboration with the senior author of the original study. In the Goldberg investigation, the head taper was divided into two regions (proximal and distal), the stem trunnion into four (medial, lateral, posterior, and anterior), and each region assigned separate fretting and corrosion scores. Because these scores were then later converted to globalized damage scores, each interface was analyzed as such in the current study. Damage scores were then dichotomized as minimal ($1 \leq score \leq 2$), or significant (score > 2).

Statistical Analysis

To conduct the time-to-event analysis, any component revised from a patient with PJI within 10 years was modeled as an event, with all other cases considered censored. The risk factors tested for their association with PJI were age, sex (female vs. male), race (white vs. other), BMI, implant type (THR vs. TKR), index surgery (primary vs. revision) and hospital type (community vs. teaching). Univariate Cox semi-parametric proportional hazards models were created for each potential risk factor to determine its relationship with time to infection. The proportional hazards assumption was assessed using by using log-log plots for all categorical variables and by using individual extended Cox models with an interaction term between the predictor and time. For the primary endpoint, a Cox model combining all predictors of interest and their interaction terms, where necessary, was created. Parametric exponential, Weibull, and log-logistic models were created for the data, with interaction terms for effect modifying variables. Frailty was also incorporated to account for the individualized effect of different hospitals. For the taper damage evaluation, risk factors for severe taper damage were initially assessed using univariate logistic regression. Multivariable logistic regression models were then generated to investigate the association between PJI and taper damage in the context of confounding variables. Model quality was assessed using the Akaike's information criterion (AIC) with model selection favoring low AIC values. All analyses were performed using SAS 9.3 (SAS Institute, Inc., Cary, North Carolina) and significance was determined at $\alpha=0.05$.

1.4 Results

As depicted in Table 1, the mean (standard deviation) age at implantation was 56.9 (14.1) years for THRs and 59.7 (10.9) years for TKRs. The majority of retrievals were implanted in patients who were female (53.2%, THRs; 59.1%, TKRs), white (81.8%, THRs; 75.6%, TKRs), had a BMI ≥25 (69.6%, THRs; 84.3%, TKRs) and during a primary surgery (53.2%, THRs; 59.1%, TKRs).

Table 1. Clinical and demographic summary for the 3097 hips and 2724 knees included in this study. As complete clinical details were not available for the entire study population, percentages are represented inclusive of missing data.

Variable	Hips (n = 3097)	Knees (n = 2724)
Age (years), mean (SD)	56.9 (14.1)	59.6 (10.9)
Sex, *n* (%)		
Male	1429 (46.1%)	1109 (40.7%)
Female	1639 (52.9%)	1599 (58.7%)
Race, *n* (%)		
White	2341 (75.6%)	1939 (71.2%)
Other	526 (17.0%)	622 (22.4%)
Body Mass Index, *n* (%)		
Underweight	182 (5.9%)	142 (5.2%)
Normal Weight	749 (24.2%)	279 (10.2%)
Overweight	1014 (32.7%)	711 (26.1%)
Obese	1105 (35.7%)	1562 (57.3%)
Index Surgery, *n* (%)		
Revision	744 (24.0%)	677 (24.9%)
Primary	1877 (60.6%)	1562 (58.4%)

Risk Factors for PJI

From the univariate time-to-event analysis, increased age (p<0.001), male sex (p<0.001), non-white race (p=0.04), BMI (p<0.001), previous revision surgery (p<0.001), TKR implants (p<0.001), and academic revision hospital (p=0.001)

were identified as risk factors for PJI. In the final multivariable log-logistic parametric survival model, which included frailty to accommodate variation among individual revising hospitals, the risk factors for PJI were increased age (p<0.001), male sex (p<0.001), BMI (underweight vs. overweight; p=0.012), previous revision surgery (p<0.001), and academic revision hospital (p=0.047).

Effect of PJI on Taper Damage

For the THRs selected for taper damage evaluation (Table 3), implants revised for PJI (n=120) were compared to those revised for all other reasons (n=410). The mean duration of implantation was 2.84 (4.79) years for cases and 6.01 (5.93) for the controls. The mean (standard deviation) age at implantation was 54.6 (14.3) years for the PJI cases and 58.4 (13.7) for the non-PJI controls. Considering implants with clinical data available, a slight majority were retrieved from males (51.7%, cases; 50.0% controls) and both patient populations were predominantly white (68.3%, cases; 73.4% controls). While the majority of non-PJI controls were implanted during primary surgery (62.4%), more than a quarter of the PJI-cases had missing index surgery details. With this consideration, there was a slight majority of revision surgeries in the PJI cases (37.5%, revision; 35.8%, primary).

The univariate analysis identified that significant predictors for increased corrosion were non-PJI diagnosis (p=0.019), male gender (p<0.001), white race (p<0.001), primary index surgery (p=0.013). In the adjusted multivariable analysis, non-PJI diagnosis (OR, 1.15; 95% CI 0.85–1.58; p=0.645) was not a significant predictor of increased corrosion after controlling for male sex (OR,

1.44; 95% CI 1.26–1.64; p=0.006) and primary index surgery (OR, 1.35; 95% CI 1.17–1.56; p=0.034).

Table 2. Results from the adjusted time-to-event analysis. The multivariable log-logistic model included frailty for revision hospital and models survival as opposed to modeling hazard. Thus, hazard ratios were calculated from by taking the exponential of the calculated coefficient's negative value.

Variable	HR (95% CI)	p-value
Age (years)	1.09 (1.16–1.25)	<0.001
Sex		
Male	1.00	
Female	0.91 (0.81–0.93)	0.011
Race		
White	1.00	
Other	1.04 (0.96–1.14)	0.416
BMI		
Underweight	1.00	
Normal	0.92 (0.72–1.07)	0.310
Overweight	0.90 (0.65–0.95)	0.012
Obese	0.97 (0.85–1.21)	0.506
Index Surgery		
Revision	1.00	
Primary	0.75 (0.48–0.56)	<0.001
Implant Type		
Knee	1.00	
Hip	0.96 (0.82–0.95)	0.351
Revision Hospital		
Teaching	1.00	
Community	0.92 (0.73–0.86)	0.047

Table 3. Clinical and demographic summary for the 530 hips selected for corrosion analysis. As complete clinical details were not available for the entire study population, percentages are represented inclusive of missing data.

Variable	PJI Cases (n = 120)	Non-PJI Controls (n = 410)
Time *in situ* (years), mean (SD)	2.84 (4.79)	6.01 (5.93)
Age (years), mean (SD)	54.6 (14.3)	58.4 (13.7)
Sex, *n* (%)		
Male	62 (51.7%)	205 (50.0%)
Female	58 (48.3%)	198 (48.3%)
Race, *n* (%)		
White	82 (68.3%)	301 (73.4%)
Other	34 (17.0%)	80 (19.5%)
Index Surgery, *n* (%)		
Revision	45 (37.5%)	63 (15.4%)
Primary	43 (35.8%)	256 (62.4%)

Table 4. Results from the adjusted corrosion analysis. A multivariable logistic regression model was used to calculate the odds for significant corrosion (corrosion score >2).

Variable	OR (95% CI)	p-value
PJI Diagnosis		
Yes	1.00	
No	1.15 (0.85–1.58)	0.645
Sex		
Female	1.00	
Male	1.44 (1.26–1.64)	0.006
Index Surgery		
Revision	1.00	
Primary	1.35 (1.26–1.64)	0.034

1.5 Discussion

Large-scale retrieval analysis results from an interdisciplinary effort that can link engineering evaluation with epidemiological assessment, and may provide insights into the *in vivo* behavior of implants. In this study using several thousand retrievals, we identified age, sex, BMI, previous revision surgery, and hospital type as risk factors for infection, consistent with the population-level findings of clinical and administrative database investigations[13-22]. In light of the increased number of corrosion-related reports in THRs and the proposed link

between inflammation and corrosion, we also assessed the association between peri-prosthetic joint infection and modular taper corrosion. Our results do not support the hypothesis that increased immune activity is associated with greater corrosion damage.

Given the projected increase in the number of THAs and TKAs through the next decade, retrieval analysis presents tremendous value for identifying factors that threaten the lifetime of orthopedic implants[10,23]. Like most retrieval studies however, the current investigation is limited by the selection bias imposed by the available collaborating surgical sites. Another limitation is the diagnosis for PJI as a proxy for immune system activity. Although the clinical summaries we used provided a diagnosis of PJI at the time of revision, no information on the latency period of the infection was available; the length of time that the implant was exposed to the infected environment is therefore unknown. Additionally, this analysis does not consider a number of implant design variables that may have an effect on taper corrosion (this limitation will be addressed in the next chapter). Nevertheless, the current retrieval study represents a unique investigation of PJI and taper corrosion, using a relatively large sample of clinical explants. Furthermore, it highlights an opportunity to increase the number of partnering hospitals and encourages collaborative activity between other implant retrieval centers.

As a known threat to the longevity of TJRs, PJI remains an opportunity for improvement within the field of arthroplasty. Of the >1 million hip and knee replacement surgeries that are performed every year, about 27,000 are revised for

PJI, and this is expected to increase through 2030[24]. The univariate results from the current study identified TKRs to have a greater hazard of revision for infection, compared to THRs. The hazard ratio was found to be time-dependent, increasing from 2.1 at five years to more than 4 at ten years. This differential in the infection risk between the two procedures was reflected in the most recent report by the Australian Orthopaedic Association National Joint Replacement Registry, which summarized that infection causes 23% of TKR revisions and 18% of THR revisions[25]. Additionally, Kurtz *et al.* reported a slightly greater incidence of infections (as a percentage of the total number of surgeries) for knees (2.05%) compared to hips (1.99%) in the United States, using the Nationwide Inpatient Sample (NIS)[24]. With consideration of reducing this burden, the effect of material selection was identified by population-based registry studies which reported lower infection rates for hip devices featuring a ceramic (vs. UHMWPE) acetabular liner[26,27]. While the use of ceramics in TKRs is still fairly limited, the increased hazard for infection in knees may illuminate an opportunity to incorporate more infection-resistant materials in TKRs. In the adjusted analysis, revision index surgery was found to have the strongest effect on the hazard of infection. Having at least one previous revision surgery increased the hazard for PJI by 200% in an investigation by Bongartz *et al.* and a greater infection risk with surgical re-entry for joint replacements has been reported by a number of clinical observations[13-15]. Additionally, we found that increased age and being male were significant risk factors for a revision due to infection. Two independent studies found that patients older than 74 have an increased risk of PJI (compared with 55-74 year olds) and Dowsey *et al.* reported that men were almost 6 times more likely than women to develop joint infection after having a primary TKR[16-18]. While

a number of studies have highlighted that obese TJR patients have a greater incidence of infection as well as higher complication and readmission rates, we identified being underweight (vs. overweight) as a significant risk factor for infection in the current analysis[28-31]. Underweight patients have been reported to have 24% lower postoperative functional health scores than those of normal weight, and have also been identified as having an increased risk of infection for TKR, as well as for TJR in patients with rheumatoid arthritis[20-22]. Lastly, we identified revision at a teaching hospital as a risk for infection, similar to the findings of Kurtz *et al.* which used the NIS database[19]. However, it was noted in that study that the trend is likely attributed to the treatment pattern for revisions, as the index surgery could have been performed at a different institution. Our identification of risk groups consistent with trends observed in the national population lends support to the opinion that our retrieval sample may be useful for insights into population-level behaviors. However, it should be noted that the current dataset skews away from some of the identified risk groups (the majority of retrievals were implanted during a primary surgery and obtained from patients who were female). Despite its considerable costs and deleterious effects, PJI remains a fairly rare outcome for all THAs; the effects of potential artifacts from the available data therefore warrant elucidation with additional retrieval studies.

Although the use of modular components in THRs had become a popular design option by the early 1990s, concerns about fretting and crevice corrosion at the modular taper junction eventually arose[12,32-36]. In light of findings that retrievals with substantially worn taper junctions exhibit adverse local tissue reactions

(ALTRs) such as pseudotumors and tissue necrosis, it has been surmised that an inflammatory and/or immune response arises in some patients as a result of adverse reactions to metal debris, caused by the processes involved in mechanically assisted corrosion[3,35,37-40]. It is still unclear why some patients respond to the presence of elevated exposure to metal debris, while others do not[7]. Additionally, the clinical relevance of the interaction between taper corrosion and immune system activity remains somewhat elusive. While laboratory studies have shown that inflammatory secretions can cause corrosion, it has also been proposed that corrosion sites on spinal implants may attract bacteria cells, leading to an increased risk of infection via hematogenous seeding[35,7,41,42]. Clinical data on the immunomodulatory behavior of metal debris in THA remains fairly limited but registry reports suggest that a reduction in the amount of polyethylene wear debris decreases the likelihood of peri-prosthetic joint infection[43]. In the current study, we were unable to identify an association between PJI and corrosion severity. Thus, our results do not provide evidence in support of corrosion's immunological origins or implications. However, we were able to identify gender and primary implant surgery to be risk factors for severe corrosion. Increased corrosion for these populations is consistent with men having greater body weight (the effect of which will be observed in the next sub-chapter) and primary surgeries tending to have longer in situ periods, which allows more time for corrosion mechanisms to have pernicious effects[12,44].

While the current study does not confirm the proposed link between corrosion severity and infection, its corroboration of population-level findings for PJI supports the incorporation of large-scale retrieval studies into surveillance

initiatives like national orthopedic implant registries. The 21st Century Cures Act defines real world evidence (RWE) as data on the usage, or the potential benefits or risks, of a drug derived from sources other than randomized clinical trials[8]. Although this regulation was enacted with a focus on drugs, the potential for RWE in medical devices has been demonstrated by the use of smartwatches to detect atrial fibrillation[45-47]. As material and design changes for implantable devices can be expected to continue, retrieval analysis appears to provide an opportunity to monitor the real world implications of developing technologies.

References

1. Lam V, Teutsch S, Fielding J. Hip and knee replacements: a neglected potential savings opportunity. *Jama.* 2018;319(10):977-978.

2. Bozic KJ, Kurtz SM, Lau E, Ong K, Vail TP, Berry DJ. The epidemiology of revision total hip arthroplasty in the United States. *JBJS.* 2009;91(1):128-133.

3. Langton DJ, Jameson SS, Joyce TJ, et al. Accelerating failure rate of the ASR total hip replacement. *J Bone Joint Surg Br.* 2011;93(8):1011-1016.

4. Hall DJ, Pourzal R, Lundberg HJ, Mathew MT, Jacobs JJ, Urban RM. Mechanical, chemical and biological damage modes within head‐neck tapers of CoCrMo and Ti6Al4V contemporary hip replacements. *Journal of Biomedical Materials Research Part B: Applied Biomaterials.* 2018;106(5):1672-1685.

5. Liu Y, Gilbert JL. The effect of simulated inflammatory conditions and Fenton chemistry on the electrochemistry of CoCrMo alloy. *Journal of Biomedical Materials Research Part B: Applied Biomaterials.* 2018;106(1):209-220.

6. Henson P. Mechanisms of exocytosis in phagocytic inflammatory cells. Parke-Davis Award Lecture. *The American journal of pathology.* 1980;101(3):494.

7. Gilbert JL, Sivan S, Liu Y, Kocagöz SB, Arnholt CM, Kurtz SM. Direct in vivo inflammatory cell‐induced corrosion of CoCrMo alloy orthopedic implant surfaces. *Journal of Biomedical Materials Research Part A.* 2015;103(1):211-223.

8. Congress U. 21st Century Cures Act. Paper presented at: 114th Congress2016.

9. Jones LC, Tsao AK, Topoleski LT. Orthopedic implant retrieval and failure analysis. *Degradation of Implant Materials*: Springer; 2012:393-447.

10. Collier JP. The value of spine implant retrieval analysis. LWW; 2008.

11. Szolwinski MP, Farris TN. Mechanics of fretting fatigue crack formation. *Wear.* 1996;198(1-2):93-107.

12. Gilbert JL, Buckley CA, Jacobs JJ. In vivo corrosion of modular hip prosthesis components in mixed and similar metal combinations. The effect of crevice, stress, motion, and alloy coupling. *Journal of biomedical materials research.* 1993;27(12):1533-1544.

13. Bongartz T, Halligan CS, Osmon DR, et al. Incidence and risk factors of prosthetic joint infection after total hip or knee replacement in patients with rheumatoid arthritis. *Arthritis Care & Research.* 2008;59(12):1713-1720.

14. Poss R, Thornhill TS, Ewald FC, Thomas WH, Batte NJ, Sledge CB. Factors influencing the incidence and outcome of infection following total joint arthroplasty. *Clinical orthopaedics and related research.* 1984(182):117-126.

15. Fitzgerald JR, Sturdevant DE, Mackie SM, Gill SR, Musser JM. Evolutionary genomics of Staphylococcus aureus: insights into the origin of methicillin-resistant strains and the toxic shock syndrome epidemic. *Proceedings of the National Academy of Sciences.* 2001;98(15):8821-8826.

16. Dowsey MM, Choong PF. Obese diabetic patients are at substantial risk for deep infection after primary TKA. *Clinical Orthopaedics and Related Research®.* 2009;467(6):1577-1581.

17. SooHoo NF, Farng E, Lieberman JR, Chambers L, Zingmond DS. Factors that predict short-term complication rates after total hip arthroplasty. *Clinical Orthopaedics and Related Research®.* 2010;468(9):2363-2371.

18. Kurtz SM, Lau E, Schmier J, Ong KL, Zhao K, Parvizi J. Infection burden for hip and knee arthroplasty in the United States. *The Journal of arthroplasty.* 2008;23(7):984-991.

19. Kurtz S, Lau E, Schmier J, Parvizi J, Halpern M. Nationwide infection burden in revision hip and knee arthroplasty. *Trans Orthop Res Soc.* 2006;31:179.

20. Sanmartin C, McGrail K, Dunbar M, Bohm E. Using population data to measure outcomes of care: the case of hip and knee replacements. *Health reports.* 2010;21(2):23.

21. Manrique J, Chen AF, Gomez MM, Maltenfort MG, Hozack WJ. Surgical site infection and transfusion rates are higher in underweight total knee arthroplasty patients. *Arthroplasty today.* 2017;3(1):57-60.

22. Somayaji R, Barnabe C, Martin L. Risk factors for infection following total joint arthroplasty in rheumatoid arthritis. *The open rheumatology journal.* 2013;7:119.

23. Kurtz S, Ong K, Lau E, Mowat F, Halpern M. Projections of primary and revision hip and knee arthroplasty in the United States from 2005 to 2030. *J Bone Joint Surg Am.* 2007;89(4):780-785.

24. Kurtz SM, Lau E, Watson H, Schmier JK, Parvizi J. Economic burden of periprosthetic joint infection in the United States. *The Journal of arthroplasty.* 2012;27(8):61-65. e61.

25. Registry TAOANJR. Annual Report 2019. 2019.

26. Graves S, Lorimer M, Bragdon C, Muratoglu O, Malchau H. Reduced risk of revision for infection when a ceramic bearing surface is used. Paper presented at: Orthopaedic Proceedings2016.

27. Pitto RP, Sedel L. Periprosthetic joint infection in hip arthroplasty: is there an association between infection and bearing surface type? *Clinical Orthopaedics and Related Research®.* 2016;474(10):2213-2218.

28. Saucedo JM, Marecek GS, Wanke TR, Lee J, Stulberg SD, Puri L. Understanding readmission after primary total hip and knee arthroplasty: who's at risk? *The Journal of arthroplasty.* 2014;29(2):256-260.

29. Zhang Z-j, Kang Y, Zhang Z-q, et al. The influence of body mass index on life quality and clinical improvement after total hip arthroplasty. *Journal of Orthopaedic Science.* 2012;17(3):219-225.

30. Wolfe F, Michaud K. Effect of body mass index on mortality and clinical status in rheumatoid arthritis. *Arthritis care & research.* 2012;64(10):1471-1479.

31. Lash H, Hooper G, Hooper N, Frampton C. Should a patients BMI status be used to restrict access to total hip and knee arthroplasty? functional outcomes of arthroplasty relative to BMI-single centre retrospective review. *The open orthopaedics journal.* 2013;7:594.

32. Collier J, Surprenant VA, Jensen RE, Mayor MB. Corrosion at the interface of cobalt-alloy heads on titanium-alloy stems. *Clinical orthopaedics and related research.* 1991(271):305-312.

33. Goldberg JR, Gilbert JL, Jacobs JJ, Bauer TW, Paprosky W, Leurgans S. A multicenter retrieval study of the taper interfaces of modular hip prostheses. *Clinical orthopaedics and related research.* 2002;401:149-161.

34. Goldberg JR, Gilbert JL. In vitro corrosion testing of modular hip tapers. *Journal of Biomedical Materials Research Part B: Applied Biomaterials.* 2003;64B(2):78-93.

35. Cooper HJ, Della Valle CJ, Berger RA, et al. Corrosion at the head-neck taper as a cause for adverse local tissue reactions after total hip arthroplasty. *The Journal of bone and joint surgery American volume.* 2012;94(18):1655.

36. Collier JP, Mayor MB, Jensen RE, et al. Mechanisms of failure of modular prostheses. *Clinical orthopaedics and related research.* 1992(285):129-139.

37. Gill I, Webb J, Sloan K, Beaver R. Corrosion at the neck-stem junction as a cause of metal ion release and pseudotumour formation. *The Journal of bone and joint surgery British volume.* 2012;94(7):895-900.

38. Lindgren J, Brismar B, Wikstrom A. Adverse reaction to metal release from a modular metal-on-polyethylene hip prosthesis. *The Journal of bone and joint surgery British volume.* 2011;93(10):1427-1430.

39. Hallab NJ, Jacobs JJ. Biologic effects of implant debris. *Bulletin of the NYU hospital for joint diseases.* 2009;67(2):182.

40. Jacobs JJ, Hallab NJ, Urban RM, Wimmer MA. Wear particles. *JBJS.* 2006;88(suppl_2):99-102.

41. del Rio J, Beguiristain J, Duart J. Metal levels in corrosion of spinal implants. *European Spine Journal.* 2007;16(7):1055-1061.

42. Beguiristain J, Del Rio J, Duart J, Barroso J, Silva A, Villas C. Corrosion and late infection causing delayed paraparesis after spinal instrumentation. *Journal of Pediatric Orthopaedics B.* 2006;15(5):320-323.

43. Vertullo CJ, Lewis PL, Peng Y, Graves SE, de Steiger RN. The effect of alternative bearing surfaces on the risk of revision due to infection in

minimally stabilized total knee replacement: an analysis of 326,603 prostheses from the australian orthopaedic association national joint replacement registry. *JBJS.* 2018;100(2):115-123.

44. Higgs GB, Hanzlik JA, MacDonald DW, Gilbert JL, Rimnac CM, Kurtz SM. Is Increased Modularity Associated With Increased Fretting and Corrosion Damage in Metal-On-Metal Total Hip Arthroplasty Devices?: A Retrieval Study. *The Journal of arthroplasty.* 2013;28(8):2-6.

45. Bumgarner JM, Lambert CT, Hussein AA, et al. Smartwatch algorithm for automated detection of atrial fibrillation. *Journal of the American College of Cardiology.* 2018;71(21):2381-2388.

46. Tison GH, Sanchez JM, Ballinger B, et al. Passive detection of atrial fibrillation using a commercially available smartwatch. *JAMA cardiology.* 2018;3(5):409-416.

47. Krivoshei L, Weber S, Burkard T, et al. Smart detection of atrial fibrillation. *Europace.* 2016;19(5):753-757.

II. Clinical and Design Factors Impacting In Vivo Corrosion of Modular Head-Neck Tapers

2.1 Abstract

Taper design has been identified as a possible contributor to fretting corrosion damage at modular connections in THA systems, but variations in as-manufactured taper interfaces may confound this analysis. This study characterizes taper damage in retrievals of two different taper sizes with comparable taper surface finishes and investigates if fretting and corrosion damage is related to taper design in the context of a multivariable analysis for metal-on-polyethylene bearings. 252 CoCrMo femoral heads were identified in a collection of retrievals: 77 with Taper A and 175 with Taper B. Implantation time averaged 5.4 ± 6.0 years (range, 0–26 years). Explants were cleaned and analyzed using a 4-point semi-quantitative method. Clinical and device factors related to head taper fretting corrosion damage were assessed using ordinal logistic regression with forward stepwise control. Components were then selected to create two balanced cohorts, matched on the significant variables from the multivariable analysis. We found that increased head offsets ($p<0.001$), longer implantation times ($p=0.002$), heavier patients ($p<0.001$) and more flexible tapers ($p<0.001$), were associated with increased taper fretting and corrosion damage. When damage scores were compared between the balanced groups, no differences were found. These results suggest that fretting and corrosion damage is insensitive to differences in taper size. The final model derived explains almost

half of the fretting corrosion damage we observed and identifies contributing factors that are consistent with other *in vitro* and retrieval studies.

2.2 Introduction

There is considerable interest within the orthopedic community in understanding the multifactorial process of modular component fretting corrosion in total hip arthroplasty (THA). Previous studies analyzing surgically retrieved hip devices have identified some patient and device factors associated with *in vivo* taper damage, including length of implantation, stem flexural rigidity, and head offset[1-5]. The increased incidence of taper-related complications in THA has also been attributed to the evolution of taper design[6]. Among implant manufacturers, there has been a trend toward more narrow and shorter stem designs to achieve increased range of motion, along with decreased risk of impingement and dislocation[7]. However, these design changes have been hypothesized to affect taper damage, as a smaller contact area may increase stress within the taper. Taper fretting corrosion is understood to be a synergistic mechanical and electrochemical phenomenon; thus, an increased localized stress that makes passive oxide film fracture more likely, may be favorable to corrosion[8].

Understanding the effect of smaller trunnions is complicated, as size is often not the only variable that can change between designs. In an experimental study that measured the taper angle of retrieved THA devices, commonly used taper options had angles of 4º, 5.6º and 6º [9]. Additionally, taper surface finish may also vary, as some contemporary trunnions incorporate surface ridges in an effort to

improve the fracture strength of a ceramic head[10]. These ridges deform when the ceramic head is impacted to provide a stress distribution that is favorable to the ceramic material given the design of the femoral head. However, these ridges have also been shown to leave imprints within metal heads via localized corrosion mechanisms [10].

The purpose of this study was to identify the effect that taper size has on taper damage while controlling for other variations in taper design. From a single manufacturer (Stryker Orthopaedics, Mahwah, NJ), we identified two different taper sizes, fashioned with similar taper angles and comparable surface finishes. The C-Taper is based on the 12/14 Euro taper design, whereas the V40 was designed with an 8% shorter taper and approximately 20% less surface area (Figure 4), but with a similar taper angle of 5° 40′. In this study, we sought to determine if there is a difference in taper fretting and corrosion damage between these two taper sizes. To test this, we analyzed a consecutive series of explanted components retrieved over a 9-year period by performing a review of the clinical records associated with the devices, combined with a semi-quantitative evaluation of the modular taper interfaces. We assessed the difference in damage using a multifactorial approach, controlling for other design and clinical factors that might affect taper damage. Thus, the preliminary goal of this study was to identify which factors are associated with taper damage in these devices.
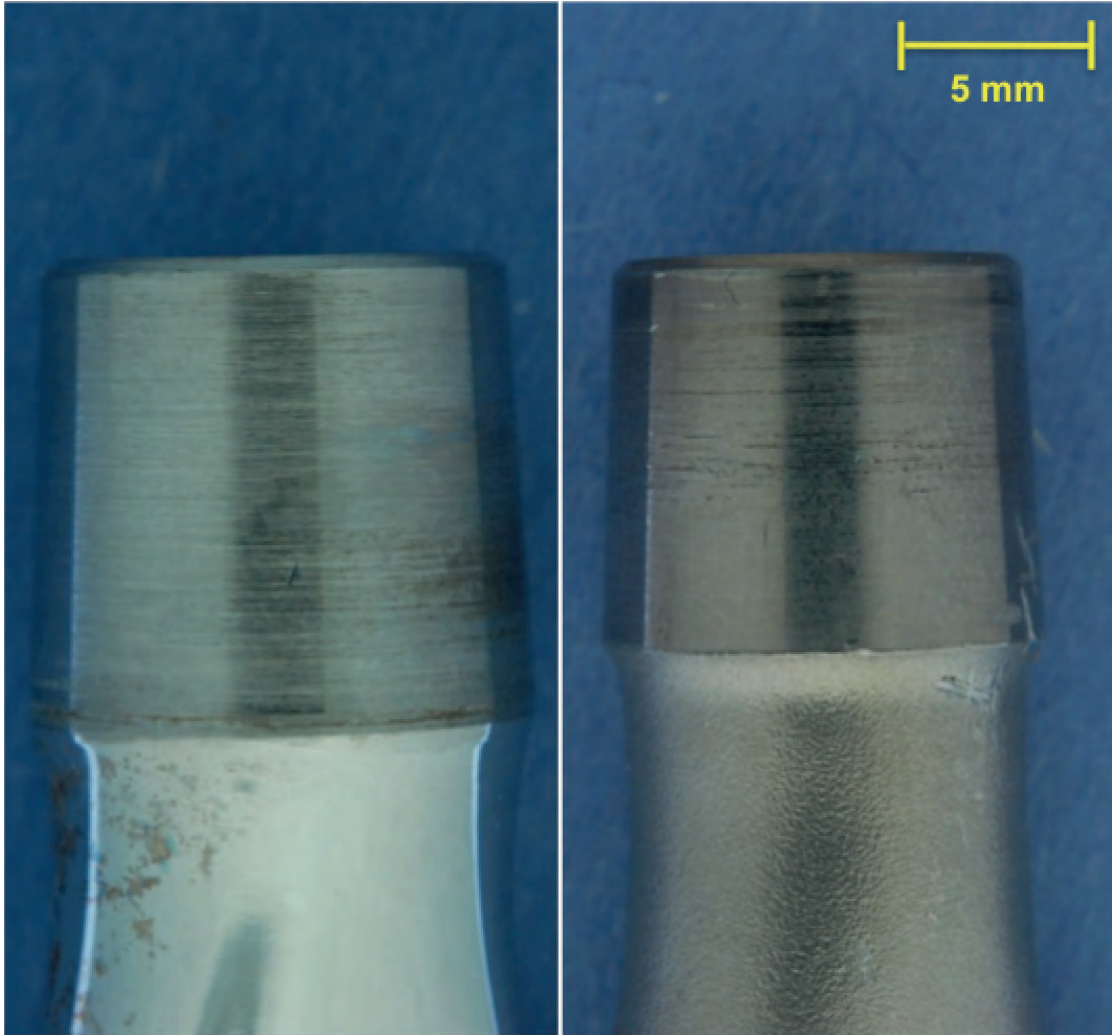
Figure 4. Comparison of the Taper A (left) and Taper B (right) designs at the same magnification

2.3 Methods

<u>Clinical and Implant Information</u>

Overall, 252 cobalt chromium (CoCrMo) femoral heads manufactured by Stryker Orthopaedics, were identified as either C-Taper or V40 from a collection of devices within a multi-institutional retrieval program. The retrieved metal-on-polyethylene (MoPE) systems were collected under an IRB-approved multi-

institutional implant retrieval program. Of the retrieved heads, 77 were C-Taper and 175 were V40. The alloy composition of the retrieved devices was confirmed using x-ray fluorescence (Niton XL3; Thermo Scientific, Waltham, Massachusetts). In cases where the femoral component was not received, stem designs were determined from radiographs and operative reports. Information on the stem material was available for 45 C-Taper devices (CoCrMo, n=18; Ti6Al4V, n=27) and 140 V40 devices (CoCrMo, n=32; Ti6Al4V, n=19; TMZF, n=53). In addition to the retrieved components, clinical information inclusive of age, gender, reason for implant revision, and length of implantation was collected for the devices (Table 5). The mean length of implantation was 5.4 ± 6.0 years (range, 0 to 26 years) and the mean patient age at implantation was 60 ± 14.3 years (range, 13 to 87 years).

Table 5. Clinical and device information corresponding to the 252 retrieved components.

Patient Summary		Device Details	
Patients		Number of Systems	252
Male	117		
Female	129	Taper A	45
Mean Age at	$60 \pm 14 \ (13 - 80)$	w/ CoCrMo Stem	18
Implantation	years	w/ Ti-6Al-4V Stem	27
Mean Time *in situ*	$5.4 \pm 6 \ (0 - 26)$ years	Taper B	104
		w/ CoCrMo Stem	32
		w/ Ti-6Al-4V Stem	19
		w/ TMZF Stem	53

Taper Damage Evaluation

All implants were cleaned by two 20-minute soaks in a 1:10 ratio of disinfecting solution (Discide®; AliMed, Dedham, Massachusetts) followed by two 30-minute

sonication periods in water. A soft nylon brush was used to help remove biological films and loose debris. Fretting and corrosion damage of the head taper was characterized using a previously described 4-point, semi-quantitative scoring system [12]. In this system, a score of 1 is assigned when the damage is considered minimal and corresponds to fretting damage occurring on less than 10% of the surface with no pronounced evidence of corrosion. A score of a 2 indicates mild damage where either more than 10% of the surface has fretting damage or there is corrosion attack confined to small areas. A score of a 3 reflects moderate damage where more than 30% of the surface has fretting damage or localized corrosion attack. A score of 4 corresponds to severe damage over the majority of the taper (>50%) with abundant corrosion debris. Irregular, acute artifacts on the surface were considered iatrogenic damage and excluded from the taper damage assessment. In an effort to achieve a consistent methodology, all components were scored in random order by three trained investigators who were initially blind to the scores of the others. In the case of discrepancies, the three scorers convened to arrive at a final score, under the supervision of the senior author. In cases where the femoral component was available, calipers were used to determine taper dimensions. The stem femoral neck taper diameter was obtained at the distal point of engagement with the femoral head when apparent, or at the distal end of the femoral stem taper in cases where the entire taper was engaged. The flexural rigidity of the taper was then calculated by multiplying the second moment of area by the elastic modulus[1].

Statistical Analysis

Clinical and device factors related to head taper fretting corrosion damage were assessed using ordinal logistic regression. Variables that have been suggested to have an effect on taper fretting corrosion damage were considered: patient age, gender, height, weight, and University of California Los Angeles (UCLA) activity score, along with head taper design (C-Taper vs. V40), head offset, head size, taper flexural rigidity, and length of implantation. First, an overall test of the statistical significance for all the predictor variables together was conducted with a standard regression model. Then, a model comprising a subset of predictor variables that explained the response variable (head taper fretting corrosion) most parsimoniously was derived using stepwise regression with forward selection and an entry threshold of $p<0.05$. The Bayesian information criterion (BIC) was used to assess the quality of each stepwise model and the final model was confirmed to have the lowest BIC value. Odds ratios (OR) with a 95% confidence interval (CI) were calculated by exponentiating the parameter estimates of the final ordinal logistic regression model that used the identified predictor variables.

To further assess the effect of taper design, two cohorts comprised of twenty-three components of each taper type were created. Each C-Taper component was matched to a V40 component based on the significant predictor variables of the final regression model. Between the two cohorts, similarities in the matching variables were confirmed using the Wilcoxon Rank Sum Test, and the proportion of components at each damage score was compared using Fisher's Exact Test with Freeman-Halton extension. Statistical analyses were performed using SAS

9.3 and JMP 11.0 (SAS Institute, Inc., Cary, North Carolina) with a significance level of α = 0.05.

2.4 Results

Head taper fretting and corrosion damage ranging from minimal to severe was observed for both taper types (Figure 5). Mild to severe damage (score≥2) was observed on 55 of 77 (71%) of C-Taper heads and 141 of 175 (81%) of V40 heads. From the final stepwise regression model, head offset, length of implantation, patient weight and taper flexural rigidity were identified as significant predictors of increased taper fretting and corrosion damage (R2 = 0.40; p<0.001). Each additional millimeter of head offset was associated with a 20% increase in the odds of a higher damage score (OR, 0.80; 95% CI, 0.72–0.88) (p<0.001). The odds of greater taper damage increased by 13% for each year the component was in situ (OR, 0.87; 95% CI, 0.79–0.95) (p=0.002). For each additional pound of patient weight, the associated elevation in the odds of increased damage was 1% (OR, 0.99; 95% CI, 0.98–0.99) (p<0.001). Stiff tapers exhibited less damage; each unit increase in flexural rigidity (x109 N□m2) was associated with a decrease of 1% in the odds of a higher damage score (OR, 1.01; 95% CI, 1.00–1.01) (p<0.001). As a guide for context, flexural rigidity ranged from 84.5–402.6 x109 N□m2 for tapers in this study. Taper size (C-Taper or V40) was not found to have an effect on head fretting and corrosion damage (p=0.21).
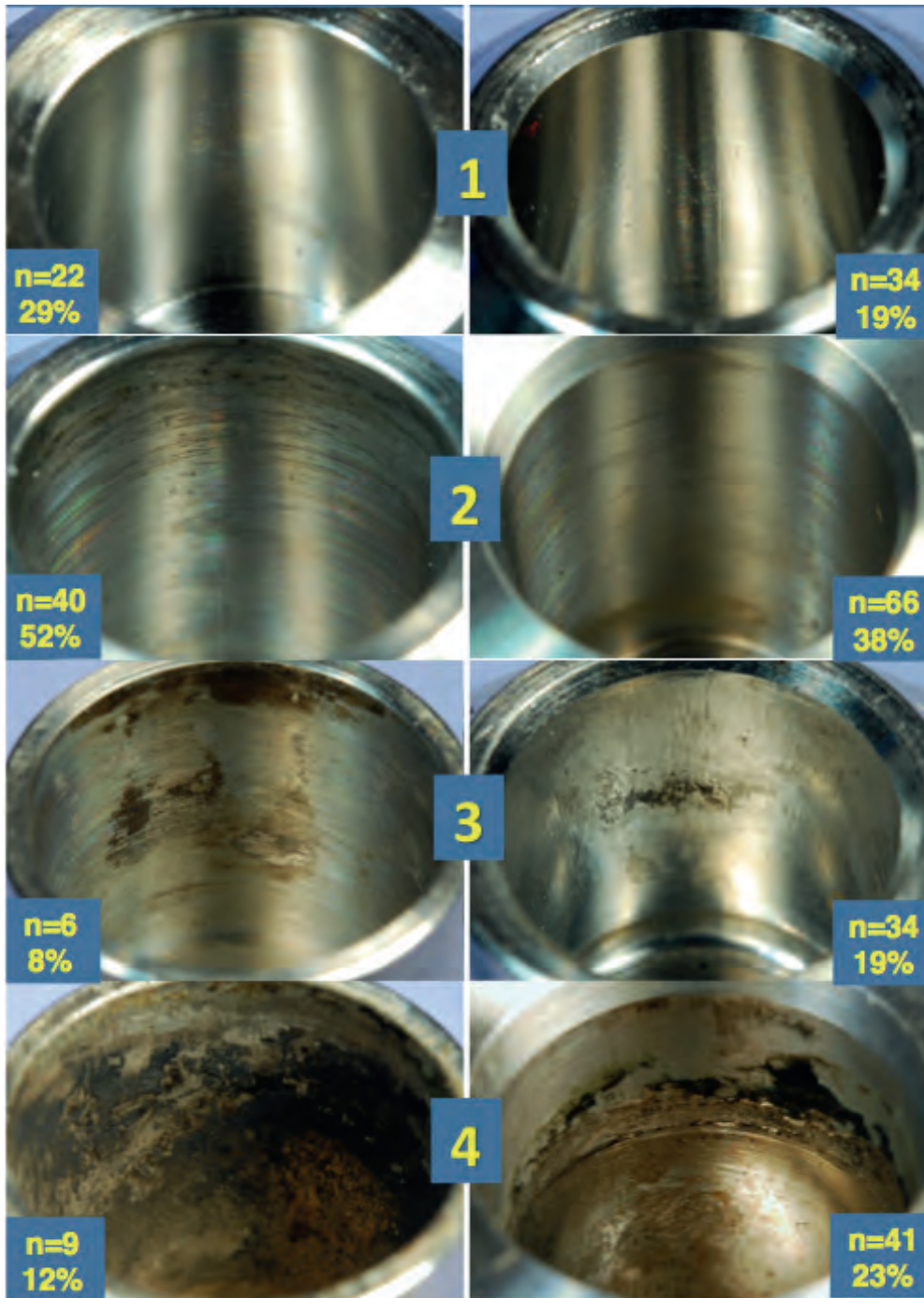
Figure 5. Photographs showing the distribution taper damage categories at the head taper, by taper design.

In the matched cohort analysis, both groups were confirmed to have similar values for head offset, length of implantation, stem material (based on flexural rigidity finding), and patient weight (Table 6). No difference was found in head fretting and corrosion damage scores (median score = 2 for both cohorts; p = 0.09) between the two taper groups (Figure 6).

Table 6. Comparison of variables between the two matched cohorts.

Variable	Taper A	Taper B	p-value
Head Offset (mm)	5.0 ± 3.6	3.5 ± 4.1	0.09
Time *in situ* (years)	6.5 ± 6.1	4.8 ± 4.4	0.11
Weight (lbs)	176 ± 53	180 ± 54	0.32
Stem Material			
CoCrMo	11/23 = 48%	11/23 = 48%	--
Ti Alloy	12/23 = 52%	12/23 = 52%	--
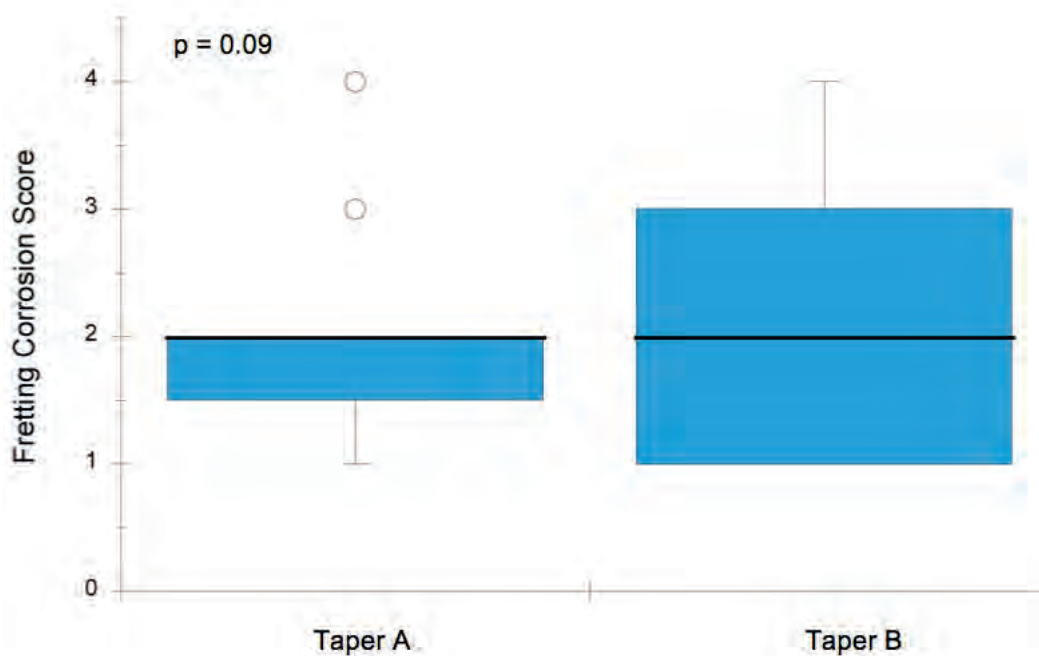
Figure 6. Box plot showing the variation in femoral head damage score between the two matched cohorts (n=23 for each cohort)

2.5 Discussion

Fretting corrosion at modular tapers in THA remains a clinical concern and a more thorough understanding of this multifactorial process is needed. While results from *in vitro* testing are useful, studying this phenomenon in surgically retrieved components allows for clinically relevant insights to be gleaned. In this retrieval study, components of two taper sizes were assessed for taper damage using multivariable and subsequent matched cohort analysis techniques. While the effect of taper design on taper damage at the head-stem junction has been explored[7,9,11], the isolated effect of taper size from taper angle and surface finish has yet to be reported. To the authors' knowledge, this is also the first retrieval study to assess this effect while controlling for other device and clinical factors. The results of this study suggest that fretting and corrosion damage is insensitive to difference in taper size within this context. The final regression model explained 40% of the variation in taper damage and identified implantation time, material combination, and head offset as contributing factors. In addition to implant factors, we found patient weight to be a predictor of fretting corrosion damage in the retrieval series.

The clinical and design factors that we found as contributors to head fretting and corrosion damage were comparable to those of previous bench-top and retrieval studies. A larger head offset is associated with an increased bending moment and has been shown to result in higher fretting currents during electrochemical tests[12,13]. The observed effect of implantation time is consistent with the understanding that more time in situ permits further progression of the fretting corrosion phenomenon[1,3,7,8]. Increased patient weight is associated with increased

stress at the head-stem junction and its effect on taper damage has been previously identified using retrievals[3]. The observed trend with flexural rigidity is consistent with the theory that necks with higher stiffness will bend less and decrease the potential for fretting corrosion[1].

Our finding that taper size (C-Taper vs. V40) has no effect on taper damage in MoPE bearings may provide some clarification to the current disagreement in the literature. Some have suggested greater damage on smaller tapers in MoM bearings due to larger moments per unit area[6]. In their analysis of 43 MoPE explants comprising six designs, Tan *et al.* reported that the narrowest taper design had the highest damage scores[11]. That study however, had relatively small sample groups (n≤6 in most groups) and did not control for the effect of stem material, which has been repeatedly identified as a contributor to taper fretting corrosion[2,8,14,15]. Conversely, Nassif *et al.* reported higher damage scores on MoM tapers that were longer and with larger diameter[9]. However, that study noted heterogeneity in the material composition between the different taper types, and did not consider variations in implantation time, head offset or patient weight between groups.

We recognize some limitations of this study. First, the semi-quantitative evaluation that was used is liable to observer subjectivity and may not comprehensively characterize the amount of material loss or corrosion debris at these interfaces. Nevertheless, having the same three trained investigators examine all devices helped to maintain consistency. Furthermore, this scoring technique has been shown to correlate highly with quantitative methods

measuring volume loss[16,17]. Second, we only investigated two taper sizes from a single manufacturer. These two designs are a subset of contemporary taper options, and the applicability of these results to all taper sizes is unclear. Third, this study only investigated MoPE articulations and did not assess taper behavior in hard-on-hard bearing couples such as ceramic-on-ceramic (CoC) or metal-on-metal (MoM). This should be noted because edge loading and low clearances may influence taper damage in large head metal-on-metal devices, but these factors were beyond the scope of the present study[18].

The results of the current study do not support the hypothesis that fretting and corrosion damage is affected by the evolution in taper size from C-Taper to V40 when considered in the context of other predictor variables in MoPE bearings. Fretting and corrosion damage is a multifactorial phenomenon and it is important to identify significant effects while considering the contribution of potential confounding variables. The reduced model derived in this analysis suggests a subset of variables that may be considered in future efforts to mitigate fretting corrosion. Further investigation with additional designs and retrievals will be useful to better understand the effect of taper design on fretting corrosion in THRs.

References

1.   Goldberg JR, Gilbert JL, Jacobs JJ, Bauer TW, Paprosky W, Leurgans S. A multicenter retrieval study of the taper interfaces of modular hip prostheses. *Clinical orthopaedics and related research.* 2002;401:149-161.

2.   Higgs GB, Hanzlik JA, MacDonald DW, Gilbert JL, Rimnac CM, Kurtz SM. Is Increased Modularity Associated With Increased Fretting and Corrosion Damage in Metal-On-Metal Total Hip Arthroplasty Devices?: A Retrieval Study. *The Journal of arthroplasty.* 2013;28(8):2-6.

3.   Kurtz SM, Kocagöz SB, Hanzlik JA, et al. Do ceramic femoral heads reduce taper fretting corrosion in hip arthroplasty? A retrieval study. *Clinical Orthopaedics and Related Research®.* 2013;471(10):3270-3282.

4.   Porter DA, Urban RM, Jacobs JJ, Gilbert JL, Rodriguez JA, Cooper HJ. Modern trunnions are more flexible: a mechanical analysis of THA taper designs. *Clinical Orthopaedics and Related Research®.* 2014;472(12):3963-3970.

5.   Lieberman JR, Rimnac CM, Garvin KL, Klein RW, Salvati EA. An analysis of the head-neck taper interface in retrieved hip prostheses. *Clinical orthopaedics and related research.* 1994;300:162-167.

6.   Langton D, Sidaginamale R, Lord J, Nargol A, Joyce T. Taper junction failure in large-diameter metal-on-metal bearings. *Bone and Joint Research.* 2012;1(4):56-63.

7.   Esposito CI, Wright TM, Goodman SB, Berry DJ. What is the Trouble With Trunnions? *Clinical Orthopaedics and Related Research®.* 2014;472(12):3652-3658.

8.   Gilbert JL, Buckley CA, Jacobs JJ. In vivo corrosion of modular hip prosthesis components in mixed and similar metal combinations. The effect of crevice, stress, motion, and alloy coupling. *Journal of biomedical materials research.* 1993;27(12):1533-1544.

9.   Nassif NA, Nawabi DH, Stoner K, Elpers M, Wright T, Padgett DE. Taper design affects failure of large-head metal-on-metal total hip replacements. *Clinical Orthopaedics and Related Research®.* 2014;472(2):564-571.

10.   Panagiotidou A, Meswania J, Hua J, Muirhead-Allwood S, Hart A, Blunn G. Enhanced wear and corrosion in modular tapers in total hip replacement is associated with the contact area and surface topography. *Journal of Orthopaedic Research.* 2013;31(12):2032-2039.

11.   Tan SC, Teeter MG, Del Balso C, Howard JL, Lanting BA. Effect of Taper Design on Trunnionosis in Metal on Polyethylene Total Hip Arthroplasty. *The Journal of arthroplasty.* 2015.

12.   Brown SA, Abera A, D'Onofrio M, Flemming C. Effects of neck extension, coverage and frequency on the fretting corrosion of modular THR bore and cone interface. *Modularity of Orthopedic Implants ASTM Special Technical Publication.* 1997;1301:189-198.

13. Gilbert JL, Mehta M, Pinder B. Fretting crevice corrosion of stainless steel stem–CoCr femoral head connections: Comparisons of materials, initial moisture, and offset length. *Journal of Biomedical Materials Research Part B: Applied Biomaterials.* 2009;88B(1):162-173.

14. Meyer H, Mueller T, Goldau G, Chamaon K, Ruetschi M, Lohmann CH. Corrosion at the cone/taper interface leads to failure of large-diameter metal-on-metal total hip arthroplasties. *Clinical Orthopaedics and Related Research®.* 2012;470(11):3101-3108.

15. Goldberg JR, Gilbert JL. In vitro corrosion testing of modular hip tapers. *Journal of Biomedical Materials Research Part B: Applied Biomaterials.* 2003;64B(2):78-93.

16. Hothi H, Matthies AK, Berber R, et al. The reproducibility of a semi-quantitative scoring method for taper corrosion and fretting, and its usefulness for predicting the volume of material loss. 2014.

17. Kocagoz SB UR, MacDonald DM, Gilbert JL, Kurtz SM. . Ceramic Heads Decrease Metal Release Caused by Head-Taper Fretting and Corrosion. . *Clin Orthop Relat Res* 2015, In Review.

18. Underwood RJ, Zografos A, Sayles RS, Hart A, Cann P. Edge loading in metal-on-metal hips: low clearance is a new risk factor. *Proceedings of the Institution of Mechanical Engineers, Part H: Journal of Engineering in Medicine.* 2012:0954411911431397.

III. Effect of Corrosion Severity on Connection Strength in Retrieved Modular Head-Neck Tapers

3.1 Abstract

Taper corrosion has been suggested as a possible contributor to *in vivo* disassociation of modular connections in total hip arthroplasty (THA) systems, but this relationship has not been explored experimentally. This study assessed whether *in vivo* taper corrosion decreases the strength of the head-stem connection, and compared these taper characteristics between clinically revised devices and cadaver retrievals. One hundred nine (109) femoral stems retrieved with an attached cobalt-chrome (CoCr) head were identified in a collection of THA retrievals: 93 from revision surgery and 16 from cadaver donors. After the explants were cleaned, the force used to disassemble each head-stem pair was recorded using a mechanical test frame with custom fixtures in accordance with ISO 7206-10. Taper corrosion was assessed using a 4-point semi-quantitative method. Femoral disassembly force was positively associated with stem taper damage (rho=0.26, p=0.007) but not significantly related to head taper damage (rho=0.14, p=0.153). There was no difference in femoral disassembly force between revision and cadaver retrievals. Revision retrievals exhibited greater damage than cadaver retrievals at both the head (OR=0.23, p=0.002) and stem (OR=0.06, p=0.001) tapers. The results of the present study do not support the hypothesis that corrosion weakens the taper junction between the head and stem of modular femoral components. Our findings from the taper damage

assessment of cadaver controls may suggest a greater prevalence of corrosion in components requiring revision surgery.

3.2 Introduction

Modular components in total hip arthroplasty devices (THAs) allow surgeons to effectively accommodate an individual patient's anatomy with a reduced implant inventory. Additionally, selective revision of malfunctioning modular components permits well-functioning fixed components to be retained, potentially reducing operation time and patient risk during revision surgery[1]. When loaded *in vivo*, implants experience fretting and corrosion at these mechanical junctions which then serve as potential sources of metal release[2]. In this regard, the modular interfaces may release metal ions and other metallic corrosion products that have been shown to have deleterious local and systemic effects[3,4]. In a recent device retrieval study involving THA devices that were revised for adverse local tissue reaction (ALTR), all had well-functioning bearing surfaces but substantially damaged metallic modular junctions[5]. Corrosion has also been shown to negatively affect the mechanical strength of femoral stems. Investigations reporting fatigue fracture of femoral stems have identified severe corrosion on the failed retrievals[6,7]. Fractures at the grain boundaries of the microstructure may result, in part, from intergranular corrosive attack initiated at the head-stem taper[6].

During a hip arthroplasty, the surgeon assembles the modular femoral head onto a stem via a tapered connection[8-10]. There are variations in the technique used to intraoperatively engage the femoral head with the stem: in some cases, the head

is manually pushed onto the stem, while in others, the head is impacted using a variety of hammer blows[11,12]. Though rare, *in vivo* dissociation of the femoral head from the stem has been reported[13-17]. The risk for this occurrence has been mitigated using standard test procedures such as ISO 7206-10, which measure the axial loads required to separate assembled connections[18]. Bench-top studies employing these methods have found that these disassembly forces are linearly related to the assembly force[12,19]. Mean disassembly force relative to the assembly force has been reported to range between 44% and 64% depending on material combination and taper geometry[12]. Thus, disassembly force measurements are being used as an indirect metric for taper strength.

Currently, little is known about how *in vivo* taper corrosion influences the strength of the taper interlock. It has been proposed that severe corrosion may compromise the taper interface and lead to loosening or disassociation of a modular junction[14,16], but this relationship has not been explored experimentally. In this study, we asked: does taper damage decrease the strength of the modular connection between a femoral head and stem? To account for potential confounding, we also sought to determine whether similar clinical and device variables were associated with taper damage and interface strength. These inquiries were assessed by analyzing a collection of intact femoral stems obtained from revision surgery and from cadaver donors. A secondary goal of this work was to answer the question: do the taper characteristics, with respect to corrosion and disassembly force, differ between components retrieved at revision surgery and those retrieved from cadaver donors?

3.3 Methods

<u>Clinical and Implant Information</u>

One hundred nine (109) femoral stems retrieved with an attached cobalt-chrome (CoCr) head were available for this analysis. Ninety-three (93) intact femoral components implanted between 1985 and 2016, and retrieved at revision surgery between 1994 and 2016, were identified from a collection of devices within an IRB-approved multi-institutional implant retrieval program based at Drexel University (Philadelphia, PA). Sixteen (16) intact femoral components were also retrieved from cadaver donors at RestoreLifeUSA (Elizabethton, TN) and the Medical Education and Research Institute (Memphis, TN). Medical records providing information on age, gender, BMI and implantation time were available for eighty-nine (89) revision retrievals (Table 7). The average implantation time was 7.4 ± 6.6 years (range, 0–24.8 years) and the mean patient age at implantation was 58 years (range, 20–89 years). The predominant reasons for revision were loosening (n=44), infection (n=17), and periprosthetic fracture (n=14). Device information (inclusive of manufacturer, design, and constituent material) was obtained from component markings and patient records. Six (6) manufacturers were represented among 103 components with identifiable designs: Zimmer Biomet, Warsaw, Indiana (n=65); Stryker, Mahwah, New Jersey (n=24); DePuy Synthes, Warsaw, Indiana (n=7); Smith and Nephew, Memphis, Tennessee (n=5); Wright Medical, Memphis, Tennessee (n=1) and Kinamed, Camarillo, CA (n=1). The alloy composition of retrieved components was confirmed using X-ray fluorescence (Niton XL3; Thermo Scientific, Waltham, MA). All implants were cleaned by two 20-minute soaks in a 1:10 ratio of disinfecting solution (Discide®;

AliMed, Dedham, Massachusetts) followed by two 30-minute sonication periods in water. A soft nylon brush was used to help remove biological films and loose debris.

Table 7. Device summary of the 109 retrieved components. Clinical information was available for 89 components from the revision cohort.

Patient Summary (Revision Cohort)		Device Material Details (All)	
Patients		Number of Systems	109
Male	45	CoCrMo Head	
Female	44	w/ CoCrMo Stem	58
Mean Age at Implantation (years)	58 (20 − 89) years	w/ Ti-6Al-4V Stem	47
		w/ TMZF Stem	4
Mean Time *in situ*	7.4 ± 6.6 (0 − 24.8) years		

Taper Interface Strength Evaluation

Femoral disassembly was performed on the cleaned retrievals using custom fixtures and a closed loop screw-driven testing frame (Instron Corporation, Norwood, Massachusetts). Head and stem fixtures were designed to accommodate the wide variety of device designs within the retrieval collection. The head fixture consists of a cradle with interchangeable slotted washers in the bottom plate, which secure the base of the femoral head. The washers were machined with different inner diameters to accommodate variations in stem neck geometries. Additionally, a universal joint was incorporated to maintain axial application of loads during testing. The stem fixture features interchangeable slotted washers in the top plate (to interface with the proximal stem), that were machined with two different inner diameters to accommodate variations in stem

body designs. All disassembly tests were conducted at a displacement rate of 0.008 mm/s in accordance with ISO 7206-10, and the peak load measured was recorded as the disassembly force[18].

Taper Damage Assessment

After disassembly, fretting and corrosion damage at the taper interface was characterized using a previously described four-point, semi-quantitative scoring system[20-22]. This system assigns a score of 1 when the damage is considered minimal, corresponding to fretting damage on less than 10% of the surface with no pronounced evidence of corrosion. A score of 2 is indicative of mild damage where either more than 10% of the surface has fretting damage or there is corrosion attack confined to small areas. Moderate damage is denoted by a score of 3 where more than 30% of the surface has fretting damage or localized corrosion attack. A score of 4 reflects severe damage over the majority of the taper (>50%) with abundant corrosion debris. Iatrogenic damage was identified as an irregular artifact on the taper surface and was excluded from the taper damage assessment. In an effort to achieve a consistent methodology, each component was scored by three trained investigators (GBH, JL and DWM) who were initially blind to the scores of the other. After scoring, the stem tapers were measured using calibrated calipers (Absolute Series 500; Mitutoyo, Sakado, Japan). The angle of the stem taper was derived from the taper design (identified from component markings) by using documentation from the manufacturer and published measurements[23].
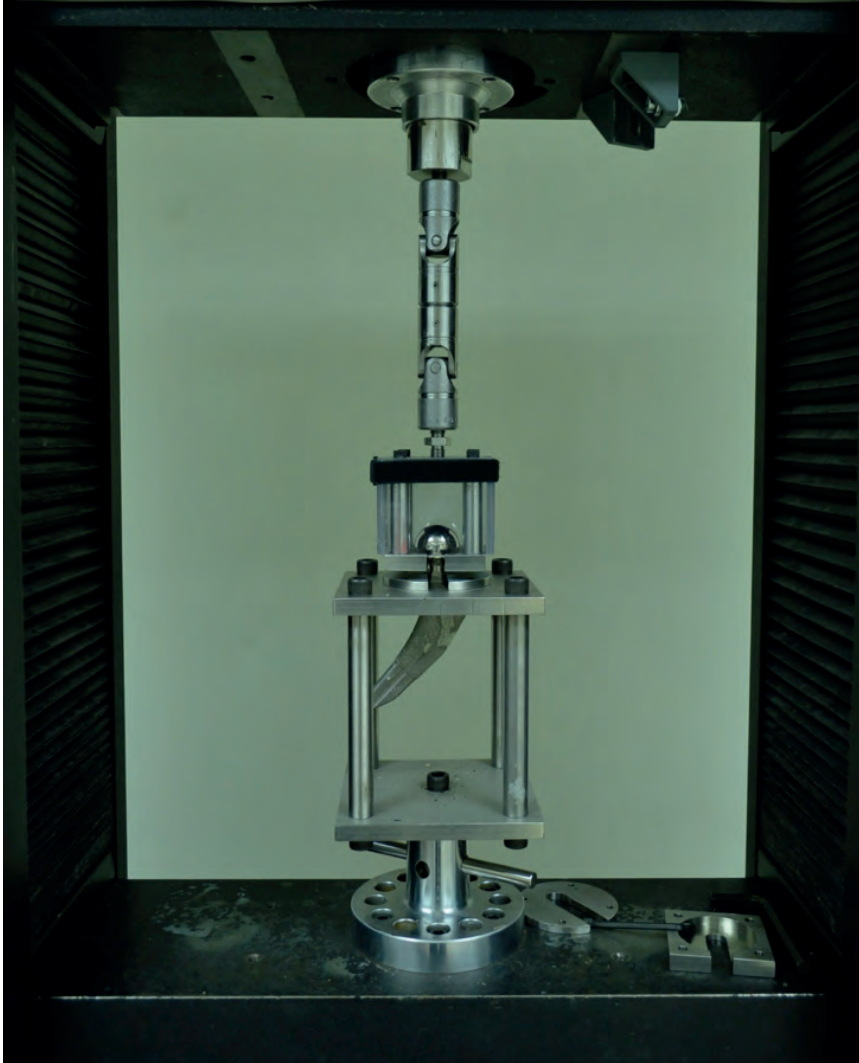
Figure 7. Photograph of disassembly apparatus with retrieved implant in place. Interchangeable slotted washers for head and stem fixtures are visible at the right.

Statistical Analysis

Due to the nonparametric nature of the data, the relationship between femoral disassembly force and taper damage was initially assessed via Spearman's correlation, with the magnitude of association denoted by rho (ϱ). To isolate the effect of clinical and component variables, univariate linear regression was used

to evaluate the association of femoral disassembly force with length of time implanted, reason for revision surgery, femoral head diameter, head offset, stem material, stem taper angle, taper length, and taper finish (smooth vs. grooved). The beta estimates (β) from the regression models provided the magnitude and direction of the linear relationship between femoral disassembly force and the modeled factors. Ordinal logistic regression was used to model the effect of these variables on the odds of greater taper damage. An odds ratio (OR) with a 95% confidence interval (CI) was calculated for each variable by exponentiating the parameter estimate of the model. Variables with significant associations between both femoral disassembly force and taper damage were identified as either confounders or effect modifiers. Confounders were included in multivariable linear regression models as covariates, while effect modifiers were included as covariates with interaction. Differences between revision retrievals and cadaver retrievals with respect to disassembly force and taper damage were initially assessed using the Wilcoxon-Mann-Whitney test, then quantified using linear or ordinal regression, as appropriate. All statistical analyses were performed using SAS 9.4 (SAS Institute, Inc., Cary, NC) with a significance threshold of p<0.05.

3.4 Results

The median femoral disassembly force for all components was 3.0 kN (range, 0.6–15.3 kN). Evidence of fretting and corrosion was observed on the majority of disassembled heads and stems: at least mild damage (score of 2) was observed on 88 of 109 (81%) head tapers, and 68 of 109 (62%) of stem tapers (Figure 8).
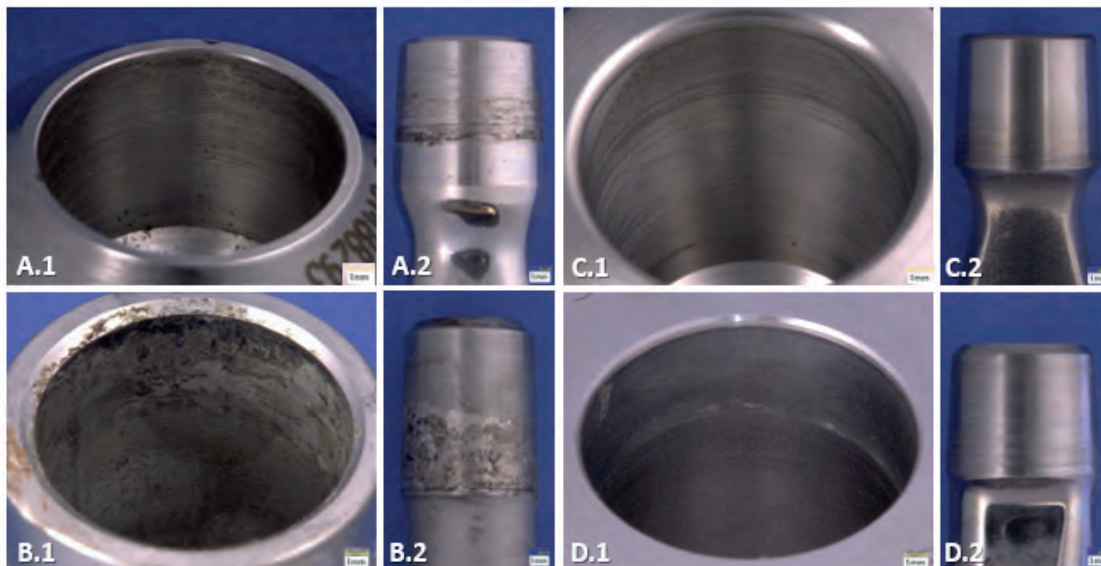
Figure 8. Macrographs showing taper damage on disassembled femoral components. Among the revision retrievals, the explant with the lowest disassembly force (0.6 kN) exhibited moderate damage (score of 3) at both the head (A.1) and stem (A.2) tapers. The revision retrieval with the highest disassembly force (15.3 kN) exhibited severe damage (score of 4) at the head and stem tapers (B.1 and B.2). The cadaver retrieval with the lowest disassembly force (0.6 kN) exhibited mild damage (score of 2) at the head (C.1) and minimal damage (score of 1) at the stem (C.2). The cadaver retrieval with the highest disassembly force (5.4 kN) exhibited mild damage (score of 2) at the head (D.1) and minimal damage (score of 1) at the stem (D.2).

Femoral disassembly force was found to have a weak positive correlation with stem taper damage ($\varrho=0.26$, $p=0.007$) but was not found to be related to head taper damage ($\varrho=0.14$, $p=0.153$; Figure 9). Larger femoral heads ($\beta= -137.7$, $p=0.030$), larger stem taper angles ($\beta= -1542.1$, $p<0.001$) and grooved tapers ($\beta= -2207.3$, $p<0.001$) were associated with a lower disassembly force, while longer stem tapers ($\beta=224.2$, $p<0.001$) were found to have a higher disassembly force. Ordinal logistic regression revealed a positive association for head taper damage with head offset ($p<0.001$) and taper finish ($p=0.002$). The odds of greater head taper damage increased by 17% for each additional millimeter of head offset ($OR=0.83$; 95% $CI=0.75–0.93$), and were 73% higher for smooth tapers ($OR=0.27$;

95% CI=0.12–0.60). Associations with stem taper damage were found for implantation time (p=0.008), reason for revision (p=0.024), femoral head size (p=0.007), head offset (p=0.032), stem taper length (p=0.012) and trunnion finish (p<0.001). The odds of greater stem taper damage increased by 8% for each year of implantation (OR=0.92; 95% CI=0.86–0.98) and were 60% higher for components revised for loosening compared to those revised for all other reasons (OR=0.40; 95% CI=0.18–0.89). Additionally, the odds of greater stem taper damage were found to increase by 10% for each additional millimeter of femoral head offset (OR=0.90; 95% CI=0.82–0.99), 12% for each additional millimeter of taper length (OR=0.88; 95% CI=0.80–0.97) and were 89% higher for smooth tapers (OR=0.11; 95% CI=0.05–0.25), but decreased by 14% for each additional millimeter of femoral head size (OR=1.14; 95% CI=1.04–1.26). In the multivariable analysis, disassembly force was not associated with head taper damage (β=558.2, p<0.068) when modeled with taper finish as an effect modifier. Disassembly force was positively associated with stem taper damage (β=782.3, p<0.028) when head size and taper length were modeled as confounders, and taper finish as an effect modifier.
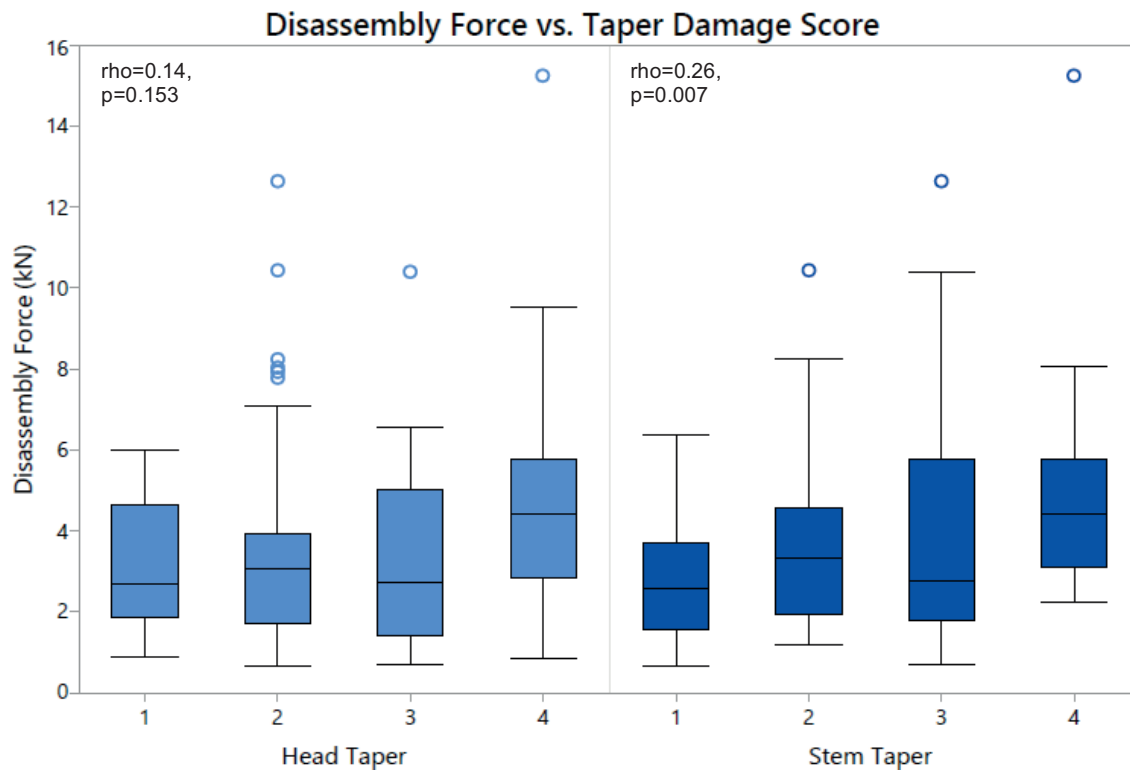
Figure 9. Box plot detailing the variation in femoral disassembly force by taper damage score. Stem taper damage was found to be positively correlated with disassembly force.

Femoral disassembly force for the cadaver retrievals (median=2.5; interquartile range=1.7 kN) was not found to differ from that for the revision retrievals (median=3.2; IQR=2.8 kN; p=0.23). Cadaver retrievals exhibited significantly less damage than revision retrievals at both the head (p=0.002) and stem (p<0.001) tapers (Figure 10). Compared to the cadaver cohort, revision retrievals were associated with a 77% increase in the odds of greater taper damage at the head (OR=0.23; 95% CI=0.08–0.67) and a 94% increase for that at the stem (OR=0.06; 95% CI=0.01–0.28).
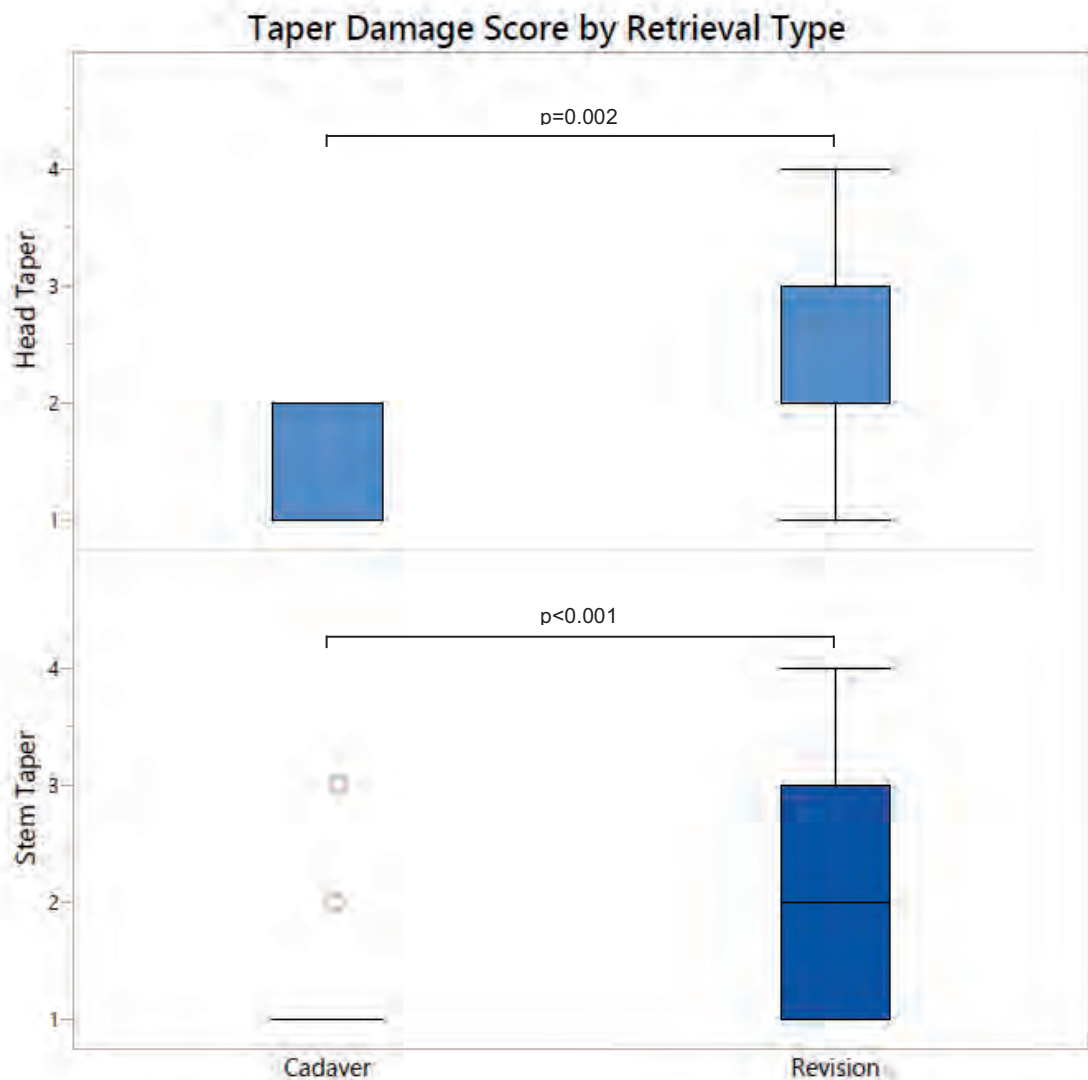
Figure 10. Box plot comparing the taper damage score between cadaver and revision retrievals. Both head and stem taper damage scores were found to be higher for retrievals from revision surgery than those from cadavers.

3.5 Discussion

The present work adds to the literature of *in vivo* taper corrosion by assessing its impact on taper strength experimentally. Modular junction corrosion damage is based on a mechanically assisted crevice corrosion mechanism (MACC).[4,24-26]

During loading, micromotion between the two metals and interfacial stresses fracture passive oxide films.[4,27] The subsequent repassivation process decreases the concentration of free oxygen in the modular junction crevice, while increasing that of reactive metal ions.[26,28] The metal chlorides that form subsequently react with water, creating metal hydroxide and hydrochloric acid.[26] With continued mechanical loading, metal oxide fracture and repassivation occurs, and the pH as well as free oxygen concentration within the crevice continues to decrease. The metal oxide however, is thermodynamically unstable in acidic conditions and the resulting passive layer may be susceptible to accelerated corrosive attack.[29] The impact of taper corrosion on taper strength has been reported by Ko and colleagues, who concluded that *in vivo* femoral head dissociation in a series of retrievals was caused by severe corrosion at the taper interface.[16] Recently, Urish *et al.* described material loss resulting from severe corrosion as a potential mechanism for *in vivo* disassociation of an initially well-fixed modular junction.[14] This study does not provide evidence that that corrosion weakens the taper junction between the head and stem of modular femoral components.

While we highlight the importance of these experimental findings in the context of observational studies, we recognize some limitations of this work. The strength of the taper connection is strongly determined by the force used at impaction, but obtaining details on the surgical technique during implantation remains a challenge for retrieval studies.[12,19] Another potential limitation is that taper damage was evaluated semi-quantitatively using a method that is liable to observer subjectivity. However, measurements of volumetric material loss from

tapers have been shown to correlate with visual damage scores[30,31] and the use of three scorers facilitated a measure of consistency for this assessment. Due to the inclusion criteria of cobalt-chrome heads, these findings are limited to femoral components with a CoCr-on-polyethylene bearing surface. It is unclear to what extent the relationships observed here would extend to cases where the head is fashioned from other alloys or ceramic materials. Despite these limitations, this study represents a variety of manufacturers and designs, facilitated by the relatively large study cohort. Other retrieval studies examining taper interface strength reported on fewer than fifteen devices.[32,33] Another strength is the inclusion of retrievals from cadaver donors, which allows these findings to be interpreted beyond components with a clinical diagnosis for revision.

Contrary to the hypothesis that corrosion results in material loss that weakens the taper interface, our results highlighted a trend toward slightly higher disassembly forces for more severely corroded stems. It has been proposed that as unordered lattice planes of the oxide form, the growing oxide scale may adhere to contacting surfaces and mediate a bond to the underlying metal.[34] An alternative explanation for the observed relationship is that the developing oxide intercalates irregularities on the contacting material and increase the interference between the two surfaces.[34] We also observed a wide range of disassembly forces for components scored as severely corroded (2.2 kN to 15.3 kN) which may signal heterogeneity in the forms of corrosion. With scanning electron microscopy and X-ray analysis, Gilbert *et al.* identified several forms of corrosive attack on the tapers of retrievals, including pitting, preferential dissolution of cobalt, interdendritic corrosion and intergranular corrosion.[26] Performing a

similar qualitative analysis on the disassembled surfaces of this study may provide insight into how individual corrosion modes affect taper strength.

To understand the taper performance of unrevised femoral components, retrievals from cadaver donors were included in this study. We identified no difference between revision and cadaver retrievals with respect to disassembly force, but observed greater taper corrosion damage for both the head and stem tapers of revision retrievals. Among the revision retrievals, we also found greater stem taper damage scores on components revised for loosening compared to all other reasons. Due to mechanical instability, loose stems may undergo greater relative movements and become more susceptible to MACC. However, this finding may also signal a biological response to more severely corroded components. Corrosion products have been shown to activate pathways that result in osteolysis, which may lead to eventual loosening. Vermes *et al.* reported that metal ions reduce osteoblast function and result in particularly necrotic local cellular responses.[35] It is therefore also possible that the greater corrosion observed on the revision retrievals may highlight the interplay of corrosion with other reasons for revision.[36,37]

The results of the present study do not support the hypothesis that corrosion weakens the taper junction between the head and stem of modular femoral components. Corrosion damage in modular tapers manifests in various ways and further investigation is therefore warranted to determine whether specific types of corrosive attack may be at risk for mechanical failure. Additionally, the

findings from the taper damage assessment of cadaver controls may suggest a greater prevalence of corrosion in components requiring revision surgery.

References

1.   Hussenbocus S, Kosuge D, Solomon LB, Howie D, Oskouei R. Head-Neck Taper Corrosion in Hip Arthroplasty. *BioMed research international.* 2015;2015.

2.   Mroczkowski ML, Hertzler JS, Humphrey SM, Johnson T, Blanchard CR. Effect of impact assembly on the fretting corrosion of modular hip tapers. *Journal of orthopaedic research.* 2006;24(2):271-279.

3.   Viceconti M, Baleani M, Squarzoni S, Tonil A. Fretting wear in a modular neck hip prosthesis. *Journal of Biomedical Materials Research Part A.* 1997;35(2):207-216.

4.   Jacobs JJ, Gilbert JL, Urban RM. Current Concepts Review-Corrosion of Metal Orthopaedic Implants. *The Journal of Bone & Joint Surgery.* 1998;80(2):268-282.

5.   Langton DJ, Jameson SS, Joyce TJ, et al. Accelerating failure rate of the ASR total hip replacement. *J Bone Joint Surg Br.* 2011;93(8):1011-1016.

6.   Gilbert JL, Buckley CA, Jacobs JJ, Bertin KC, Zernich MR. Intergranular corrosion-fatigue failure of cobalt-alloy femoral stems. A failure analysis of two implants. *JBJS.* 1994;76(1):110-115.

7.   Huot Carlson JC, Van Citters DW, Currier JH, Bryant AM, Mayor MB, Collier JP. Femoral stem fracture and in vivo corrosion of retrieved modular femoral hips. *The Journal of arthroplasty.* 2012;27(7):1389-1396. e1381.

8.   Cameron HU. Modularity in primary total hip arthroplasty. *The Journal of arthroplasty.* 1996;11(3):332-334.

9.   Barrack RL. Modularity of prosthetic implants. *Journal of the American Academy of Orthopaedic Surgeons.* 1994;2(1):16-25.

10.   McCarthy JC, Bono JV, O'Donnell PJ. Custom and modular components in primary total hip replacement. *Clinical orthopaedics and related research.* 1997;344:162-171.

11.   Heiney JP, Battula S, Vrabec GA, et al. Impact magnitudes applied by surgeons and their importance when applying the femoral head onto the Morse taper for total hip arthroplasty. *Archives of orthopaedic and trauma surgery.* 2009;129(6):793-796.

12.   Rehmer A, Bishop NE, Morlock MM. Influence of assembly procedure and material combination on the strength of the taper connection at the head–neck junction of modular hip endoprostheses. *Clinical Biomechanics.* 2012;27(1):77-83.

13.   Star MJ, Colwell Jr CW, Donaldson III WF, Walker RH. Dissociation of modular hip arthroplasty components after dislocation: a report of three cases at differing dissociation levels. *Clinical orthopaedics and related research.* 1992;278:111-115.

14. Urish KL, Hamlin BR, Plakseychuk AY, et al. Trunnion Failure of the Recalled Low Friction Ion Treatment Cobalt Chromium Alloy Femoral Head. *The Journal of Arthroplasty.* 2017.

15. Banerjee S, Cherian JJ, Bono JV, et al. Gross trunnion failure after primary total hip arthroplasty. *The Journal of arthroplasty.* 2015;30(4):641-648.

16. Ko LM, Chen AF, Deirmengian GK, Hozack WJ, Sharkey PF. Catastrophic femoral head-stem trunnion dissociation secondary to corrosion. *JBJS.* 2016;98(16):1400-1404.

17. Talmo CT, Sharp KG, Malinowska M, Bono JV, Ward DM, Lareau J. Spontaneous modular femoral head dissociation complicating total hip arthroplasty. *Orthopedics.* 2014;37(6):e592-e595.

18. Richter HG, Willmann G, Wimmer M, Osthues FG. Influence of the ball/stem-interface on the load bearing capability of modular total hip endoprostheses. *Modularity of orthopedic implants*: ASTM International; 1997.

19. Pennock AT, Schmidt AH, Bourgeault CA. Morse-type tapers: factors that may influence taper strength during total hip arthroplasty. *The Journal of arthroplasty.* 2002;17(6):773-778.

20. Goldberg JR, Gilbert JL, Jacobs JJ, Bauer TW, Paprosky W, Leurgans S. A multicenter retrieval study of the taper interfaces of modular hip prostheses. *Clinical orthopaedics and related research.* 2002;401:149-161.

21. Higgs GB, Hanzlik JA, MacDonald DW, Gilbert JL, Rimnac CM, Kurtz SM. Is Increased Modularity Associated With Increased Fretting and Corrosion Damage in Metal-On-Metal Total Hip Arthroplasty Devices?: A Retrieval Study. *The Journal of arthroplasty.* 2013;28(8):2-6.

22. Higgs GB, MacDonald DW, Gilbert JL, Rimnac CM, Kurtz SM, Committee IRCW. Does taper size have an effect on taper damage in retrieved metal-on-polyethylene total hip devices? *The Journal of arthroplasty.* 2016;31(9):277-281.

23. Nassif NA, Nawabi DH, Stoner K, Elpers M, Wright T, Padgett DE. Taper design affects failure of large-head metal-on-metal total hip replacements. *Clinical Orthopaedics and Related Research®.* 2014;472(2):564-571.

24. Jacobs J, Cooper H, Urban R, Wixson R, Della Valle C. What do we know about taper corrosion in total hip arthroplasty? *The Journal of arthroplasty.* 2014;29(4):668-669.

25. Gilbert JL, Jacobs JJ. The mechanical and electrochemical processes associated with taper fretting crevice corrosion: a review. *Modularity of Orthopedic Implants.* 1997;1301:45.

26. Gilbert JL, Buckley CA, Jacobs JJ. In vivo corrosion of modular hip prosthesis components in mixed and similar metal combinations. The effect of crevice, stress, motion, and alloy coupling. *Journal of biomedical materials research.* 1993;27(12):1533-1544.

27. Hallab NJ, Messina C, Skipor A, Jacobs JJ. Differences in the fretting corrosion of metal–metal and ceramic–metal modular junctions of total hip replacements. *Journal of Orthopaedic Research.* 2004;22(2):250-259.

28. Hoeppner D, Chandrasekaran V. Fretting in orthopaedic implants: a review. *Wear.* 1994;173(1):189-197.

29. West JM. Basic corrosion and oxidation. 1986.

30. Kocagoz SB, Underwood RJ, MacDonald DW, Gilbert JL, Kurtz SM. Ceramic Heads Decrease Metal Release Caused by Head-taper Fretting and Corrosion. *Clinical Orthopaedics and Related Research®.* 2016;474(4):985-994.

31. Hothi HS, Matthies AK, Berber R, Whittaker RK, Skinner JA, Hart AJ. The reliability of a scoring system for corrosion and fretting, and its relationship to material loss of tapered, modular junctions of retrieved hip implants. *The Journal of arthroplasty.* 2014;29(6):1313-1317.

32. Nganbe M, Louati H, Khan U, Speirs A, Beaule PE. Retrieval analysis and in vitro assessment of strength, durability, and distraction of a modular total hip replacement. *Journal of Biomedical Materials Research Part A.* 2010;95(3):819-827.

33. Lieberman JR, Rimnac CM, Garvin KL, Klein RW, Salvati EA. An analysis of the head-neck taper interface in retrieved hip prostheses. *Clinical orthopaedics and related research.* 1994;300:162-167.

34. Werber T. The phenomenon of adherence of a growing scale to the surface of a solid substance. *Materials Science and Engineering.* 1987;88:283-285.

35. Vermes C, Glant TT, Hallab NJ, Fritz EA, Roebuck KA, Jacobs JJ. The potential role of the osteoblast in the development of periprosthetic osteolysis: review of in vitro osteoblast responses to wear debris, corrosion products, and cytokines and growth factors. *The Journal of arthroplasty.* 2001;16(8):95-100.

36. McGrory BJ, McKenney BR. Revision for taper corrosion at the head-neck junction: pearls and pitfalls. *Current reviews in musculoskeletal medicine.* 2016;9(1):97-102.

37. Osman K, Panagiotidou A, Khan M, Blunn G, Haddad F. Corrosion at the head-neck interface of current designs of modular femoral components. *Bone Joint J.* 2016;98(5):579-584.

IV A Quantitative Method to Assess the Severity of Taper Corrosion

4.1 Abstract

Visual assessment of taper damage has been a useful tool for obtaining a semi-quantitative understanding of corrosion severity in retrieved and *in vitro* tested modular femoral components, but this method is challenged by its inherent subjectivity and the inability to distinguish the degree of corrosion beyond binned categories. This study leveraged the electrochemical nature of taper corrosion to develop a quantitative assessment of damage severity, and explored whether these continuous measurements could provide insight into the effects of head taper corrosion on interface strength. Twenty CoCrMo (20) femoral heads were characterized: 19 from the previously described study that evaluated the effect of corrosion on the strength of the taper interface, and one unimplanted control. The taper surface of these components was evaluated using electrochemical impedance spectroscopy under the frequency domain and electrochemical behavior was modeled using a Randle's circuit. Corrosion damage had significant correlations with low frequency impedance, max phase angle, polarization resistance, and constant phase element (CPE) capacitance along with its associated exponent. Three of these electrochemical determinants of corrosion (impedance, phase angle, polarization resistance and capacitance) were also associated with increased taper strength. These results highlight the potential of electrochemical measurements to assess taper corrosion severity and corroborate earlier findings of increased taper strength for more severely corroded femoral stems.

4.2 Introduction

A large number of studies assessing taper corrosion have relied on visual scoring to provide a semi-quantitative estimate of corrosion severity[1-5]. While this approach is useful for a preliminary assessment, corrosion is more aptly described as a continuous process and an ordinal measure limits the granularity with which this phenomenon can be studied. Methods to measure volumetric wear have also been developed, and their utility in quantifying the amount of material released during simulation or while *in vivo* will remain paramount in understanding the burden of debris at risk to the patient[1,6]. Nonetheless, this measure of an effect does not allow for an un-confounded understanding of the corrosion processes that can cause it, and mechanistic studies to evaluate new candidate alloys for biomedical applications are warranted.

The corrosion resistance of medical alloys is largely dependent on the ability of these materials to spontaneously form nanometer-scale oxide films.[7] This process of self-passivation provides a barrier between the base alloy and its surrounding biological environment, which impedes corrosion reactions and facilitates biocompatibility. Within orthopedics, implants fashioned from cobalt-based alloys feature chromium to impart spontaneous passivation characteristics and molybdenum to provide local corrosion resistance. Additionally, manufacturers routinely treat CoCrMo devices with an immersion in nitric acid at an elevated temperature to further passivate the material and increase corrosion resistance[8]. In the case of femoral heads however, the oxide may be disrupted by interfacial stresses within the modular taper connection crevice under *in vivo* loading, resulting in mechanically assisted crevice corrosion as previously described. The

cascading effects of this process create an autocatalytic phenomenon that compromises the ability of the alloy to re-form the protective oxide. Thus, corroded tapers of CoCrMo femoral heads can be expected to exhibit impaired passivation behavior, as compared to their as-manufactured condition.

Electrochemical impedance spectroscopy is a technique that has been employed to understand the corrosion resistance of dielectric materials such as paints and organic coatings on metal substrates[9,10]. Frequency-dependent EIS involves applying a sinusoidal perturbation to the substrate, typically at the millivolt (mV) scale, and measuring the amount of current that passes through the protective coating. The measure of a system's opposition to current flow is described as its impedance, and can be modeled as an equivalent electrical circuit consisting of some combination of resistive, capacitive, and inductive circuit elements. The purpose of the current study was to leverage the self-passivating behavior of CoCrMo orthopedic alloys to quantify the corrosion severity of retrieved femoral heads. With the understanding that corrosion at the taper surface manifests with disruption of the protective metal oxide, we anticipate that more severely corroded tapers would exhibit decreased impedance. A secondary goal of this work was to identify whether this quantitative measure could provide further insight into how corrosion may be implicated in the strength of the taper interface.

4.3 Methods

<u>Implant Information</u>

Twenty (20) cobalt-chrome (CoCr) femoral heads were identified for this assessment. Ten (10) severely corroded retrieved femoral heads were selected from the population previously evaluated for taper interface strength, comprising components from taper connections with the five (5) highest and five (5) lowest disassembly forces. Using the same selection criteria, an additional nine (9) heads were selected to represent moderate (n=7) and mild (n=2) corrosion damage, with one unimplanted femoral head included as a control. The dimensions of the female tapers for these components were obtained using calibrated calipers (Absolute Series 500; Mitutoyo, Sakado, Japan).

<u>Electrochemical Impedance Spectroscopy</u>

Components were electrochemically characterized using a potentiostat (PARSTAT 3000A; Princeton Applied Research–Ametek, Berwyn, PA) and a three electrode cell (Figure 11). The femoral head was connected to the working electrode terminal via an electrical wire that was secured to the external base of the femoral head with copper tape. A platinum (Pt) counter electrode was constructed by coiling a 0.012″ diameter 99.9% Pt wire (Alfa Aesar, Haverhill, MA) around the tip of a glass pipette. This increased the effective surface area of the counter electrode in an effort to mitigate a charge build-up that could hinder current flow between the working electrode. An Ag/AgCl reference electrode was constructed by first cleaning a 0.015″ Ag wire (A-M Systems, Sequim, WA) with ethanol to remove surface oils. The dry wire was then incubated at room

temperature in a solution of sodium hypochlorite for 36 hours. Using a voltmeter, the potential of the constructed electrode was cross-referenced with an Ag/AgCl standard lab electrode that was co-immersed in a 0.01 M solution of phosphate buffer solution (PBS). The inside of the femoral head taper was filled with 0.01 M PBS, and a lint-free wipe (Kimwipe; Kimberly-Clark, Irving, TX) was used to ensure the liquid level was consistent for all samples.
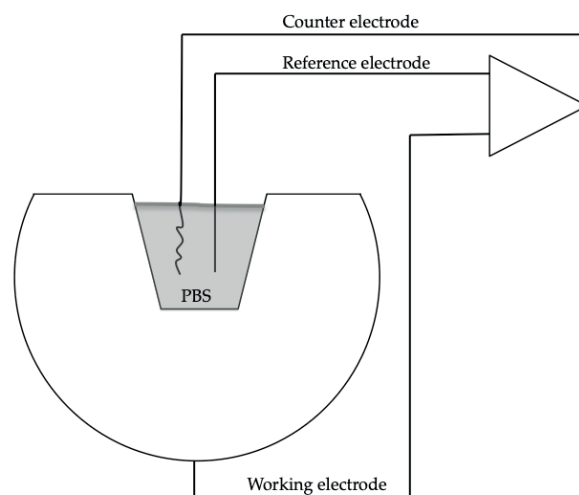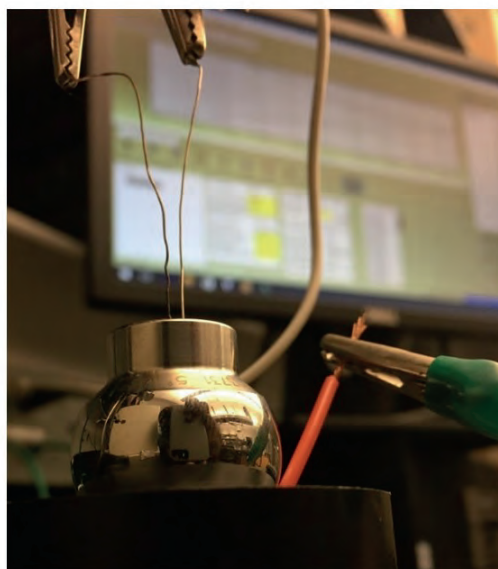
Figure 11. Photograph of electrochemical impedance apparatus with retrieved femoral head in place. A schematic of the 3-electrode experimental system is depicted on the right.

To conduct EIS testing, the open circuit potential (OCP) was measured for 1 hour, and a 10 mV sinusoidal voltage (relative to OCP) was applied over a range of frequencies: beginning at 20 kHz and ending at 2 mHz. At high-frequencies the impedance results represent the solution behavior, while the characteristics

of the taper surface are captured at low frequencies. Therefore, corrosion severity was assessed relative to the impedance measurement at 2 mHz, (|Z-minfreq|) and max phase angle (θ-max). The data were then modeled as a Randle's circuit with a constant phase element (CPE), using a least-squares fitting algorithim (ZView; Scribner Associates, Southern Pines, NC). A CPE was employed in place of a traditional capacitor to account for the imperfect capacitive behavior expected for metallic biomaterials. The impedance of a CPE is given in Equation 6:

$$Z_{CPE} = \frac{1}{((i\omega)^{\alpha} Q)}$$ *Equation 6*

where α is the constant phase exponent which can vary from 1 to 0 and Q is the capacitive-like value of the CPE. When α is 1, the CPE acts like an ideal capacitor, while at values less than 1, the CPE takes on more and more of a resistive character. Circuit elements: polarization resistance (R-P), CPE-capacitance, and α were then also evaluated relative to corrosion severity. To control for the mathematical effect of surface area on capacitive and resistive components, the measured taper dimensions were used to calculate the surface area of each working electrode, and the area-dependent metrics were scaled accordingly.

Statistical Analysis

Nonparametric analysis techniques were employed due to the lack of normality for these data. Thus, the relationship between the continuous electrochemical variables and taper damage was initially assessed using Spearman's correlation

coefficient, denoted by rho (ϱ). The effect of these electrochemical variables on taper strength was also assessed, and this analysis was repeated after stratification by taper strength category. Differences in electrochemistry between the low taper strength and high taper strength cohorts were assessed using the Wilcoxon-Mann-Whitney test. Statistical analyses were performed using SAS 9.4 and JMP 13 (SAS Institute, Inc., Cary, NC) with a significance threshold of $p<0.05$.

4.4 Results

Representative Bode spectra depicting impedance and phase angle as a function of frequency are presented in Figure 12. Generally, high impedance values were observed for these components. The median |Z-minfreq| was 1.73×10^5 Ω (range 1.03×10^5–5.34×10^6 Ω), indicating passive film formation on the taper surfaces. Impedance was found to decrease with corrosion severity, evident by the strong inverse relationship between the two metrics ($\varrho=-0.857$, $p<0.001$; Figure 13). Phase angle values deviated from 90° for the majority of components: median |θ-max| was 80.2° (range 62.8–89.8°). This deviation was moderately correlated with corrosion severity ($\varrho=-0.483$, $p=0.031$; Figure 14).
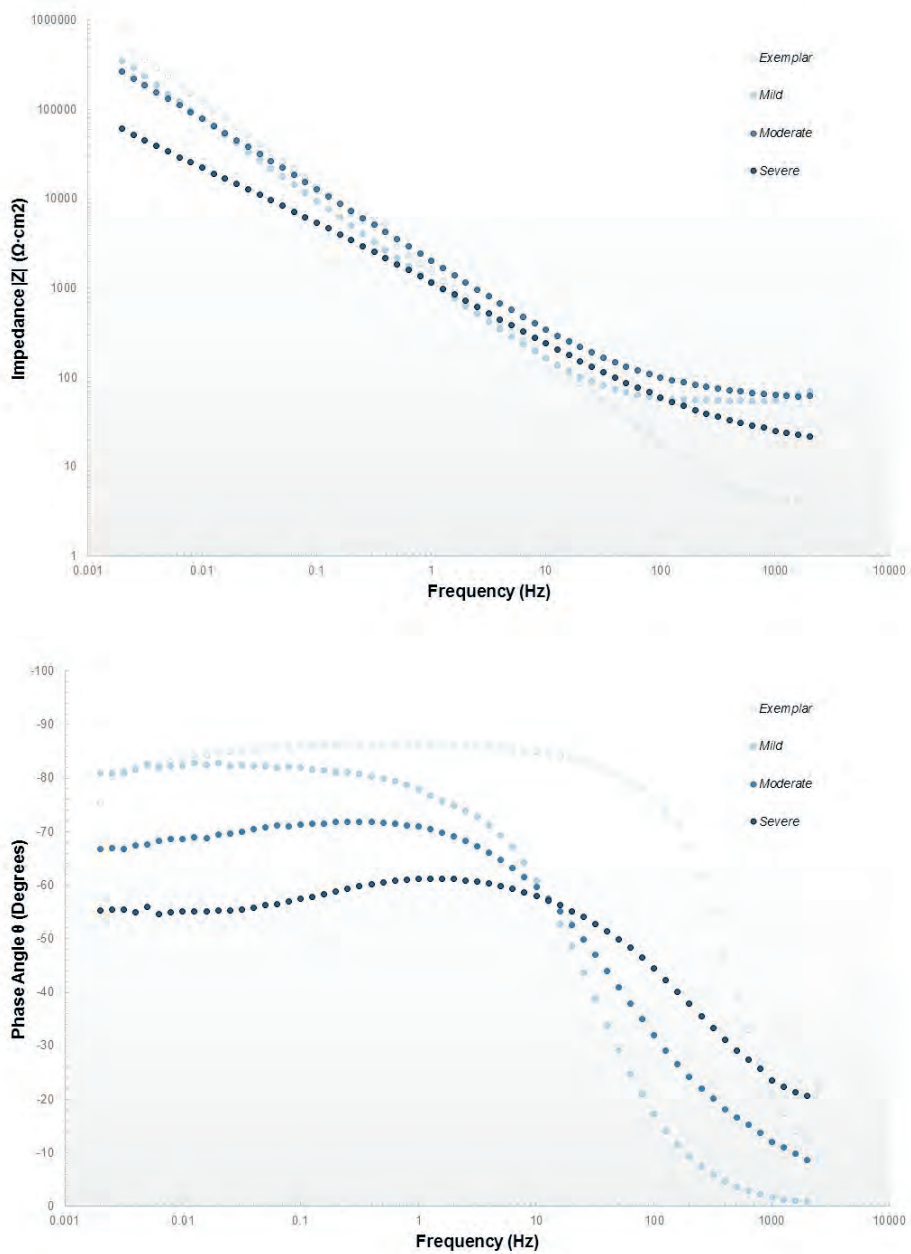
Figure 12. Representative Bode plots showing the variation in impedance (top) and phase angle (bottom) as a function of frequency for different categories of corrosion severity.
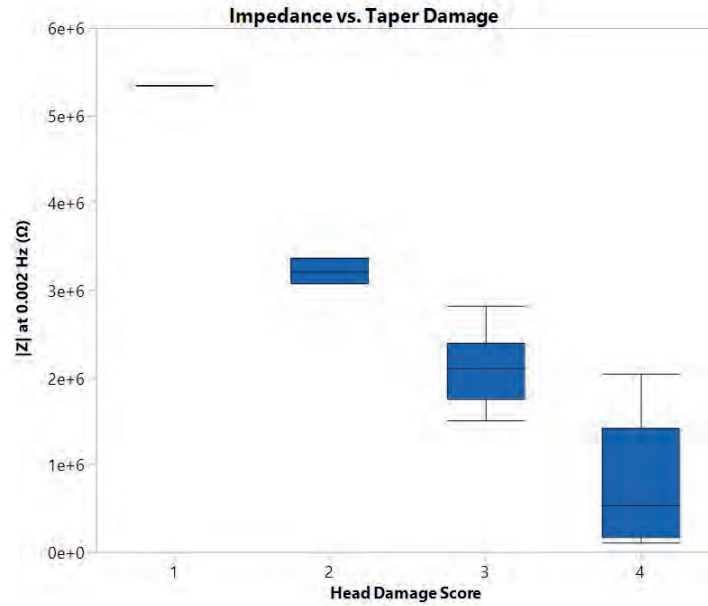
Figure 13. Box plot detailing the variation in impedance by taper damage score. Increased corrosion severity was strongly correlated with lower impedance values (ρ=-0.857, p<0.001).
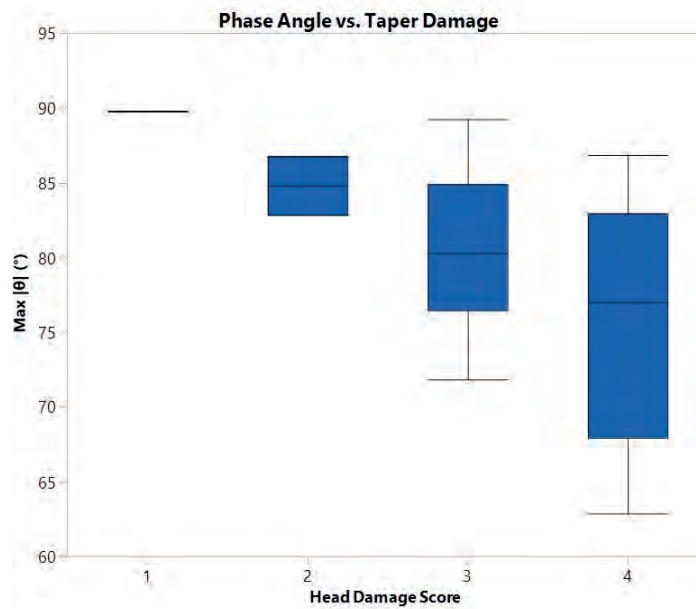
Figure 14. Box plot detailing the variation in phase angle by taper damage score. Increased corrosion severity was moderately correlated with increased deviation from 90° (ρ=-0.483, p=0.031).

From the least-squares fitting procedure, we were able to estimate the relative contributions of the various circuit elements to the overall impedance. The median capacitance of the CPE was 2.16×10^{-5} F · $s^{\alpha-1}$ (range 1.77×10^{-5}–5.62×10^{-4} F · $s^{\alpha-1}$) and its associated exponent (α) was 0.87 (range 0.51–0.97). As the α of an ideal capacitor is 1, values closer to 0 indicate a greater relative resistive character for the CPE. Both of these variables were found to be associated with corrosion severity: CPE-capacitance exhibited a strong positive correlation ($\varrho = 0.913$, $p < 0.001$; Figure 15), while a moderate inverse relationship was observed between α and damage score ($\varrho = -0.653$, $p = 0.002$; Figure 16). The median resistance to polarization was found to be 6.94×10^6 Ω (range 6.89×10^5–3.64×10^{13} Ω). Additionally, a moderate correlation was seen between R-P and corrosion damage score ($\varrho = 0.556$, $p = 0.011$; Figure 17).
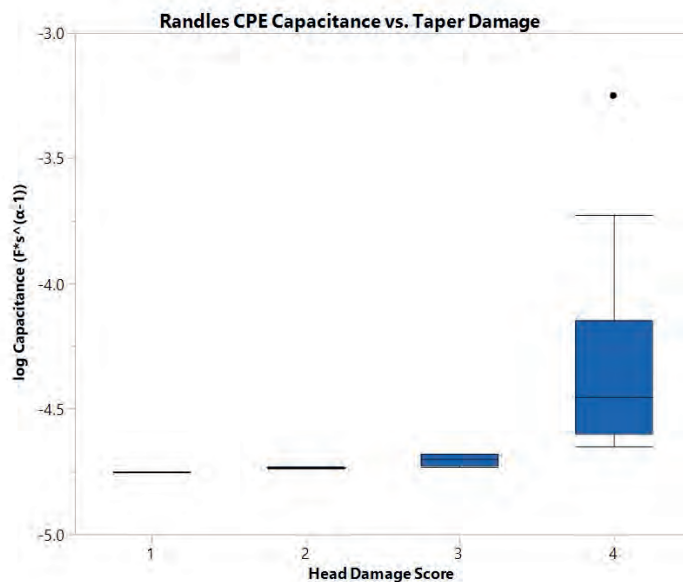
Figure 15. Box plot detailing the variation in CPE-capacitance by taper damage score. Increased corrosion severity was strongly correlated with higher capacitance values (ρ=0.913, p<0.001). A log scale was used to better visualize the positively skewed CPE-capacitance data.
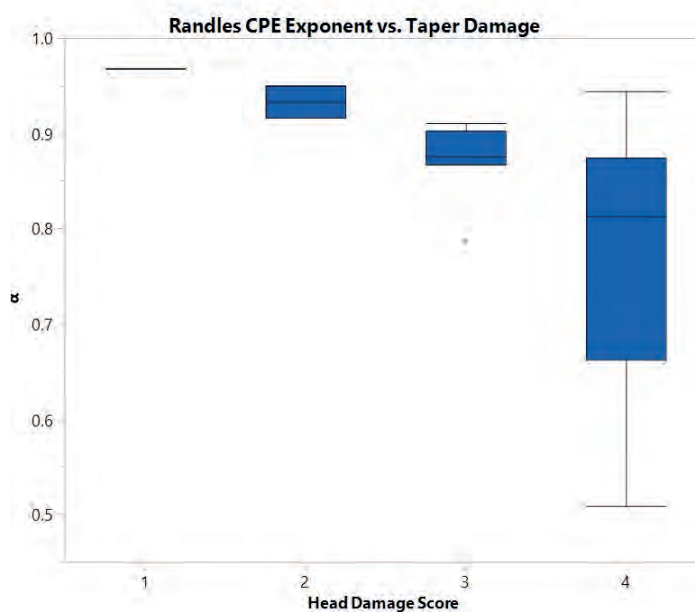
Figure 16. Box plot detailing the variation in the exponent of the CPE, by taper damage score. Increased corrosion severity was moderately correlated with greater deviation from ideal capacitive behavior (ρ= -0.653, p=0.002).
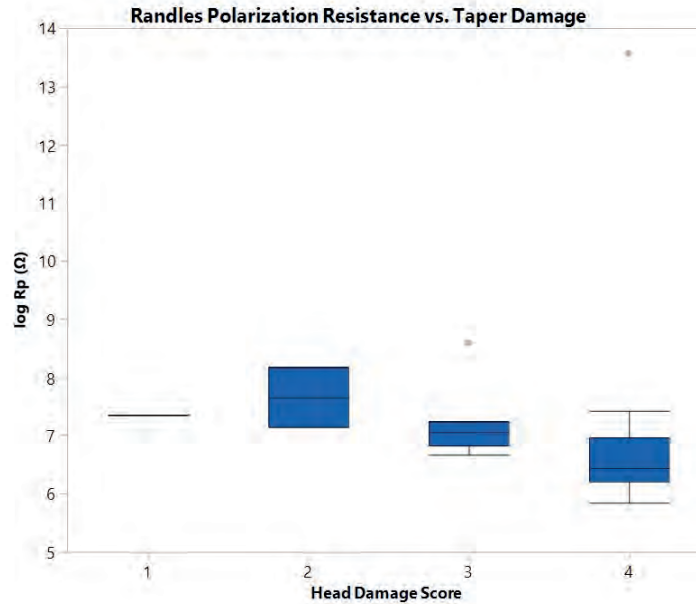
Figure 17. Box plot detailing the variation in polarization resistance by taper damage score. Increased corrosion severity was strongly correlated with lower impedance values (ρ=-0.857, p<0.001). A log scale was used to better visualize the positively skewed polarization resistance data.

Median taper strength was 1.9 kN (range, 0.6–3.2 kN) and 5.4 kN (range, 4.0–15.3 kN) for the low and high taper strength cohorts, respectively (p<0.001). From the overall assessment, none of the electrochemical variables were found to have significant associations with taper strength (|Z-minfreq|: ϱ=-0.244, p=0.314; θmax: ϱ=-0.114, p=0.642; CPE-capacitance: ϱ=0.291, p=0.226; α: ϱ=-0.053, p=0.831; RP: ϱ=-0.107, p=0.663). For the low taper strength cohort within the stratified analysis however, CPE-capacitance increased with taper strength (ϱ=0.782, p=0.008) while |Z-minfreq| (ϱ=-0.855, p=0.002), α (ϱ=-0.818, p=0.004) and R-P (ϱ=-0.673, p=0.033) all exhibited negative correlations. No such associations were observed in the high taper strength cohort. Additionally, no

differences were found between the two cohorts with respect to any of the electrochemical variables.

4.5 Discussion

This work draws on the electrochemical foundation for the corrosion resistance of orthopedic alloys to develop a quantitative evaluation of taper corrosion. The self-passivating property of biomedical alloys is based on the development of a highly adherent compact thin oxide film, which covers the metal surface and results in a physical barrier that kinetically limits corrosion reactions. This process of oxidation involves an increase in the valence state of the metal from atomic element to ion, constituting a chemical change. Furthermore, the Cabrera and Mott theory proposes that high electric fields can develop across this oxide. Oxidation at the metal-oxide interface results in a buildup of cations in the oxide adjacent to the metal, with electrons concentrating in the metal adjacent to the oxide. Similarly, reduction at the solution-oxide interface results in a negative charge buildup in the oxide adjacent to the solution with positive charges concentrating at the solution-oxide interface, forming an electrical double layer. In addition to the charge storage behavior of this metal-oxide-solution system, charges may also be transported through the oxide. Electrons tunnel from the metal to the solution due to their affinity with oxygen, and ions migrate across the oxide in response to its electrical gradient. Thus, these oxide films may be considered to be dynamic electrical structures consisting of capacitive and resistive electrical elements. The results of this study support the hypothesis that electrochemical impedance spectroscopy is a suitable tool to study the kinetics

CoCrMo passive films and can be used to quantify the severity of taper corrosion.

The quantitative framework developed here overcomes several challenges of visual scoring, but we recognize some limitations. EIS measurements may be affected by instrumental variations such as electrode area and positioning; consideration should therefore be given to these variables when designing similar experiments. Additionally, impedance is highly dependent on variables such as solution temperature and time of immersion. The former is based on reaction kinetics and was partially accounted for by conducting all experiments within a temperature-controlled lab. The latter is based on hydration of the oxide and was a motivating factor for the 1 hour OCP measurement prior to each EIS test. However, the oxides of biological retrievals can be highly variable and individualized immersion periods may be warranted. The electrical equivalent circuit modeling may be another potential limitation of this work. The Randle's circuit assumed for these data resulted in fairly large errors of estimation for a small number of cases, which may be addressed with alternative circuit models depicted in Figure 18.
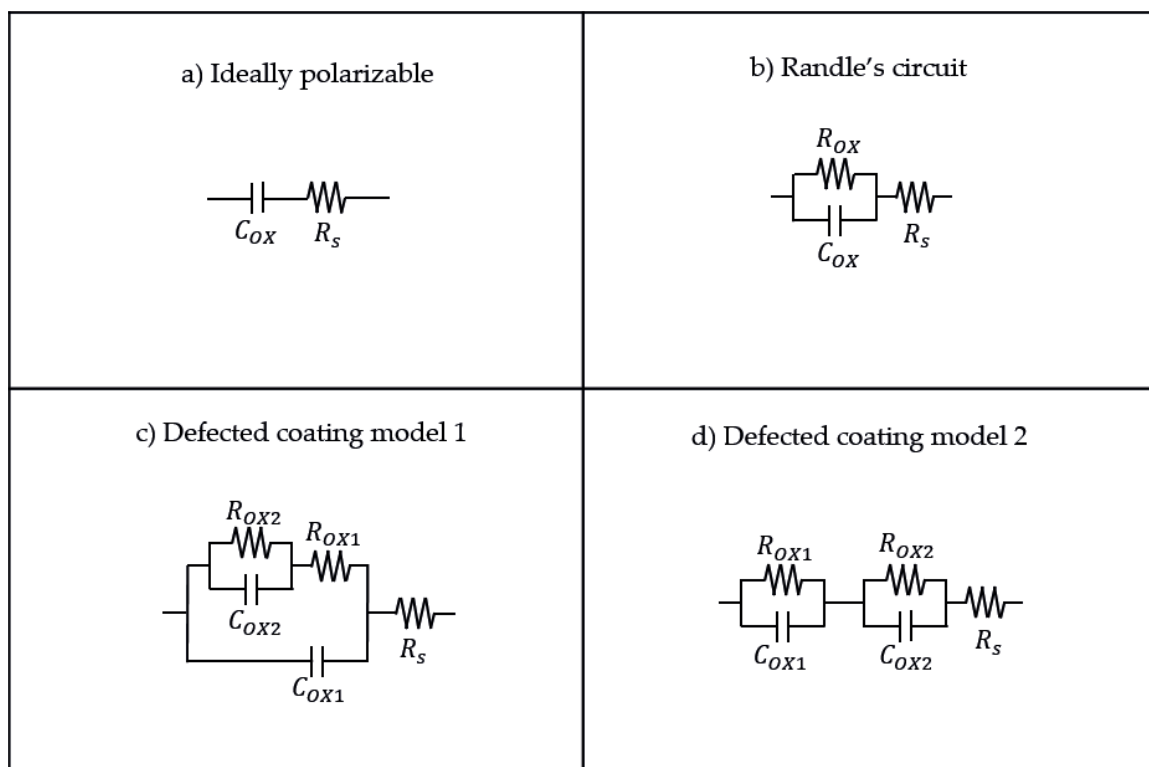
Figure 18. Circuit models that may be used to analyze the electrochemical impedance properties of metallic biomaterials. Ideally polarizable electrodes have no currents through the surface (a). Randle's circuit used in the current analysis to describe the oxide thin film surfaces (b). Defected coating models used for analyses involving thicker coatings on metal surfaces (c and d).

In practice however, additional elements were found to result in increased error values during circuit modeling. Despite these limitations, the use of retrievals in this study allowed for clinically relevant corrosion to be electrochemically evaluated. Additionally, the use of components previously evaluated for taper strength permitted the empirical value of these continuous corrosion variables to be demonstrated.

The decreased impedance observed for more severely corroded femoral head tapers is consistent with the expectation that corrosion disrupts the passive oxide

film on CoCrMo materials. This overall impedance is dominated by capacitive character, which results from the metal-oxide capacitance, oxide capacitance, and the electrical double layer capacitance. In response to a sinusoidal voltage, current is out of phase with voltage by 90° for an ideal capacitor[11]. A decreased phase angle was associated with increased corrosion and suggests non-ideal behavior with partial resistive nature. The frequency dependent behavior of a capacitor allows for an evaluation of these dynamics. As previously outlined, the Randle's circuit models the taper surface as having a solution resistance connected in series to the parallel connection of oxide polarization resistance and oxide capacitance. At high frequencies, the impedance of a capacitor is 0 and results in short-circuit behavior. This results in solution resistance being the only contributor to the overall impedance. As frequency decreases, the relative contribution of the capacitor begins to increase until it arrives at an inflection point where the capacitive impedance becomes higher than the polarization resistance. At this point, the resistor becomes the "easier path" for the flow of current and the relative contribution of the capacitor to the overall impedance decreases. In the case of this analysis, increased corrosion introduces defects that result in decreased resistance, as these defect provide additional avenues for the transport of charges. Therefore, the resistive contribution of the oxide begins to have an effect before the capacitive contribution reaches its maximum value, thus the maximum phase angle has a resistive quality. The results from the equivalent circuit analysis elucidate this behavior. RP was found to decrease with corrosion severity. An increase in the number of defects increases the surface area of the electrode, which has an inverse relationship with resistance. Capacitance however, is directly proportional to surface area, which is consistent with the

positive relationship observed between CPE-capacitance and taper damage. As the exponent of a CPE is a measure of the deviation from ideal, it makes sense that we observed an inverse relationship with alpha and corrosion severity.

In the previous analysis, it was determined that more severely corroded femoral stems had stronger taper connections, but no significant association was found for femoral heads. The head corrosion measurements derived in the current study were unable to account for variations in overall taper strength, but we did observe an increase in electrochemical determinants of corrosion for components with lower disassembly forces. Taper mechanics dictate that the force required to separate the connection is linearly related to the force with which it is assembled, but the mechano-biological environment of a replacement hip can result in deviations from this theorized behavior. In their in-vitro assessment, Pennock *et al.* reported a maximum disassembly force of 3.42 kN, which suggests that all components in the high taper strength category exhibited some in-vivo adhesion mechanism[12]. We were unable to distinguish electrochemical differences between taper strength cohorts however, thus the relative contribution of corrosion to this behavior is unclear.

This study demonstrates the feasibility of electrochemical measurements to determine the severity of clinically relevant corrosion for CoCrMo femoral heads. EIS provides a method to quantitatively evaluate corrosion without the subjectivity associated with visual scoring approaches. Additionally, the significant associations observed between these electrochemical corrosion measures and taper strength highlight the potential of using continuous

variables to design studies with smaller sample sizes and greater statistical power. Furthermore, these results support our earlier findings that corrosion may be associated with increased taper strength.

References

1.   Hothi HS, Matthies AK, Berber R, Whittaker RK, Skinner JA, Hart AJ. The reliability of a scoring system for corrosion and fretting, and its relationship to material loss of tapered, modular junctions of retrieved hip implants. *The Journal of arthroplasty.* 2014;29(6):1313-1317.

2.   Higgs G, Hanzlik J, MacDonald D, et al. Method of characterizing fretting and corrosion at the various taper connections of retrieved modular components from metal-on-metal total hip arthroplasty. *Metal-on-metal total hip replacement devices*: ASTM International; 2013.

3.   Higgs GB, Hanzlik JA, MacDonald DW, Gilbert JL, Rimnac CM, Kurtz SM. Is Increased Modularity Associated With Increased Fretting and Corrosion Damage in Metal-On-Metal Total Hip Arthroplasty Devices?: A Retrieval Study. *The Journal of arthroplasty.* 2013;28(8):2-6.

4.   Ko LM, Chen AF, Deirmengian GK, Hozack WJ, Sharkey PF. Catastrophic femoral head-stem trunnion dissociation secondary to corrosion. *JBJS.* 2016;98(16):1400-1404.

5.   Lange J, Wach A, Koch CN, et al. Do Well-functioning THAs Retrieved at Autopsy Exhibit Evidence of Fretting and Corrosion? *Clinical Orthopaedics and Related Research®.* 2018;476(10):2017-2024.

6.   Kocagoz SB, Underwood RJ, MacDonald DW, Gilbert JL, Kurtz SM. Ceramic Heads Decrease Metal Release Caused by Head-taper Fretting and Corrosion. *Clinical Orthopaedics and Related Research®.* 2016;474(4):985-994.

7.   Gotman I. Characteristics of metals used in implants. *Journal of endourology.* 1997;11(6):383-389.

8.   Allen R. Standard practice for surface preparation and marking of metallic surgical implants (F86). *Annual Book of ASTM Standards, Medical Devices and Services.* 1998.

9.   Loveday D, Peterson P, Rodgers B. Evaluation of organic coatings with electrochemical impedance spectroscopy. *JCT coatings tech.* 2004;8:46-52.

10.   Akbarinezhad E, Bahremandi M, Faridi H, Rezaei F. Another approach for ranking and evaluating organic paint coatings via electrochemical impedance spectroscopy. *Corrosion Science.* 2009;51(2):356-363.

11.   Arulepp M, Permann L, Leis J, et al. Influence of the solvent properties on the characteristics of a double layer capacitor. *Journal of Power Sources.* 2004;133(2):320-328.

12.   Pennock AT, Schmidt AH, Bourgeault CA. Morse-type tapers: factors that may influence taper strength during total hip arthroplasty. *The Journal of arthroplasty.* 2002;17(6):773-778.

V. Nondestructive Identification of Subsurface Corrosion Features

5.1 Abstract

Orthopedic alloys undergo a variety of *in vivo* corrosion mechanisms, some of which may penetrate into the structure beneath the surface. This study builds from the quantitative evaluation of corrosion severity provided by electrochemical impedance spectroscopy to assess whether the technique could distinguish corrosion damage features. Ten (10) severely corroded components previously characterized with EIS were visually examined using optical and scanning electron microscopy, then grouped according to corrosion damage features. The majority of components exhibited mechanically-dominated damage, while evidence of electrochemically-dominated damage was observed on four (4) components. Components with electrochemical damage were found to have significantly lower $|Z_{0.002Hz}|$ and higher CPE-capacitance. Metallographic inspection of the electrochemically-dominated cohort identified subsurface penetration of the corrosion damage that was absent in the mechanically-dominated cohort. These results highlight the potential of EIS to distinguish corrosion damage modes and non-destructively evaluate features beneath the alloy surface.

5.2 Introduction

Although the process of taper corrosion in total hip arthroplasty (THA) is generally described as mechanically-assisted crevice corrosion, the complexity of the *in vivo* environment can result in a variety of corrosion damage features. Some of the more commonly studied corrosion modes include etching, fretting,

intergranular corrosion, pitting, film formation, and selective leaching[1,2]. There have also been reports of other damage modes such as inflammatory cell induced corrosion (ICIC), material transfer from the Ti6Al4V stem to the CoCrMo head, and imprinting – a phenomenon in which the stem taper topography is transferred to the head taper)[3-6]. These damage features have recently been categorized as being primarily mechanical (plastic deformation, fretting, material transfer), electrochemical (pitting corrosion, etching, intergranular corrosion, phase boundary corrosion, column damage) or a combination of both (fretting corrosion, formation of thick oxide films, imprinting). While taper corrosion in general remains a clinical concern, these electrochemical damage mechanisms have been shown to penetrate into the material resulting in subsurface material loss[7].

Whether these damage modes occur and the extent to which they exist can depend on a number of factors including the material of the mating stem, and the microstructure of the CoCrMo alloy. A thorough understanding of individual corrosion mechanisms is integral to designing new implants, as developing countermeasures for one damage mode has the potential to enhance another. Pre-clinical evaluation of orthopedic implants is routinely conducted by device manufacturers in an effort to obtain an understanding of how new materials and designs may behave *in vivo*. These tests are generally conducted according to systematized methodology developed and maintained by organizations such as International Organization for Standardization (ISO) and ASTM International (formerly known as the American Society for Testing and Materials). Efforts to evaluate the propensity for taper corrosion have chiefly relied on measuring

fretting currents generated under *in vivo* loading conditions[a]. Additionally, accelerated aging studies to simulate corrosion generally use visual or volumetric assessment to estimate corrosion damage severity, which provides limited information on the individual corrosion damage features that are present. Thus, the extent to which *in vitro* studies of simulated corrosion accurately represents the distinct *in vivo* phenomena that threaten implant longevity is unclear.

In our previous work, we showed that electrochemical impedance spectroscopy (EIS) can provide a quantitative measure of corrosion severity. The purpose of this study was to assess whether electrochemical assessment could be used to distinguish clinically-relevant corrosion damage features. Mathematically, the surface area of an electrode is inversely proportional to its impedance and directly proportional to its capacitance. Under this premise, corrosion damage that penetrates into the bulk material may be quantitatively identified from the increased effective area of the electrode. Thus, we anticipate that EIS could be used to identify electrochemically-dominated corrosion damage with subsurface features. A secondary goal of this work was to determine if these distinct corrosion damage features had a differential effect on the strength of the taper connection.

5.3 Methods

<u>Nondestructive Evaluation of Corrosion Damage Features</u>

Ten (10) severely corroded CoCrMo femoral heads were previously assessed using electrochemical impedance spectroscopy under the frequency domain.

Prior to electrochemical characterization, the taper surfaces were imaged using optical microscopy for a preliminary evaluation of corrosion damage features. Corrosion was identified as black deposits, white or shiny haziness, and discoloration[b]. Imprinting (cases in which the rougher topography of the stem taper imprinted into the smoother head taper) was also determined using optical microscopy. After EIS analysis, the taper surfaces for seven (7) components were further investigated with scanning electron microscopy. Specifically, evidence of damage features described by Hall *et al.*[c] were assessed: plastic deformation (local flattening of machining mark peaks), pitting corrosion (large accumulation of round pits with size range 0.1–12μm), intergranular or phase boundary corrosion (large areas of material dissolution along grain/phase boundaries), fretting damage (roughened appearance of CoCrMo substrate and/or fine ridges that stretched roughly along the taper axis), etching (visible slip planes, fine grain structure, and twin boundaries), oxide films/deposits (thick flake-like deposits of chromium or titanium oxide), and column damage (column-like banded pattern that stretched in the proximal-distal direction). Components were then grouped according to whether or not they exhibited evidence of chemically-dominated damage features (pitting corrosion, etching, intergranular corrosion, phase boundary corrosion, column damage).

Destructive Evaluation of Corrosion Damage Features

For a more thorough assessment of the taper surfaces, two (2) components from each group were sectioned in the longitudinal direction along the head-taper axis using a cutoff saw with abrasive wheels. With this unobstructed access to the taper, the surfaces were imaged with SEM and elemental evaluation was

conducted using energy dispersive X-ray spectroscopy (EDS). EDS permitted detection of material transfer, a damage feature involving the deposit of titanium rich material from the femoral stem onto the taper surface of the CoCrMo femoral (for mixed alloy couples). To confirm subsurface features, these samples were embedded in an epoxy resin for metallographic examination. Samples were ground and polished using a standard preparation technique. Grounding was conducted sequentially, ending with a 320-grit sheet. Polishing was also done sequentially using 9-, 3-, and 1-µm diamond suspension. The polished samples were imaged using a metallurgical light microscope to evaluate the presence of damage features through the cross-section. Metallographic etching was then performed to visualize the individual grains of the samples and distinguish CoCrMo alloy microstructure (as-cast or wrought). The etchant used was composed of 95 mL hydrochloric acid, 5 mL sulfuric acid, and 3 mL nitric acid. After the etching process, the samples were re-evaluated with the light microscope for microstructural observation. In addition to grain size assessment, light microscopic images of the etched samples were used to reveal inhomogeneity of the alloy's microstructure such as banding and dendritic structures, as well as microstructural features such as slip bands (parallel, step-like features indicative of local deformation and lattice defects) and twin boundaries (parallel lines within grains)[10].

Statistical Analysis

Electrochemical determinants of corrosion (low frequency impedance, max phase angle, polarization resistance, and constant phase element (CPE) capacitance along with its associated exponent) were analyzed with respect to the observed

damage features. Differences between components with and without evidence of electrochemical damage features were assessed using Wilcoxon-Mann-Whitney test. The relationship between subsurface damage and taper strength was also evaluated: the proportion of components with subsurface corrosion in the low taper strength group (measured in the disassembly force study, and grouped for the previous electrochemical analysis) was compared to that in the high taper strength group using Fisher's exact test. Additionally, the median taper strength of those with electrochemical damage was compared to those without, using the Wilcoxon-Mann-Whitney test. For all statistical analyses, significance was determined at α=0.05.

5.4 Results

Representative images from optical microscopy assessment are revealed a number of damage features (Figure 19–Figure 28). Deposits of black debris were found on all femoral heads. Four (4) of the 10 components (40%) had areas with a white or hazy appearance, while 3/10 (30%) showed imprinting, and 2/10 (20%) had evidence of discoloration.
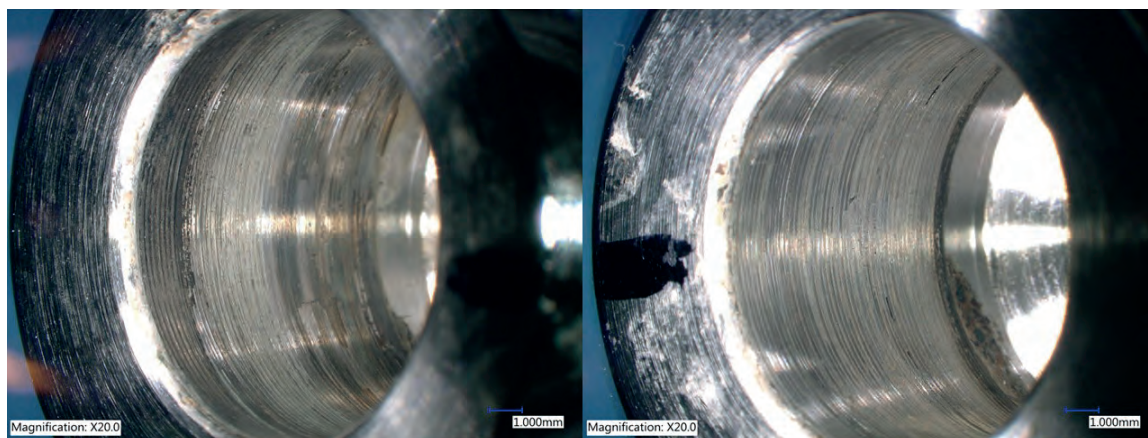
Figure 19. Optical micrographs of sample HUMC-H1087, exhibiting imprinting with dark discoloration.
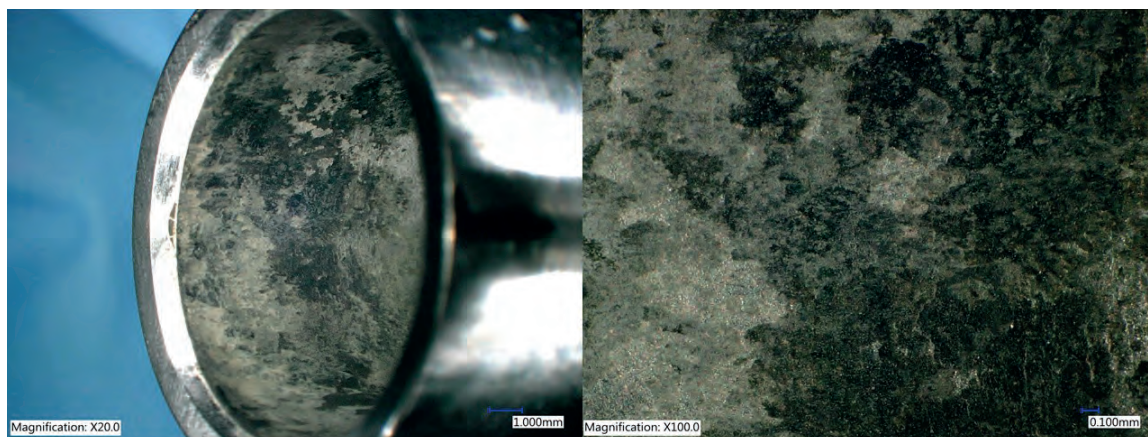
Figure 20. Optical micrographs of sample HUMC-H0658, showing areas of white haziness with black deposits.

Figure 21. Optical micrographs of sample CW-H0915, showing black deposits throughout the taper.
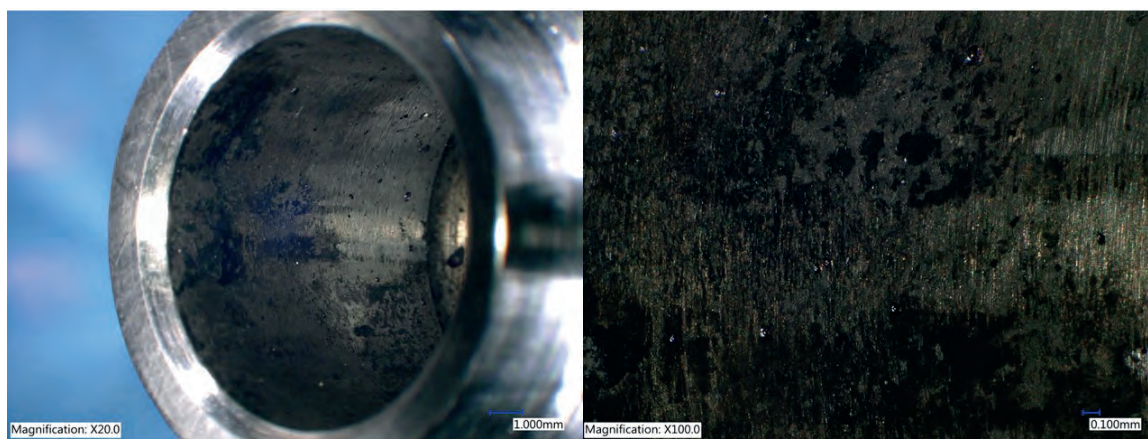
Figure 22. Optical micrographs of sample RI-H0596, showing black deposits throughout the taper.
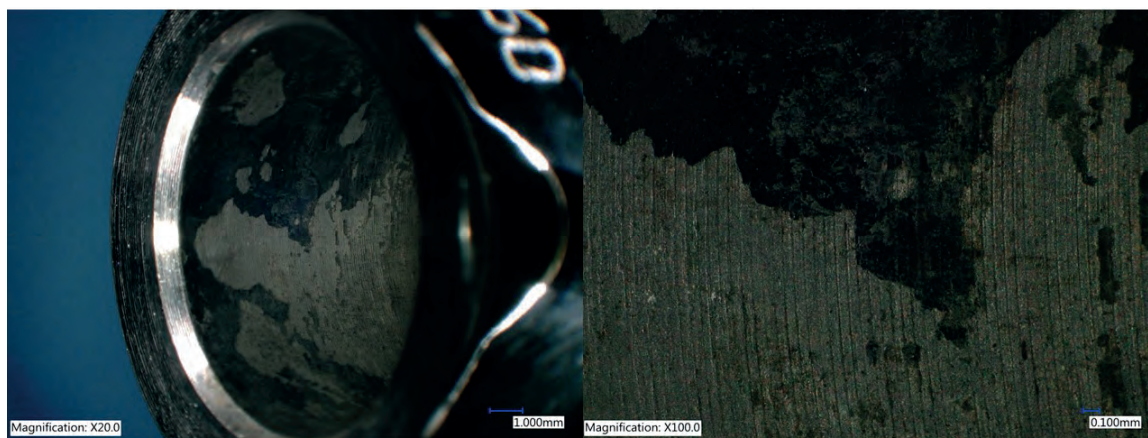
Figure 23. Optical micrographs of sample RI-H0940, showing large areas of black deposits.
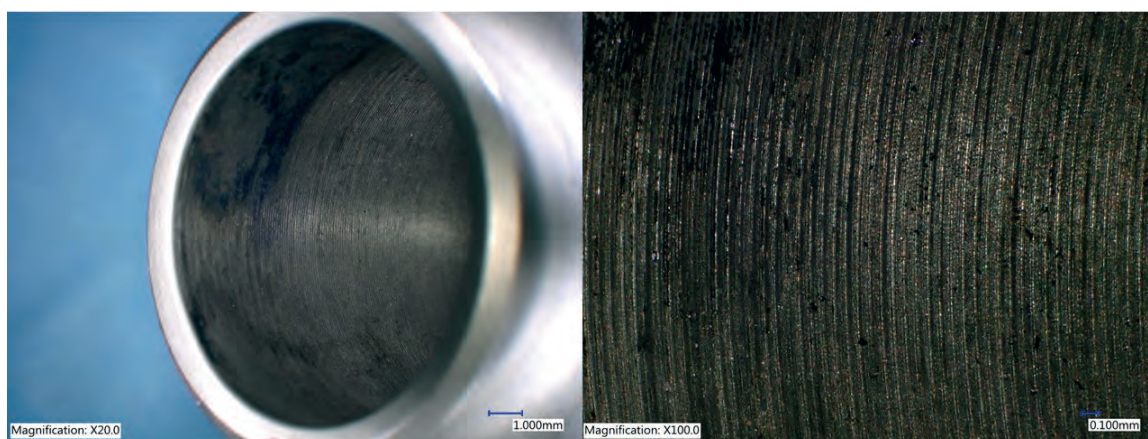
Figure 24. Optical micrographs of sample CW-H0460, exhibiting imprinting proximally with black deposits distally.

Figure 25. Optical micrographs of sample CW-H0616 exhibiting imprinting with black deposits.

Figure 26. Optical micrographs of sample CW-H0201, with black deposits proximally and areas with a shiny appearance.

Figure 27. Optical micrographs of sample RI-H0801, exhibiting proximal discoloration, black deposits and areas with a shiny appearance.

Figure 28. Optical micrographs of sample SHB-H0689, with black deposits distally and a hazy appearance throughout the taper.
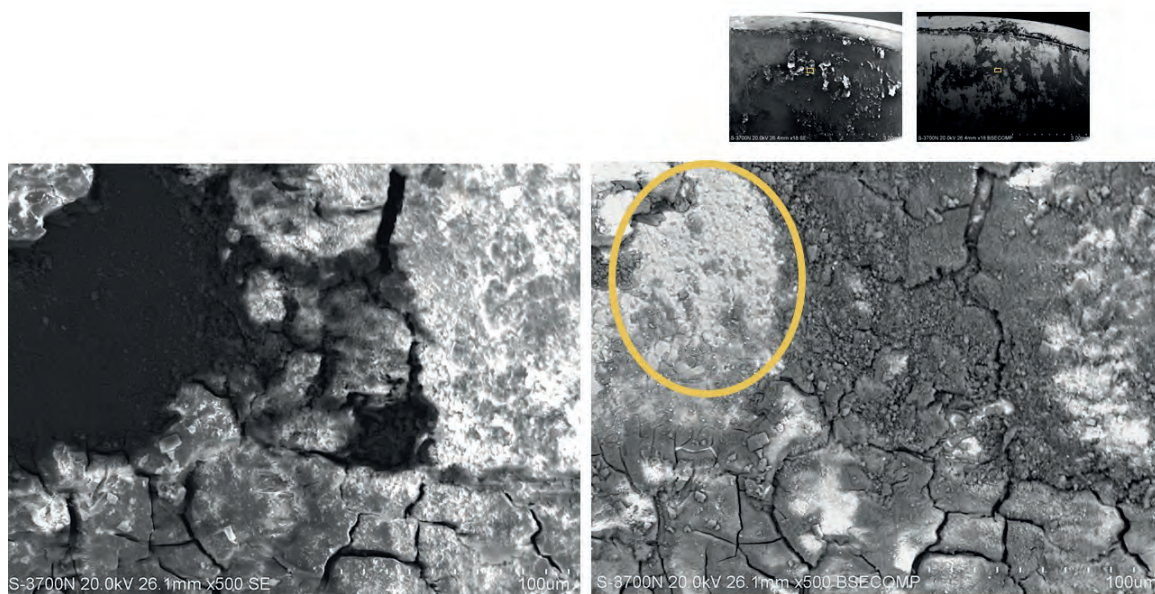
Figure 29. Scanning electron micrographs of sample HUMC-H0658 showing thick oxides with a "lake-bed" appearance overtop CoCrMo base with roughened appearance indicative of fretting (yellow oval). In the backscattered electron (BSE) image on the right, higher density materials (i.e. base alloy) appear light, while lower density materials (i.e. oxides) appear darker.
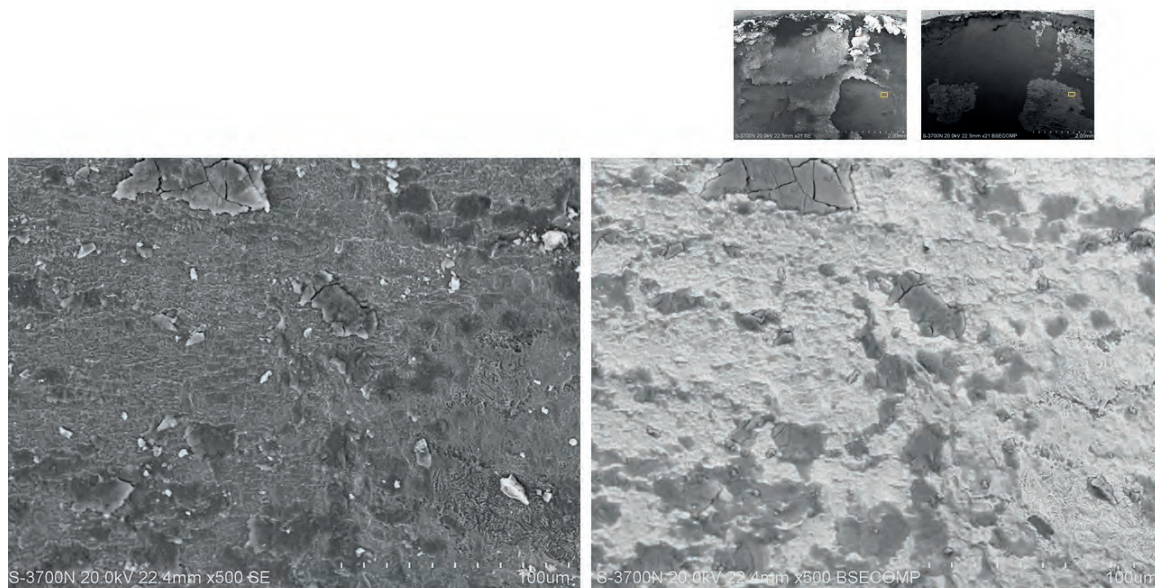
Figure 30. Scanning electron micrographs of sample RI-H0940 showing areas of thick oxide film with fretting of the CoCrMo beneath the oxide.
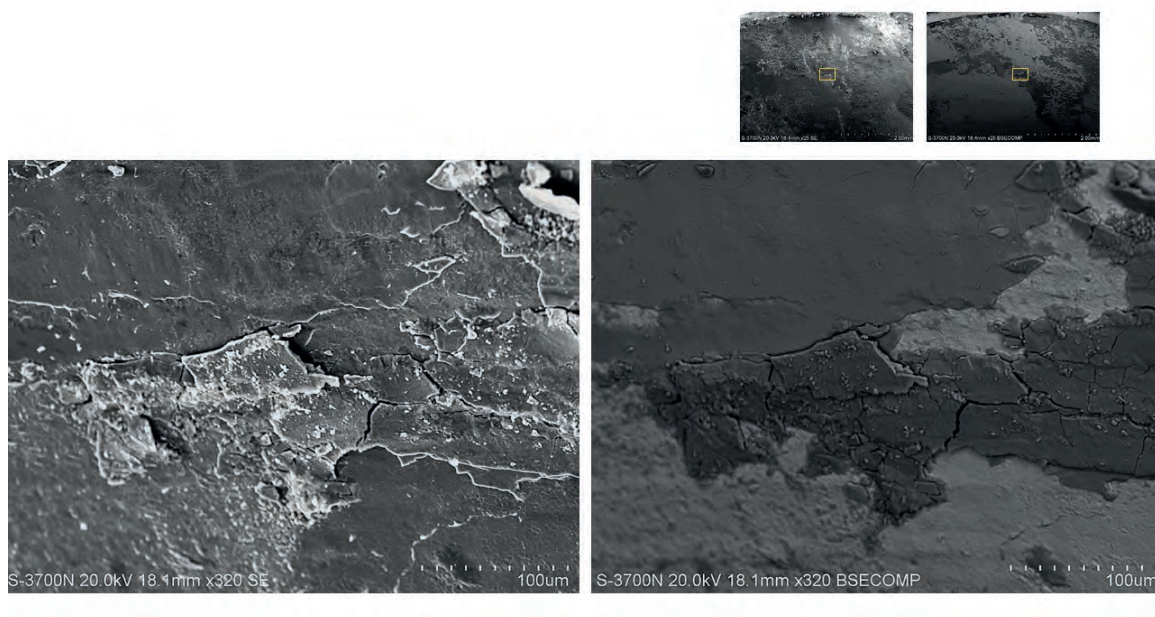
Figure 31. Scanning electron micrographs of sample RI-H0940 showing areas of thick oxide film.
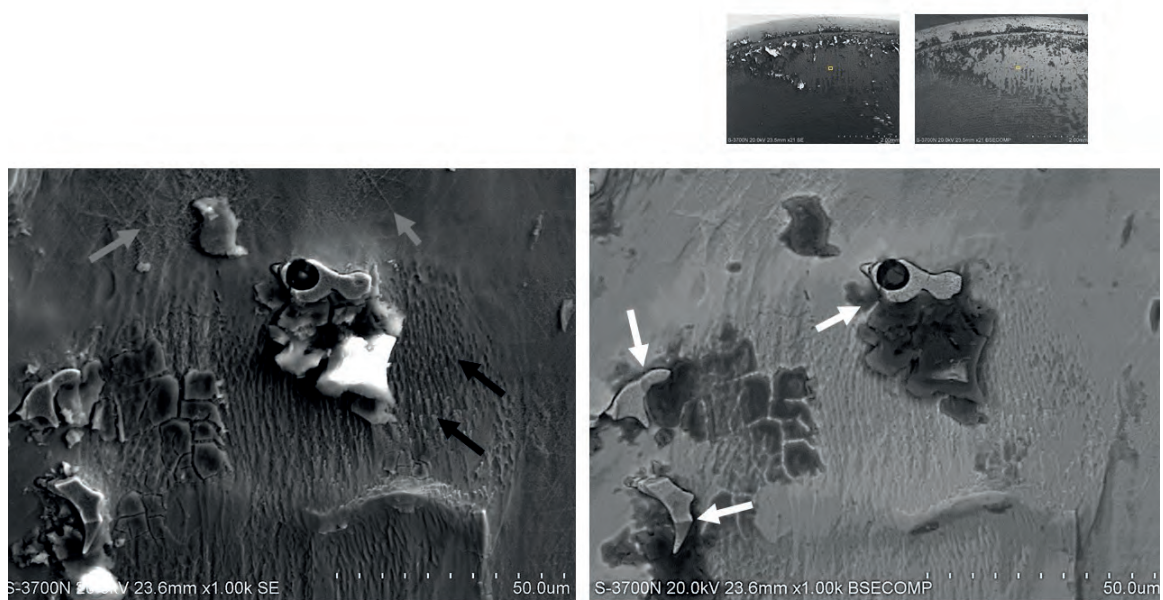
Figure 32. Scanning electron micrographs of sample CW-H0616 showing etching (gray arrows) with evidence of selective leaching (black arrows) and boundary corrosion (white arrows).
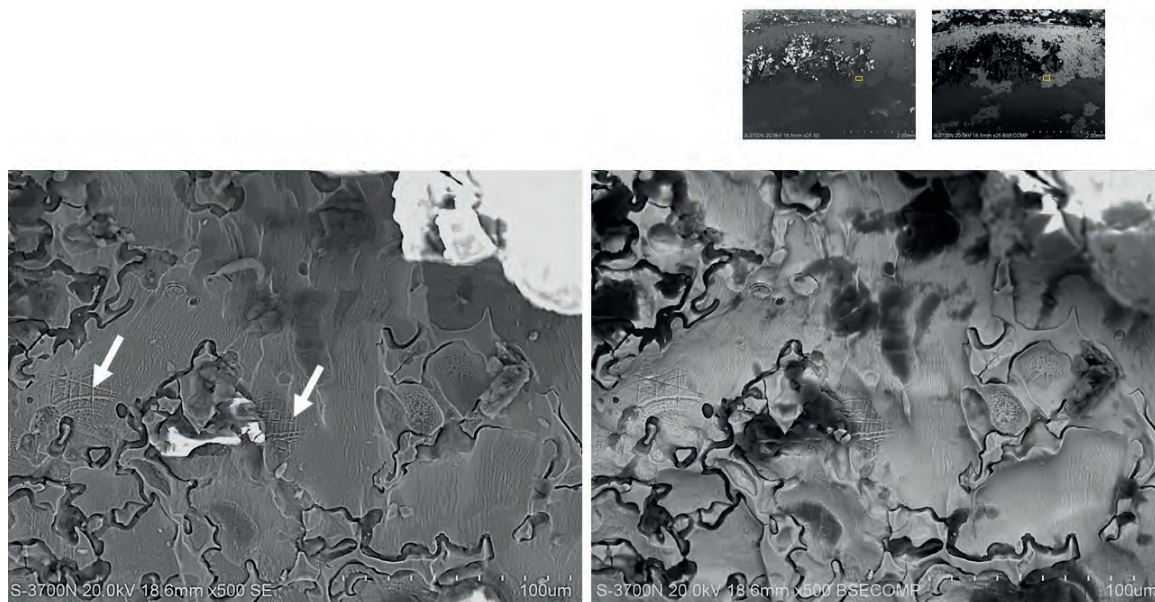
Figure 33. Scanning electron micrographs of sample CW-H0201 exhibiting etching with exposure of slip planes and deformation patterns of the crystalline microstructure (white arrows).
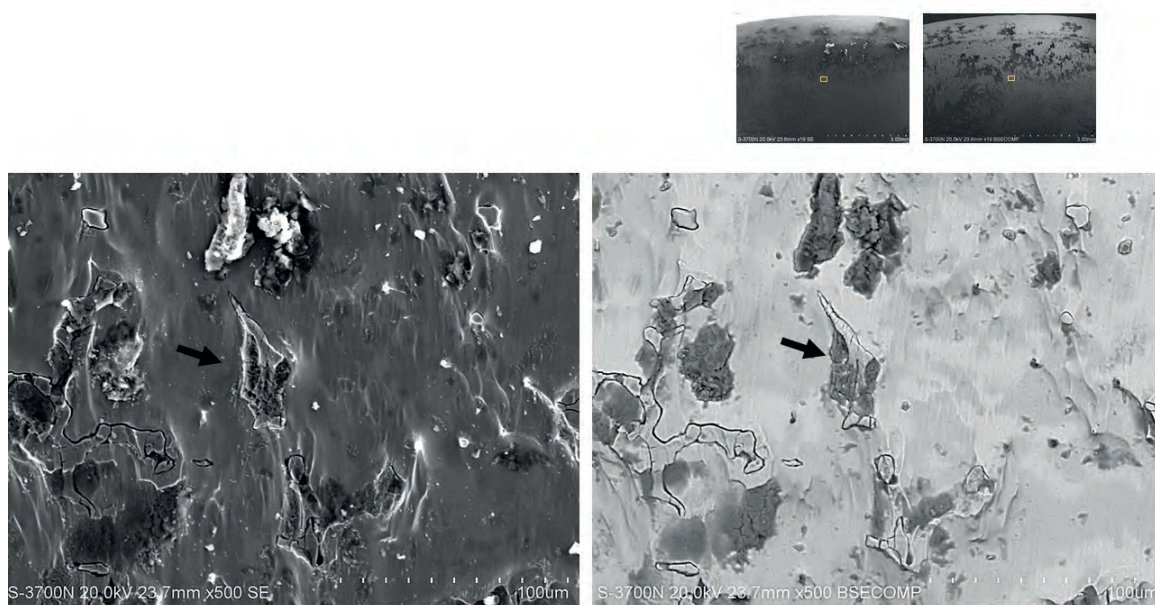
Figure 34. Scanning electron micrographs of sample RI-H0801 showing boundary corrosion with accumulation of oxide debris at the boundary (black arrows).
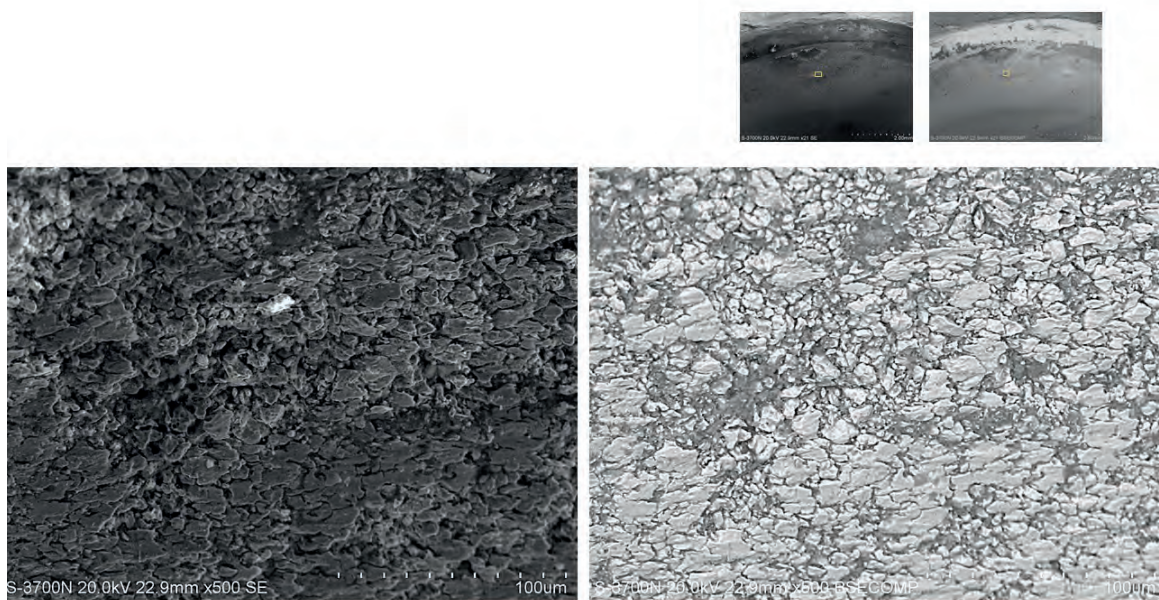
Figure 35 Scanning electron micrographs of sample SHB-H0689 showing intergranular corrosion with dissolution of the grain structure revealing grain sizes within the range of 10-20 µm.

The predominant damage features identified in the SEM analysis were thick oxide films and intergranular/phase boundary corrosion, observed on 4/7 (57%) of components. Evidence of fretting was found on 3/7 (43%) of the femoral heads, and the underlying crystal structure (indicative of etching) was visible on 2/7 (29%) components. In total, four (4) femoral heads were found to exhibit some form of electrochemical damage. The |Z-minfreq| for these components (median=1.56×10^5; IQR=$2.96\times10^5\Omega$) was found to be lower than those only exhibiting mechanical damage (median=1.29×10^6; IQR=$1.25\times10^6\Omega$; p=0.019) (Figure 36). A difference was also observed for CPE-capacitance, for which the electrochemical group (1.19×10^{-4}; IQR=4.18×10^{-4} F·s^{a-1}) had significantly higher values than the mechanical group (2.63×10^{-5}; IQR=1.08×10^{-5} F·s^{a-1}; p=0.011)

(Figure 37). No differences were observed for max phase angle (p=0.831), polarization resistance (p=0.522) or CPE-exponent (p=0.286). The significant EIS relationships were used to generate an electrochemical summary of the femoral heads assessed in this study. Log plots were used to account for the positively skewed data observed for both |Z-minfreq| and CPE-capacitance. Components exhibiting electrochemical damage features were all found to have a log CPE-capacitance >-4.4 (Figure 38).
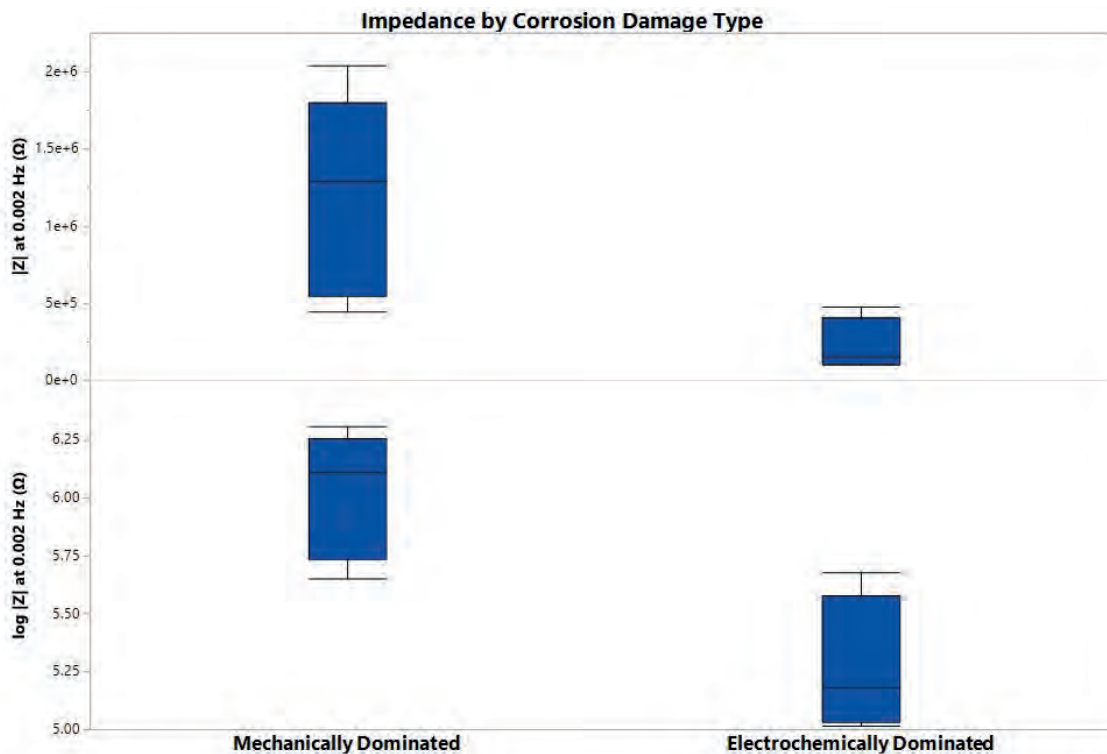
Figure 36. Box plot detailing the difference in impedance values between components exhibiting mechanically dominated damage features and those exhibiting electrochemically dominated damage. Components in the electrochemical group were found to have significantly lower impedance values (top). Log plots of impedance are shown (bottom) to represent the positively skewed impedance data
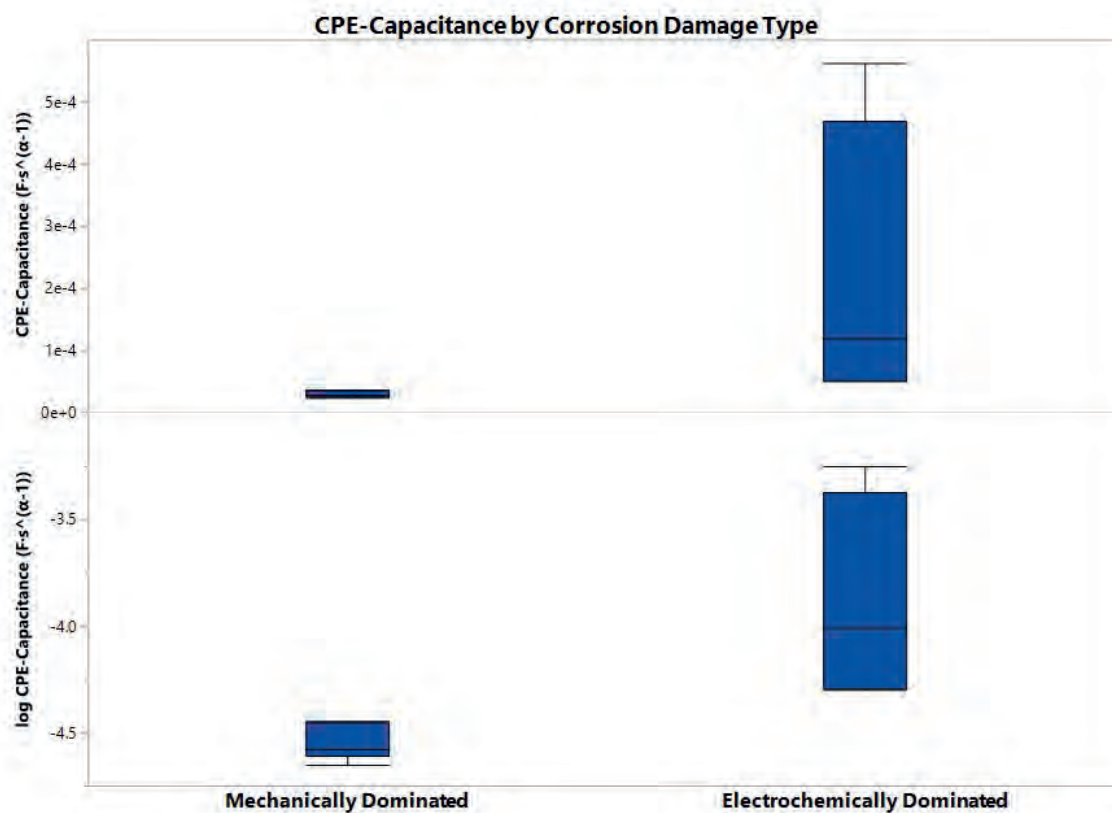
Figure 37. Box plot detailing the difference in CPE-capacitance values between components exhibiting mechanically dominated damage features and those exhibiting electrochemically dominated damage. Components in the electrochemical group were found to have significantly higher CPE-capacitance values (top). Log plots of CPE-capacitance are shown (bottom) to represent the positively skewed CPE-capacitance data.
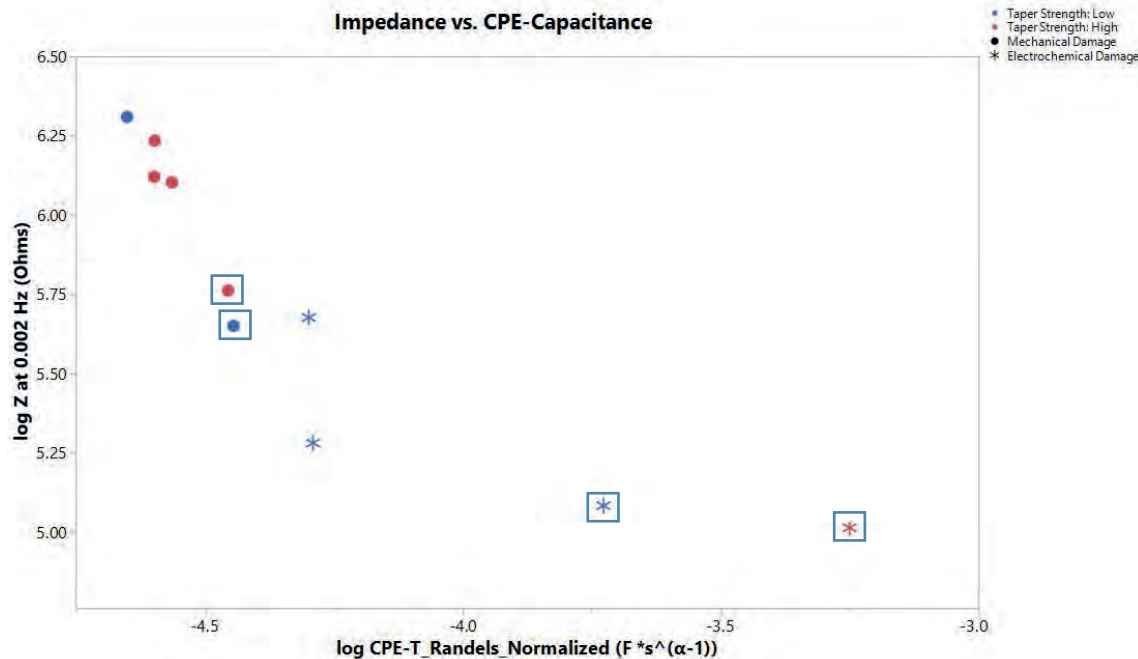
Figure 38. Scatterplot showing the monotonic log-log relationship between impedance and CPE-capacitance. Components exhibiting electrochemically dominated corrosion damage were all found to have log CPE-capacitance >-4.4. Components selected for destructive evaluation are identified by the blue boxes. A measure of taper strength (obtained in Aim I and categorized in Aim II) for these components is also shown.

Elemental analysis of a sample with electrochemical damage revealed evidence of grain boundary corrosion around molybdenum-rich grains, with the surrounding areas filled with titanium and oxygen (Figure 39). Preferential dissolution of Co over Cr was also observed. EDS spectra of the other specimen with electrochemical damage showed the presence of titanium along with aluminum, indicative of material transfer from its associated TI6Al4V stem (Figure 40). This component was also associated with characteristically high taper connection strength. Metallographic evaluation of components in this electrochemical group confirmed corrosion damage that penetrated into the subsurface of the material (Figure 41). These localized damage features exposed a

difference in the underlying microstructure of the two samples with electrochemical damage, prior to chemical etching. Such observations were absent in the mechanical group. After etching, an as-cast microstructure was confirmed for one sample from the electrochemical group, with grain sizes that exceeded 100 µm and a prevalence of dendritic structures (Figure 42). The other electrochemically-corroded sample was confirmed to be a wrought CoCrMo alloy with much smaller grains (<10 µm) and the presence of banding (Figure 43). Twin boundaries were also visible in this sample. Both samples from the mechanical group were wrought alloys with a fine grain structure that exhibited banding along with some twin boundaries and numerous slip band reliefs. These striations within the grains were indicative of the alloy having been cold worked.

Categorical analysis comparing the groups of femoral heads exhibiting the two types of corrosion damage did not reveal a significant difference with respect to the proportion of components in the two taper strength categories (p=0.524). The median taper strength of the samples with electrochemical damage features (median=3.1; interquartile range=5.5 kN) was not found to differ from that of the mechanically damaged components (median=4.8; IQR=7.7 kN; p=0.670).
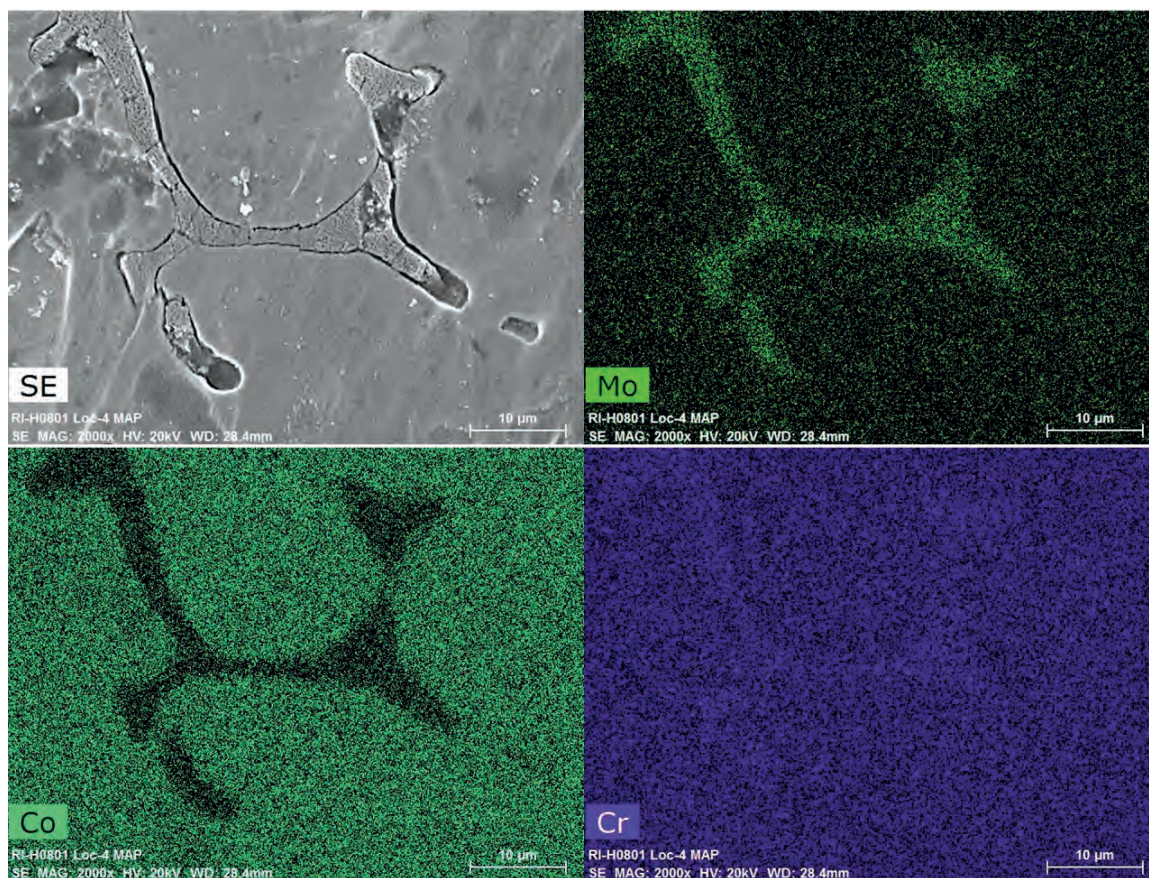
Figure 39. Scanning electron micrograph with energy dispersive spectroscopy for elemental evaluation of sample RI-H0801 showing grain boundary corrosion around molybdenum-rich grains (top), along with preferential dissolution of cobalt over chromium (bottom).
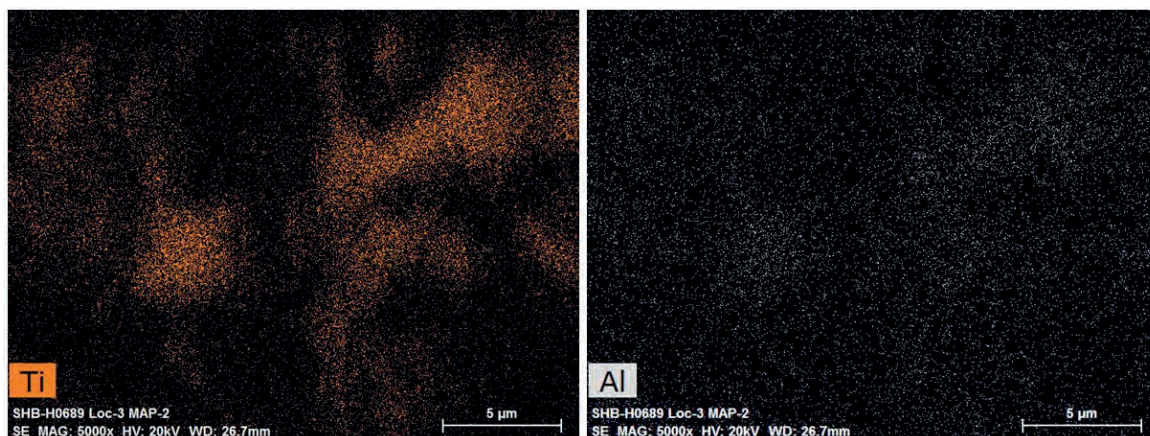
Figure 40 EDS map of SHB-H0689 showing evidence of aluminum along with titanium on the surface of the CoCrMo head taper.
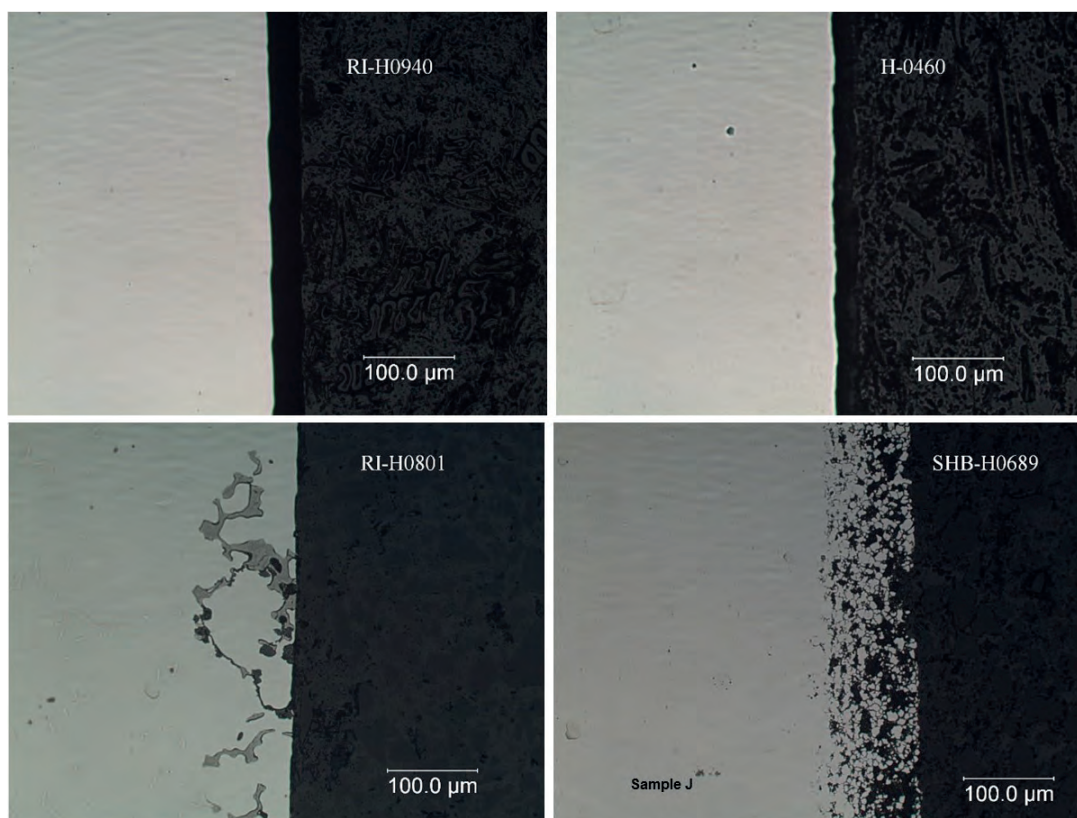
Figure 41. Optical micrographs of components sectioned for metallography. Unlike samples RI-H0940 and CW-H0460 in the mechanically damaged group, samples RI-H0801 and SHB-H0689 components exhibited boundary corrosion that extended into the subsurface, exposing differences in the microstructure of RI-H0801 (as-cast) and SHB-H0689 (wrought) in the absence of chemical etching.
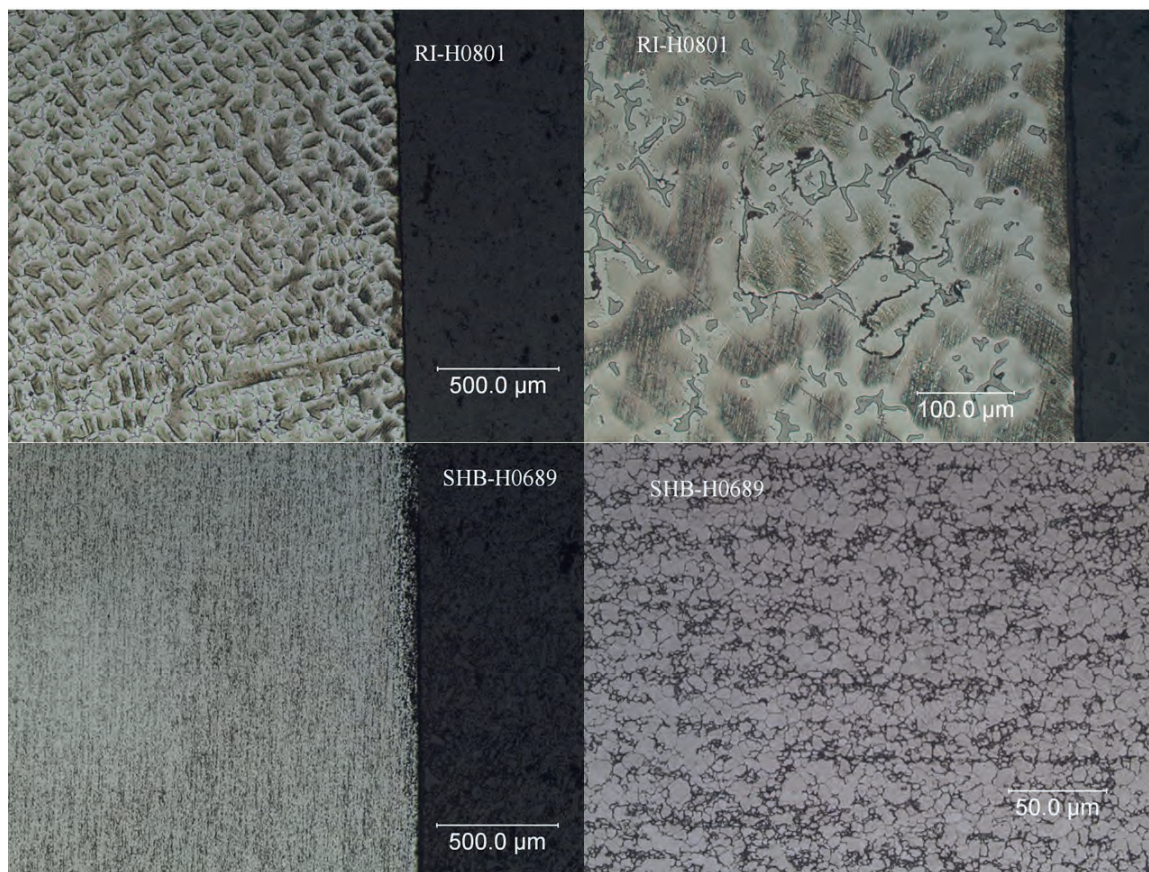
Figure 42. Optical micrographs of etched samples from the electrochemical corrosion group. An as-cast microstructure can be seen in sample RI-H0801, evident by inhomogeneity with dendritic structures (top-left) and the visible boundary around a singular large grain ~200μm (top-right). The wrought alloy microstructure of SHB-H0689 is apparent in the much finer grain structure (bottom-right) and longitudinal banding (bottom-left).
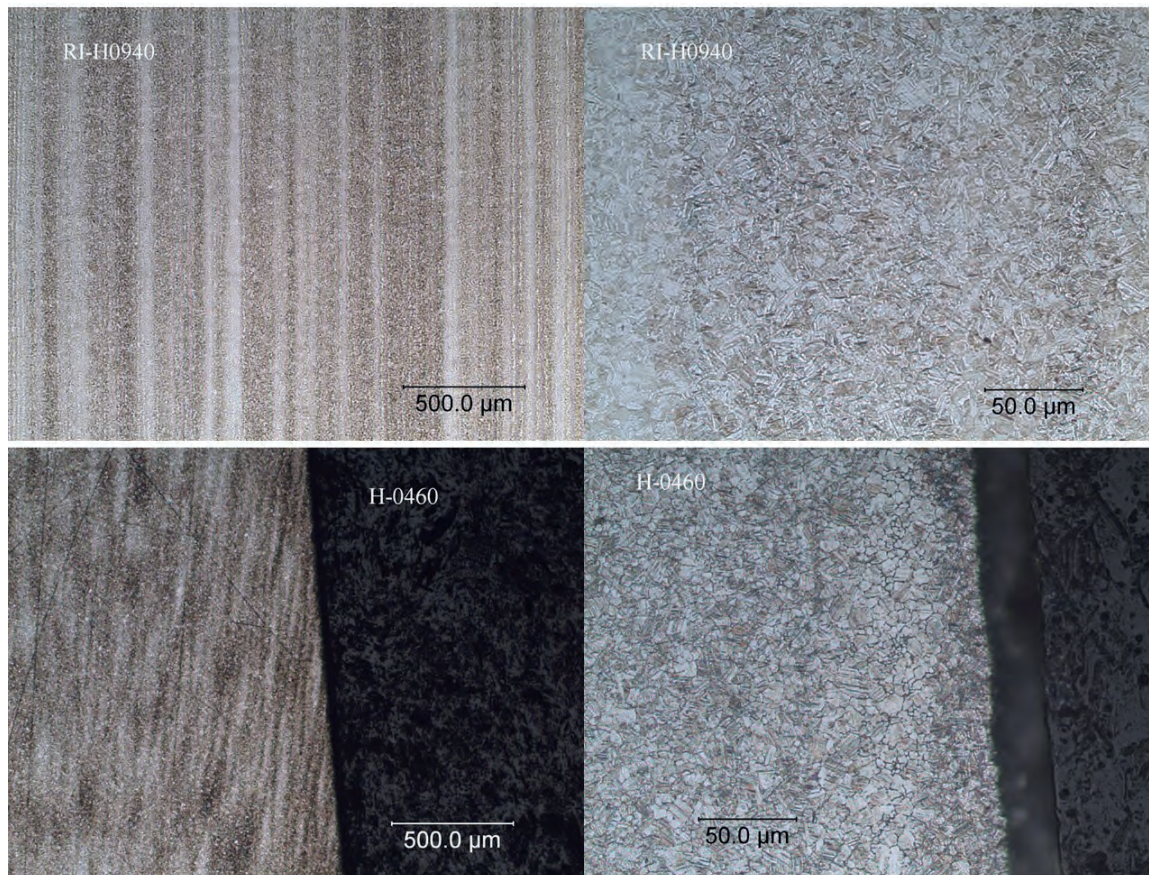
Figure 43. Optical micrographs of etched samples from the mechanical corrosion group, identifying a wrought alloy structure for both components. RI-H0940 exhibited pronounced longitudinal banding (top-left) with twin boundaries and slip lines visible at higher magnification (top-right). CW-H0460 showed off-axis longitudinal banding (top right) RI-H0940 with evidence of twin boundaries and slip lines.

5.5 Discussion

The purpose of this investigation was to identify whether electrochemical evaluation could be used to distinguish corrosion modes that occur at the taper connection of femoral heads in THA. Under the general category of corrosion, uniform corrosion occurs most commonly and describes a process that proceeds at approximately the same rate over the entire corrosion surface[11]. However, cobalt-based alloys used in orthopedics feature chromium, which imparts self-passivation properties, and molybdenum, which improves mechanical properties and local corrosion resistance[10,12,13]. Two commonly used types of CoCrMo used for THA are the as-cast alloy and the wrought alloy, which have characteristically different microstructures. The unequal cooling of the molten alloy within the mold can result in inhomogeneous microstructures for the cast alloy. This limitation is overcome in wrought alloys in which large castings are thermo-mechanically processed after being hot forged, resulting in smaller more uniform grains[14,15]. Additionally, CoCrMo alloys may feature additions of carbon, resulting in hard phases which increase wear resistance[12,13]. Localized corrosion may occur at the boundaries of these different grains/phases resulting in accelerated non-uniform attack, and analysis of retrieved CoCrMo femoral heads has shown that localized corrosion may penetrate into the subsurface[7]. The results of this study support the hypothesis that electrochemical impedance spectroscopy can identify such subsurface corrosion without the need to section the sample to confirm this phenomenon.

This study is not without limitations. Firstly, the sample size constrains our conclusions to the diversity represented within the ten femoral heads assessed by

EIS, and the four samples examined with metallographic analysis. Although implant manufacturers adhere to the mechanical and chemical specifications outlined in ASTM F75 (as-cast) and ASTM F1537 (wrought), differences in manufacturing practices can result in large variations with respect to grain size, and hard phases[10]. Furthermore, Pourzal *et al.* showed that microstructure can dictate cyclic potentiodynamic polarization behavior, and the extent to which our EIS results may be affected by this variable is unknown. Another limitation is the contact-dependent nature of EIS. In order to influence electrochemical behavior, the damage feature of interest must appreciably engage with the electrolyte (which permits the flow of current within the experimental system). In instances such as pitting corrosion, which can have large cavities with small openings, surface tension dynamics might hinder percolation of the electrolyte into the subsurface. It should also be noted that in-depth analysis of local damage features was conducted with SEM and this qualitative evaluation of the taper surface is largely dependent on sampling area. The high magnification required makes it laboriously time-consuming to thoroughly scan the entire taper surfaces for all cases, and the areas selected for assessment may not have comprehensively represented the damage features present on the components. Despite these limitations, the methods employed in this study provide a foundation to quantitatively evaluate clinical corrosion features nondestructively. Additionally, the incorporation of well-established destructive techniques allows the diagnostic value of this electrochemical approach to be demonstrated.

Of the individual damage modes assessed in this study, the predominant finding was the presence of corrosion deposits, observed on 100% of components. This supports work done by Hall *et al.* who reported the presence of oxide films/deposits on 100% of femoral heads paired with a Ti6Al4V stem, and 90% of those coupled with a CoCrMo stem[6]. Another common observation was intergranular/phase boundary corrosion, though this was only exhibited by heads paired with Ti6Al4V stems (67% of Co/Ti couples) and was more prevalent than that previously reported (7.7% Co/Ti couples). This electrochemically-dominated damage was identified as having characteristically high impedance values, and was confirmed to have subsurface penetration during metallographic evaluation. It should be mentioned that several corrosion modes can occur simultaneously, and as such, a number of damage features may be represented in EIS measurements of the entire taper. If we consider that these features are electrochemically connected in parallel, circuit theory can be used to help elucidate their combined impact on the overall impedance. Parallel impedances sum as the reciprocal, so features with the smallest impedance will dominate the overall behavior of the system. Thus, the most severe damage feature will dictate the total impedance, which may allow this technique to be used as a screening tool. The potential for EIS to evaluate penetrative corrosion has also been demonstrated by Li and colleagues[16]. This study involved inducing various degrees of localized corrosion on 2024T3 (aluminum alloy widely used as an aircraft structural material) using an alternating immersion test. Using EIS under the time domain, an inverse relationship was found between low frequency impedance and corrosion depth, which was confirmed using optical

microscopy. The results of the current study demonstrate the potential of frequency-based EIS to quantitatively identify subsurface corrosion features.

Although we did not observe significant relationships between corrosion damage features and taper strength, this qualitative analysis does shed some light on earlier results. The observation of titanium material along with aluminum (as opposed to the presence of titanium in the absence of co-alloying elements) is indicative of material transfer[6]. This may suggest that micro-joints were established between the two surfaces and is consistent with the relatively high taper connection strength that was found for this sample (>9.5 kN). The subsurface corrosion on this component was most severe proximally and distally, which may have resulted from toggling of the femoral head on the stem *in vivo*. Our results also highlighted microstructural consequences of corrosion. The observed preferential dissolution of cobalt around molybdenum rich areas may be indicative of micro-galvanic corrosion. It has been proposed that such boundaries may act as a sacrificial anode and protect the rest of implant material from corrosion[17,18]. From our observation of this unetched as-cast sample however, corrosion penetrating to the subsurface appeared to occur along these boundaries. This inhomogeneity can be reduced with thermomechanical treatment, but all of the wrought alloys in our study were found to exhibit longitudinal bands after etching. This banded microstructure has been linked to local molybdenum depletion leading to column damage, and has been associated with inferior corrosion behavior[10,19].

This study demonstrates the value of electrochemical impedance spectroscopy as a tool to distinguish between different types of corrosion that can occur at the taper connection of CoCrMo femoral heads *in vivo*. This technique leverages the area-dependent characteristic of impedance behavior to detect corrosion damage features that penetrate into the subsurface of the material. As the orthopedic community works toward the development of more predictive pre-clinical evaluation methods, these results may prove to be useful as a quantitative framework for a variety of clinically relevant corrosion features, to which *in vitro* studies of simulated corrosion may be compared. This nondestructive technique supports observations from the unetched evaluation, highlighting some potential for this method to be used in instances where traditional metallographic inspection may not be feasible. Additional work with a greater number of samples is necessary to determine the whether impedance measurements can be leveraged to gain insight into microstructural differences among these alloys.

References

1. Gilbert JL, Buckley CA, Jacobs JJ. In vivo corrosion of modular hip prosthesis components in mixed and similar metal combinations. The effect of crevice, stress, motion, and alloy coupling. *Journal of biomedical materials research.* 1993;27(12):1533-1544.

2. Goldberg JR, Gilbert JL, Jacobs JJ, Bauer TW, Paprosky W, Leurgans S. A multicenter retrieval study of the taper interfaces of modular hip prostheses. *Clinical orthopaedics and related research.* 2002;401:149-161.

3. Bishop N, Witt F, Pourzal R, et al. Wear patterns of taper connections in retrieved large diameter metal-on-metal bearings. *Journal of Orthopaedic Research.* 2013;31(7):1116-1122.

4. Van Citters D, Martin A, Currier J, Park S-H, Edidin A. Factors related to imprinting corrosion in modular head-neck junctions. *Modularity and Tapers in Total Joint Replacement Devices*: ASTM International; 2015.

5. Gilbert JL, Sivan S, Liu Y, Kocagöz SB, Arnholt CM, Kurtz SM. Direct in vivo inflammatory cell‐induced corrosion of CoCrMo alloy orthopedic implant surfaces. *Journal of Biomedical Materials Research Part A.* 2015;103(1):211-223.

6. Hall DJ, Pourzal R, Lundberg HJ, Mathew MT, Jacobs JJ, Urban RM. Mechanical, chemical and biological damage modes within head‐neck tapers of CoCrMo and Ti6Al4V contemporary hip replacements. *Journal of Biomedical Materials Research Part B: Applied Biomaterials.* 2018;106(5):1672-1685.

7. Mali SA. *Mechanically assisted corrosion performance of metallic biomaterials: Implant retrieval, material analyses and device testing*, Syracuse University; 2015.

8. ASTM F. 98 (Reapproved 2004). *Standard Practice for Fretting Corrosion Testing of Modular Implant Interfaces: Hip Femoral Head-Bore and Cone Taper Interface.* 1875.

9. Higgs G, Hanzlik J, MacDonald D, et al. Method of characterizing fretting and corrosion at the various taper connections of retrieved modular components from metal-on-metal total hip arthroplasty. *Metal-on-metal total hip replacement devices*: ASTM International; 2013.

10. Pourzal R, Hall DJ, Ehrich J, et al. Alloy microstructure dictates corrosion modes in THA modular junctions. *Clinical Orthopaedics and Related Research®.* 2017;475(12):3026-3043.

11. Crolet J. Mechanisms of uniform corrosion under corrosion deposits. *Journal of materials science.* 1993;28(10):2589-2606.

12. Sinnett-Jones P, Wharton J, Wood R. Micro-abrasion–corrosion of a CoCrMo alloy in simulated artificial hip joint environments. *Wear.* 2005;259(7-12):898-909.

13. Bellefontaine G. *The corrosion of CoCrMo alloys for biomedical applications*, University of Birmingham; 2010.

14. Berry G, Bolton JD, Brown JB, McQuaide S. The production and properties of wrought high carbon Co-Cr-Mo alloys. *Cobalt-Base Alloys for Biomedical Applications*: ASTM International; 1999.

15. Lee S-H, Takahashi E, Nomura N, Chiba A. Effect of carbon addition on microstructure and mechanical properties of a wrought Co–Cr–Mo implant alloy. *Materials transactions.* 2006;47(2):287-290.

16. Li D, Hu Y, Guo B. Study on the evaluation of localized corrosion of 2024T3 aluminum alloy with EIS. *Materials Science and Engineering: A.* 2000;280(1):173-176.

17. Talbot DE, Talbot JD. *Corrosion science and technology.* CRC press; 2018.

18. Panigrahi P, Liao Y, Mathew MT, et al. Intergranular pitting corrosion of CoCrMo biomedical implant alloy. *Journal of Biomedical Materials Research Part B: Applied Biomaterials.* 2014;102(4):850-859.

19. Hall D, McCarthy S, Ehrich J, et al. Imprinting and column damage on CoCrMo head taper surfaces in total hip replacements. *Beyond the Implant: Retrieval Analysis Methods for Implant Surveillance*: ASTM International; 2018.

Conclusions and Future Work

This body of work provides a practical, albeit indirect assessment of the link between immune system activity and *in vivo* taper corrosion, assesses the effect of clinical contributors to corrosion, and elucidates corrosion's impact on the mechanical performance of the taper interface. Additionally, it establishes a quantitative metric for a phenomenon that has predominantly been assessed qualitatively. The use of impedance spectroscopy may allow for more quantitative evaluation of results from electrochemical interactions at the taper surface, providing unique insights into the oxide behavior of the passivated film. This novel approach can be leveraged for earlier detection of corrosion as well as non-destructive identification of sub-surface corrosion features during preclinical testing and design evaluation.

In the first few sections of this dissertation, the use of retrievals to understand the *in vivo* performance of modular head-neck tapers was highlighted. Despite their limitations, artificial joints have revolutionized the treatment of arthritic and injured joints over the last century by allowing for increased patient activity, decreased comorbidities, and improved quality of life. In an effort to improve *in vivo* performance, medical device companies have constantly innovated, providing new and improved devices. Unfortunately, pre-clinical testing and even limited clinical trials, cannot always predict what the impact on patients will be when the product becomes commercially available[1]. With this consideration, the FDA has increased their focus on real world evidence, which includes electronic medical records, insurance claims information, and even social media data[2]. Real-world evidence has been practically employed to

facilitate regulatory approvals, as well as post-market surveillance requirements. Thus, methods to accurately capture how these devices are changing in the body remains paramount, as there are a host of different implant designs that can be challenging to assess in the context of patient and surgical variables. The Implant Research Center at Drexel University has partnered with hospitals around the United States to collect retrieved implants from revision surgeries in an effort to identify and troubleshoot the mechanisms that necessitate a revision. By using this collection of implants that includes over 8000 devices, the current work has demonstrated the potential of large-scale retrieval analysis. While incorporating techniques of epidemiology into engineering evaluation, these analyses have facilitated a deeper look into the specific factors that affect implant performance, and may provide a potential source of real world evidence to help guide implant design. The use of this retrieval dataset to confirm some of the findings of national databases, such as increased risk of infection for older patients, male sex, increased BMI and previous revision surgery, is promising. Additionally, it was identified that clinical factors that increase the risk of implant corrosion may include male gender and white race. Ultimately, the approaches detailed here may serve as tools to help design the best implants for specific demographics, and thus move toward using real world evidence as an opportunity for data-driven technological advancements.

One motivation for this work was the increase in clinical reports of gross trunnion failure (GTF), which results in the release of a large but generally unknown quantity of metallic debris into the patient[5,6]. Although a validated technique to measure material loss for femoral stem tapers has been developed[7],

the method relies on features of the taper that may not be present after GTF (Figure 44a). While not an objective of the overall study, a preliminary technique was developed to estimate material loss for femoral stems with a wear pattern that precludes analysis using currently recognized techniques. Nine (9) femoral stems with GTF were identified in the available retrieval collection. Mean patient age at implantation was 58 years (range, 40 to 73 years) and implantation time averaged 9.06 ± 1.8 years (range, 7.3 to 12.5 years). Based on femoral stem catalog numbers, each case was matched to a femoral stem with negligible wear to serve as its control. A polyurethane replica of the proximal stem was created for each case and each control by first creating a silicone negative mold, into which the polyurethane resin was poured and allowed to harden (Smooth-On, Inc.; Macungie, PA). The replicas were then scanned using micro-computed tomography (μCT 80, Scanco Medical; Brüttisellen, Switzerland) and each case was registered against its respective control (Figure 44b). The registrations were clipped 30 mm distally from the proximal tip of the unworn taper and the estimated material loss was taken as the difference in volume between the clipped registrations of each pair of case and control replicas. To assess the integrity of the replicas as a surrogate for the actual component, one femoral stem with a case of GTF, along with its respective control, was scanned directly using high powered micro-computed tomography (X50, North Star Imaging; Rogers, MN) and material loss was estimated as previously described (Figure 44c). The mean estimated material loss of the GTF replicas was 937 ± 847 mm^3 (range, 314 to 2535 mm^3). The component measured using both methods was found to have an estimated wear of 529 mm^3 based on scans of the replica, and an estimated wear of 488 mm^3 using direct scans of the component. This estimated

material loss from the GTF components was more than 3 orders of magnitude larger than the mean wear volume recently reported for a cohort of 28 retrieved stems without GTF (0.14mm3 (range, 0.04 to 0.28 mm³))[5]. One benefit of estimating wear from polyurethane replicas of the components is that lower powered microCT units, unable to penetrate the alloys used in femoral stems, may be used to estimate material loss. The initial results from the method of direct measurement revealed an 8% difference in the wear, compared to that which was estimated using the replicas. Further validation of this technique using components with known material loss is warranted. Nevertheless, the use of micro-computed tomography to evaluate *in vivo* damage of femoral tapers in THRs is promising and may be worth additional investigation.
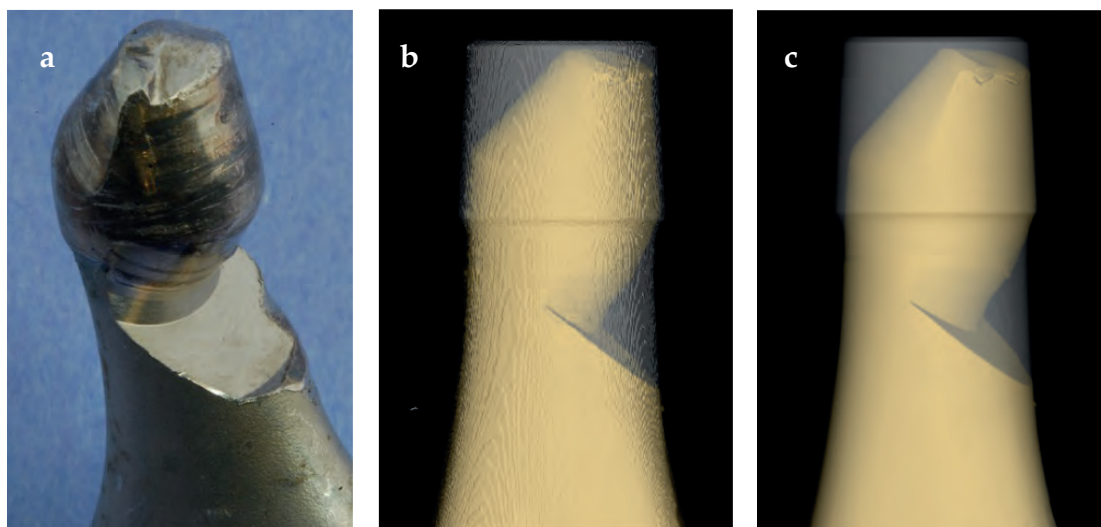
Figure 44. Picture of a component with GTF (a), 3-D registrations for scans of the replicas (b) and direct scans of the components (c). Material loss (taken as the difference in volume between the case and control) was estimated to be 529 mm³ based on scans of the replica (b), and 488 mm³ based on direct scans of the component (c).

The findings of this dissertation dovetail with ongoing efforts to better understand the *in vivo* performance of orthopedic devices. The FDA expects manufacturers to use the total product life cycle to develop products. As part of that process, there is a need to examine the clinical performance of devices and compare that clinical performance to that which is derived during verification and validation of the device. The electrochemical methods developed here may serve as tools that can be incorporated into ongoing efforts at standardization bodies such as ASTM International and the International Organization for Standardization (ISO), to regularize methods that evaluate corrosion at modular taper interfaces. In addition to the techniques already outlined in this body of work, our collection of explanted THR systems was leveraged for the purpose of validating preclinical testing methodology. It was postulated that insights into the ongoing concern of *in vivo* taper damage might be obtained by incorporating

standard electrochemical equipment into a mechanical test configuration to measure the corrosion behavior at modular metallic interfaces. To demonstrate this, an MTS Acumen Electrodynamic Test System (MTS Systems Corporation; Eden Prairie, MN) was adapted to simulate physiological loading of explanted hip components by applying custom fixtures, designed to accommodate the specimen orientation guidelines of ISO 7206. To measure the corrosion behavior during loading, a Gamry 600 potentiostat (Gamry Instruments; Warmister, PA) was used in conjunction with the mechanical test system. The potentiostat was arranged as a three-electrode system: a loaded femoral explant (working electrode), a carbon counter electrode, and an Ag/AgCl reference electrode. The explant used to evaluate this configuration comprised a Zimmer Versys Ti6Al4V stem and 32 mm CoCr head couple that was retrieved from a cadaveric donor. After the specimen was potted, 0.01 M PBS was added to the proximal test chamber such that the head-neck interface of the explant was submerged. Electrodes were added to the solution and the system was allowed to stabilize for one hour. The explant was then held at a constant potential (-50 mV vs. Ag/AgCl) and subjected to ten 3-minute increments of 2 Hz cyclic loading, with the max load at each stage increasing from 600N to 2.9 kN. The resulting current was measured at a sampling rate of 10 points/second and the load to initiate fretting was identified as the loading period where the generated current exceeded system noise (1 μA).
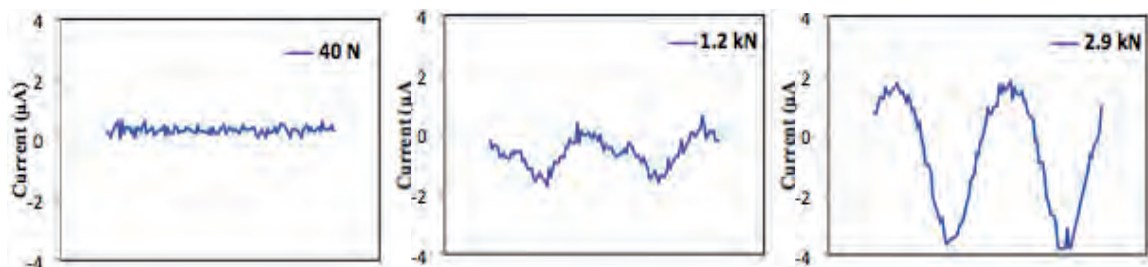
Figure 45. Increased fretting current was observed with increased cyclic load. The load to initiate fretting was 1.2 kN

The fretting current (measured as the height of the waveform) was found to increase with greater cyclic load (Figure 45). The maximum fretting current was 5.6 μA and was measured during the 2.9 kN loading period. The load to initiate fretting was 1.2 kN. The observed current generation is consistent with the MACC theory: breakdown of the interfacial passive layer during loading, resulting in repassivation reactions and the liberation of electrons. Evaluating explanted medical devices with minimal manipulation may provide unique insight into their "as-implanted" behavior. The femoral explant was mounted within an electrodynamic test frame, with no need for major destructive preparation of the sample. These results encourage further testing with additional retrievals to gain a more thorough understanding of *in vivo* device performance.

In summary, this body of work distills a number of approaches that all work toward understanding the impact of head-neck taper corrosion on the *in vivo* performance of this modular interface. It must be emphasized that these analyses are generally limited by implant selection and the availability of clinical information. Nevertheless, the interdisciplinary approach was able to corroborate trends observed in larger database studies, while also identifying

previously unreported patient demographics that may be at risk for increased corrosion at the modular head-neck taper. Furthermore, the electrochemical corrosion assessments provide opportunities for more comprehensive evaluation of corrosion, whether for retrieved implants or for *in vitro* preclinical testing.

References

1.   Redberg RF. Improving the Safety of High-Risk Medical Devices. *DePaul L Rev.* 2018;68:327.

2.   Jarow JP, LaVange L, Woodcock J. Multidimensional evidence generation and FDA regulatory decision making: defining and using "real-world" data. *Jama.* 2017;318(8):703-704.

3.   Banerjee S, Cherian JJ, Bono JV, et al. Gross trunnion failure after primary total hip arthroplasty. *The Journal of arthroplasty.* 2015;30(4):641-648.

4.   Ko LM, Chen AF, Deirmengian GK, Hozack WJ, Sharkey PF. Catastrophic Femoral Head-Stem Trunnion Dissociation Secondary to Corrosion. *J Bone Joint Surg Am.* 2016;98(16):1400-1404.

5.   Spanyer J, Hines J, Beaumont CM, Yerasimides J. Catastrophic Femoral Neck Failure after THA with the Accolade® I Stem in Three Patients. *Clinical Orthopaedics and Related Research®.* 2016;474(5):1333-1338.

6.   Talmo CT, Sharp KG, Malinowska M, Bono JV, Ward DM, Lareau J. Spontaneous modular femoral head dissociation complicating total hip arthroplasty. *Orthopedics.* 2014;37(6):e592-e595.

7.   Kocagoz SB, Underwood RJ, MacDonald DW, Gilbert JL, Kurtz SM. Ceramic Heads Decrease Metal Release Caused by Head-taper Fretting and Corrosion. *Clinical Orthopaedics and Related Research®.* 2016;474(4):985-994.

8.   Bone MC, Sidaginamale RP, Lord JK, et al. Determining material loss from the femoral stem trunnion in hip arthroplasty using a coordinate measuring machine. *Proceedings of the Institution of Mechanical Engineers, Part H: Journal of Engineering in Medicine.* 2015;229(1):69-76.

9.   Gilbert JL, Buckley CA, Jacobs JJ. In vivo corrosion of modular hip prosthesis components in mixed and similar metal combinations. The effect of crevice, stress, motion, and alloy coupling. *Journal of biomedical materials research.* 1993;27(12):1533-1544.

Appendix A: Risk for PJI Analysis SAS Script

```
/************************ANALYSING HIPS AND KNEES DATA
SETS***************************/

proc format;
value locationF
0 = "Hip"
1 = "Knee";

value sexF
0 = "Male"
1 = "Female";

value bmiF
0 = "Underweight"
1 = "Normal Weight"
2 = "Overweight"
3 = "Obese";

value revisionF
0 = "First"
1 = "Repeat";

value raceF
0 = "Other"
1 = "White";

run;

*import datasets;
proc import datafile = 'H:\Genymphas Paper\10.28.17 Datasets\Hips.xlsx'
      dbms = xlsx out=fhips replace;
run;

proc import datafile = 'H:\Genymphas Paper\10.28.17
Datasets\Knees.xlsx'
      dbms = xlsx out=fknees replace;
run;

*look at data;
proc contents data=fhips varnum; run;

proc contents data=fknees varnum; run;

*data steps for cleaning data;
data hipsnew (drop = Age_at_Insertion);
      *ensure proper matching lengths of variables;
      length site $10 race_new $10;
      format Standardized_Reason $55. Study__ $25.;
   informat Standardized_Reason $55. Study__ $25.;

      set fhips;
      *convert age from character to numeric;
```

```
        if Age_at_Insertion = "?" then age = .;
        else age = input(Age_at_Insertion, 10.);
        *recode abnormal age/height/weight as missing;
        if age = 0 then age = .;
        if Height__in_ = 0 then Height__in_ = .;
        if Weight__lbs_ = 0 then Weight__lbs_ = .;
        *generate new variable of site ID from the patient ID - extract
substring before hyphen;
        if find(Study__,"-",'i') ge 1 then site =
substr(Study__,1,(index(Study__,"-")-1));
             *else if find(Study__,'HUMC','i') ge 1 then site = "HUMC";
             else if Study__ = "" then site = " ";
        bmi = (Weight__lbs_/(Height__in_**2))*703;
        *create variable defining event of interest as infection and all
others (including missing) are censored;
        if find(Standardized_Reason,'infection','i') ge 1 then event = 1;
             else event = 0;
        *limit decimals on implantation time;
        format Implantation_Time 10.2;
        *recode race;
        if race = "A" then race_new = "Other";
             else if race = "AL" then race_new = "Other";
             else if race = "Blk" then race_new = "Other";
             else if race = "H" then race_new = "Other";
             else if race = "Other" then race_new = "Other";
             else if race = "Other/Blank" then race_new = "Other";
             else if race = "Pac" then race_new = "Other";
             else if race = "W" then race_new = "White";
        if Study__ = "HUMC 0667" then site = "HUMC";
             else if Study__ = "HUMC 623" then site = "HUMC";
        *Only select individuals with a reasonable age value;
        if age < 200;
run;


proc freq data=hipsnew;
        tables event / list missing;
run;


proc print data=hipsnew (obs=5); run;


data kneesnew (drop = Age_at_Insertion);
        *ensure proper matching lengths of variables;
        length site $10 race_new $10;
        format Standardized_Reason $55. Study__ $25.;
   informat Standardized_Reason $55. Study__ $25.;


        *remove blank rows;
        set fknees (where=(Study__ ne " "));
        *rename revision number so names match;
        rename Number_of_Previous_Revision =
Number_of_Previous_Revisions;
        *convert age from character to numeric;
        if Age_at_Insertion = "?" then age = .;
        else age = input(Age_at_Insertion, 10.);
        *recode abnormal age/height/weight as missing;
        if age = 0 then age = .;
        if Height__in_ = 0 then Height__in_ = .;
```

```
        if Weight__lbs_ = 0 then Weight__lbs_ = .;
        *generate new variable of site ID from the patient ID - extract
substring before hyphen;
        if find(Study__,"-",'i') ge 1 then site =
substr(Study__,1,(index(Study__,"-")-1));
             else if anydigit(Study__) ge 1 then site =
substr(Study__,1,anydigit(Study__)-1);
             else if Study__ = "" then site = " ";
        bmi = (Weight__lbs_/(Height__in_**2))*703;
        *create variable defining event of interest as infection and all
others (including missing) are censored;
        if find(Standardized_Reason,'infection','i') ge 1 then event = 1;
             else event = 0;
        *limit decimals on implantation time;
        format Implantation_Time 10.2;
        *recode race;
        if race = "A" then race_new = "Other";
             else if race = "AL" then race_new = "Other";
             else if race = "Blk" then race_new = "Other";
             else if race = "H" then race_new = "Other";
             else if race = "Other" then race_new = "Other";
             else if race = "Other/Blank" then race_new = "Other";
             else if race = "Pac" then race_new = "Other";
             else if race = "W" then race_new = "White";
        *Only select individuals with a reasonable age value;
        if age < 200;
run;

proc freq data=kneesnew;
        tables event / list missing;
run;

*look at data;
proc contents data=hipsnew varnum;
        title "hipsnew";
run;

proc contents data=kneesnew varnum;
        title "kneesnew";
run;

proc print data=hipsnew (obs=10);
        title "hipsnew";
run;

proc print data=kneesnew (obs=10);
        title "kneesnew";
run;

*frequencies by site;
proc freq data=hipsnew;
        tables site;
run;
proc freq data=kneesnew;
        tables site;
run;
```

```
*look at missing sites;
proc print data=hipsnew;
      title "hipsnew";
      where site = "";
run;

proc print data=kneesnew;
      title "kneesnew";
      where site = "";
run;

/*****

*distribution of implantation time across both groups - determine
cutoff point = 10 years;
proc means data=hipsnew n mean median min max p25 p50 p75 p90 p95 p99;
      title "hipsnew means";
      var Implantation_Time;
run;

proc means data=kneesnew n mean median min max p25 p50 p75 p90 p95 p99;
      title "kneesnew means";
      var Implantation_Time;
run;

*number of previous revisions;
proc freq data=hipsnew;
      title "hipsnew freq";
      tables race_new Number_of_Previous_Revisions;
run;

proc freq data=kneesnew;
      title "kneesnew freq";
      tables race_new Number_of_Previous_Revisions;
run;

*distribution of ages, height, weight;
proc means data=hipsnew;
      title "hipsnew numeric vars ";
      var age Height__in_ Weight__lbs_ Number_of_Previous_Revisions;
run;

proc means data=kneesnew;
      title "kneesnew numeric vars ";
      var age Height__in_ Weight__lbs_ Number_of_Previous_Revisions;
run;

*FREQUENCIES OF GENDER;
proc freq data=hipsnew;
      title "hipsnew gender";
      tables Gender;
run;

proc freq data=kneesnew;
      title "kneesnew gender";
      tables Gender;
run;
```

```
*FREQUENCIES OF site;
proc freq data=hipsnew;
     title "hipsnew site";
     tables site;
run;

proc freq data=kneesnew;
     title "kneesnew site";
     tables site;
run;

***/

proc print data=hipsnew (obs=5); title "hipsnew"; run;

proc print data=kneesnew (obs=5); title "kneesnew";run;

***** reformat both data sets so they can be combined ******;

data hipsnew2;
     length location 4;
     set hipsnew;
     *remove triage information;
     drop Triage_Information__Bearing_Coup
Triage_Information__Liner_Materi Triage_Information__Head_Materia;
     *add variable to indicate location;
     location = 0;
     *cutoff of 10 years - if they got the event after 10 years we
didn't see it;
     if Implantation_Time > 10 and event = 1 then do;
          new_time = 10;
          event = 0;
          end;
     else if Implantation_Time > 10 and event = 0 then do;
          new_time = 10;
          event = 0;
          end;
     else new_time = Implantation_Time;
     where Implantation_Time > 0;
run;

data kneesnew2;
     length location 4;
     *put variables in the same order;
     keep location site race_new Standardized_Reason Study__
Implantation_Time Gender Race Height__in_ Weight__lbs_
Number_of_Previous_Revisions age bmi event new_time;
     set kneesnew;
     *add variable to indicate location;
     location = 1;
     *cutoff of 10 years of followup - if they got the event after 10
years we didn't see it;
     if Implantation_Time > 10 and event = 1 then do;
          new_time = 10;
          event = 0;
          end;
```

```sas
        else if Implantation_Time > 10 and event = 0 then do;
             new_time = 10;
             event = 0;
             end;
        else new_time = Implantation_Time;
        where Implantation_Time > 0;
run;

proc print data=hipsnew2 (obs=5); title "hipsnew2"; run;

proc print data=kneesnew2 (obs=5); title "kneesnew2";run;




*append data sets together into single data set;

data combined;
      set hipsnew2 kneesnew2;
      *only select for people with an implantation time > 0;
      if Implantation_Time > 0;
      site = strip(site);

      /*add in variables for urban/teaching;
      if site in ("STA","UTHSA","C-UT","DRLU","UPMC","CW","UP","RI")
then do;
             urban = 1;
             teaching = 1;
             end;
        else if site in ("KP","NOC","LU","SHB") then do;
             urban = 1;
             teaching = 0;
             end;
        else if site in ("HUMC") then do;
             urban = 0;
             teaching = 1;
             end;
        else if site in ("TOC","JH","HN") then do;
             urban = 0;
             teaching = 0;
             end; */


      *all sites are urban, teaching classified in Excel Spreadsheet;
      if site in ("STA","UTHSA","C-
UT","DRLU","UPMC","CW","HUMC","UP","RI") then teaching = 1;
             else teaching = 0;

      *make site uppercase;
      site = upcase(site);

      if Number_of_Previous_Revisions = 0 then revision = 0;
      else if Number_of_Previous_Revisions > 0 then revision = 1;
run;

proc print data=combined(obs=10);
```

```
        title "Combined";
run;

proc freq data=combined;
     tables site*teaching;
run;

/********************** summary statistics on population
*********************/

proc freq data=combined;
     tables event; run;

proc means data = combined n mean median min p25 p50 p75 max maxdec=2;
     var Implantation_Time new_time;
     *implantation time is prior to cutting of at 10 years follow-up;
     title "Number of people who got event";
     where event=1;
run;

proc means data = combined n mean median min p25 p50 p75 max maxdec=2;
     var Implantation_Time new_time;
     *implantation time is prior to cutting of at 10 years follow-up;
     title "Number of people who got event by 10 years";
     where event=1 and Implantation_Time <= 10;
run;

proc sort data = combined; by location; run;

proc means data = combined n mean median min p25 p50 p75 max maxdec=2;
     var Implantation_Time new_time;
     *implantation time is prior to cutting of at 10 years follow-up;
     by location;
     title "Continuous Variables Summary Statistics";
run;


proc freq data=combined;
tables site / out = site_counts;
run;

proc print data=site_counts; run;

proc transpose data=site_counts
     out = site_counts_new;
     id site;
     where PERCENT >= 2;
run;

proc print data = site_counts_new; run;

*SITES TO KEEP: CW HN HUMC JH LGH RI SHB TOC UP;




proc print data=combined n;
```

```
       where find(Standardized_Reason,'infection','i') = 0 and event =
0;
run;



data intermed (drop = Number_of_Previous_Revisions);
       set combined (drop=race Standardized_Reason Height__in_
Weight__lbs_ );
       *CW HN HUMC JH LGH RI SHB TOC UP UPMC ;
       where site in ("CW", "HN", "HUMC", "JH", "LGH", "RI", "SHB",
"TOC", "UP");

       *recode variables into numeric;
       if gender = "M" then sex_num = 0;
             else if gender = "F" then sex_num = 1;

       if race_new = "Other" then race_num = 0;
                    else if race_new = "White" then race_num = 1;

       *create extra copies of continuous variables for standardization;
       agestd = age;
       timestd = new_time;

       rename Study__ = id;
run;

*standardize variables;
proc standard data=intermed mean=0 std=1 out=intermediate;
       var agestd;
run;

*check that variables have been correctly standardized;
proc means data=intermediate; run;

*new site distribution;
proc freq data=intermediate;
       tables site;
run;

proc print data=intermediate (obs=5);
       title "combined";
run;

proc freq data=intermediate;
       tables location*event;
       format location locationF.;
run;

proc freq data=intermediate;
       tables site*teaching / list missing;
run;

*1407 people didn't get event because had time maxed at 10;
proc print data=intermediate n;
       where event = 0 and new_time=10;
run;
```

```
/******start by looking at a KM curve stratified by location*****/
proc lifetest data = intermediate plots = (S);
      time new_time*event(0);
      strata location;
      title "KM Curves Stratified by Implant Location";
      format location locationF.;
run;
*from this basic curve it looks like hip implants have a better
survival time as compared to knees;
*log rank statistic p <.0001, suggesting the curves are statistically
different;

/******Univariate models to test for associations between implant
failure and covariates of interest*****/

*location p <.0001;
proc phreg data = intermediate;
      class location;
      model new_time*event(0) = location / rl;
      title "Univariate: Location Only";
      format location locationF.;
run;

*gender p = 0.0001;
proc phreg data = intermediate;
      class Gender;
      model new_time*event(0) = Gender/ rl;
      title "Univariate: Gender Only";
run;

*race_new p = 0.0443 BORDERLINE SIGNIFICANT;
proc phreg data = intermediate;
      class race_new;
      model new_time*event(0) = race_new / rl;
      title "Univariate: Race Only";
run;

*agestd p <.0001;
proc phreg data = intermediate;
      model new_time*event(0) = agestd / rl;
      title "Univariate: Age Only";
run;

*site p <.0001;
proc phreg data = intermediate;
      class site;
      model new_time*event(0) = site / rl;
      title "Univariate: Site Only";
run;

*previous revision status <.0001;
proc phreg data = intermediate;
      class revision (ref="0") / param=ref;
      model new_time*event(0) = revision / rl;
      title "Univariate: Revisions Only";
run;
```

```
*bmi p <.0001;
proc phreg data = intermediate;
      model new_time*event(0) = bmi / rl;
      title "Univariate: BMI Only";
run;

/*urban p <.0001;
proc phreg data = intermediate;
      class urban;
      model new_time*event(0) = urban / rl;
      title "Univariate: Urban Only";
run; */

*teaching p = 0.0010 ;
proc phreg data = intermediate;
      class teaching;
      model new_time*event(0) = teaching / rl;
      title "Univariate: teaching Only";
run;

/* create new categorization for BMI into groups

Below 18.5             Underweight
18.5 - 24.9            Normal or Healthy Weight
25.0 - 29.9            Overweight
30.0 and Above         Obese

Source: https://www.cdc.gov/healthyweight/assessing/bmi/adult_bmi/

*/

data final;
      set intermediate;

      *categorize continuous predictors;
      if bmi < 18.5 then bmi_cat = 0;
            else if bmi >= 18.5 and bmi <= 24.9 then bmi_cat = 1;
            else if bmi >= 25.0 and bmi <= 29.9 then bmi_cat = 2;
            else if bmi >= 30.0 then bmi_cat = 3;
run;




*re-run the model with bmi_cat;
*bmi_cat p <.0001;
proc phreg data = final;
      class bmi_cat (ref="0") / param=ref;
      model new_time*event(0) = bmi_cat / rl;
      title "Univariate: BMI_cat Only";
      *format bmi_cat bmiF.;
run;

/******Create Cox Model including relevant predictors *****/

*All predictors excep race and age sig,  AIC = 12179.299;
proc phreg data = final;
```

```
      class location gender race_new revision (ref="First") bmi_cat
teaching / param=ref;
      model new_time*event(0) = location gender race_new revision
bmi_cat teaching agestd / rl;
      title "Model 1: Full Model No Interaction";
      format location locationF. bmi_cat bmiF. revision revisionF.;
run;

****************** even though not all predictors are significant, full
model has lowest AIC
*****************************************************************;


/****** Check PH Assumption for Predictors in Cox Model *****/

*****log-log for location - roughly parallel, especially for longer
time - PH HOLDS***;

      *KM curves and dataset for Location;
      proc lifetest data = final method = km outsurv = one noprint;
            time new_time*event(0);
            title "KM Curves for Location";
            strata location;
            format location locationF.;
      run;
      /*Create a new dataset that takes the log-log*/
      data one_new;
            set one;
            lls = -log(-log(survival));
      run;
      /*Plot the log-log survival curve with the new dataset*/
      proc gplot data = one_new;
            plot lls*new_time = location;
            symbol1 interpol=stepLJ h=1 c=black;
            symbol2 interpol=stepLJ h=1 c=red;
            title "-log(-log(Survival)) Curves for Location";
            format location locationF.;
      run;

*****log-log for gender - roughly parallel, especially for longer time
- PH HOLDS***;

      *KM curves and dataset for Location;
      proc lifetest data = final method = km outsurv = two noprint;
            time new_time*event(0);
            title "KM Curves for Gender";
            strata gender;
      run;
      /*Create a new dataset that takes the log-log*/
      data two_new;
            set two;
            lls = -log(-log(survival));
      run;
      /*Plot the log-log survival curve with the new dataset*/
      proc gplot data = two_new;
            plot lls*new_time = gender;
            symbol1 interpol=stepLJ h=1 c=black;
```

```
        symbol2 interpol=stepLJ h=1 c=red;
        title "-log(-log(Survival)) Curves for Gender";
    run;

    *****log-log for race - roughly parallel, especially for longer
time - PH HOLDS***;

    *KM curves and dataset for Location;
    proc lifetest data = final method = km outsurv = three noprint;
        time new_time*event(0);
        title "KM Curves for Race";
        strata race_new;
    run;
    /*Create a new dataset that takes the log-log*/
    data three_new;
        set three;
        lls = -log(-log(survival));
    run;
    /*Plot the log-log survival curve with the new dataset*/
    proc gplot data = three_new;
        plot lls*new_time = race_new;
        symbol1 interpol=stepLJ h=1 c=black;
        symbol2 interpol=stepLJ h=1 c=red;
        title "-log(-log(Survival)) Curves for Race";
    run;

*****log-log for urban - roughly parallel - PH holds ***;
/*

    *KM curves and dataset for site;
    proc lifetest data = final method = km outsurv = four noprint;
        time new_time*event(0);
        title "KM Curves for Urban";
        strata urban;
    run;
    *Create a new dataset that takes the log-log*;
    data four_new;
        set four;
        lls = -log(-log(survival));
    run;
    *Plot the log-log survival curve with the new dataset;
    proc gplot data = four_new;
        plot lls*new_time = urban;
        title "-log(-log(Survival)) Curves for Urban";
    run;

    */

*****log-log for teaching - roughly parallel - PH holds ***;
    *KM curves and dataset for site;
    proc lifetest data = final method = km outsurv = five noprint;
        time new_time*event(0);
        title "KM Curves for teaching";
        strata teaching;
    run;
    /*Create a new dataset that takes the log-log*/
    data five_new;
```

```
            set five;
            lls = -log(-log(survival));
      run;
      /*Plot the log-log survival curve with the new dataset*/
      proc gplot data = five_new;
            plot lls*new_time = teaching;
            title "-log(-log(Survival)) Curves for teaching";
      run;

*****log-log for previous revision status - roughly parallel - PH holds
***;

      *KM curves and dataset for site;
      proc lifetest data = final method = km outsurv = six noprint;
            time new_time*event(0);
            title "KM Curves for Number of Previous Revisions";
            strata revision;
      run;
      /*Create a new dataset that takes the log-log*/
      data six_new;
            set six;
            lls = -log(-log(survival));
      run;
      /*Plot the log-log survival curve with the new dataset*/
      proc gplot data = six_new;
            plot lls*new_time = revision;
            title "-log(-log(Survival)) Curves for Number of Previous
Revisions";
      run;

*****log-log for bmi_cat - crossing between groups - PH assumption MAY
NOT HOLD***;

      *KM curves and dataset for bmi_cat;
      proc lifetest data = final method = km outsurv = seven noprint;
            time new_time*event(0);
            title "KM Curves for bmi_cat";
            strata bmi_cat;
            format bmi_cat bmiF.;
      run;
      /*Create a new dataset that takes the log-log*/
      data seven_new;
            set seven;
            lls = -log(-log(survival));
      run;
      /*Plot the log-log survival curve with the new dataset*/
      proc gplot data = seven_new;
            plot lls*new_time = bmi_cat;
            title "-log(-log(Survival)) Curves for bmi_cat";
            format bmi_cat bmiF.;
      run;

/*****Log-Log Summary: Holds for Essentially All predictors
*********************************************************/
```

```
/****** Use Time-Dependent Covariates to test PH Assumption: g(t) = t
*****/

*location > interaction p = 0.0006 indicating PH VIOLATION;
proc phreg data = final;
      class location;
      model new_time*event(0) = location tlocation;
      tlocation = location*new_time;
      title "Univariate Test PH Using Time-Dependent Predictor:
Location Only";
run;

*sex > interaction p = 0.2311 indicating no PH violation;
proc phreg data = final;
      class sex_num;
      model new_time*event(0) = sex_num tsex;
      tsex = sex_num*new_time;
      title "Univariate Test PH Using Time-Dependent Predictor: Sex
Only";
run;

*race > interaction p = 0.0055 indicating PH VIOLATION;
proc phreg data = final;
      class race_num;
      model new_time*event(0) = race_num trace;
      trace = race_num*new_time;
      title "Univariate Test PH Using Time-Dependent Predictor: Race
Only";
run;

/*
*urban > interaction p <.0001 indicating PH VIOLATION;
proc phreg data = final;
      class urban;
      model new_time*event(0) = urban turban;
      turban = urban*new_time;
      title "Univariate Test PH Using Time-Dependent Predictor: Urban
Only";
run;
*/

*number of revisions > interaction p = 0.0004 indicating PH VIOLATION;
proc phreg data = final;
      class revision (ref="0")/param=ref;
      model new_time*event(0) = revision trev;
      trev = revision*new_time;
      title "Univariate Test PH Using Time-Dependent Predictor: Rev
Only";
run;

*bmi_cat > interaction p = 0.5137 indicating no PH violation;
proc phreg data = final;
      class bmi_cat;
      model new_time*event(0) = bmi_cat tbmi;
      tbmi = bmi_cat*new_time;
      title "Univariate Test PH Using Time-Dependent Predictor: BMI Cat
Only";
```

```
run;

*teaching > interaction p 0.7114 indicating no PH violation;
proc phreg data = final;
      class teaching;
      model new_time*event(0) = teaching tteaching;
      tteaching = teaching*new_time;
      title "Univariate Test PH Using Time-Dependent Predictor:
Teaching Only";
run;

*age > interaction p = 0.9967 indicating no PH violation;
proc phreg data = final;
      model new_time*event(0) = agestd tage;
      tage = agestd*new_time;
      title "Univariate Test PH Using Time-Dependent Predictor: Age
Only";
run;


/*****Extended Cox Summary: PH does not hold for location, race_num,
and reveision
*************************************************************************
*********/

/******* New Cox Model with Interaction Terms ****/

*AIC = 12152.257 - age and location main effects not sig but all
interactions are sig;
proc phreg data = final;
      class location (ref="Knee") gender (ref="M") revision
(ref="First") bmi_cat (ref="Underweight") race_num (ref="Other")
teaching (ref="0")/ param = ref;
      model new_time*event(0) = location gender race_num revision
bmi_cat teaching agestd tlocation trace trev/ rl covb;
      tlocation = location*new_time;
      trace = race_num*new_time;
      trev = revision*new_time;
      title "Model 3: Full Model with Interaction for Location, Race,
and Revision";
      format location locationF. race_num raceF. bmi_cat bmiF. revision
revisionF.;
run;




/******************************** NOW TRY PARAMETRIC MODELS with same
covariates - removed site to help model convergence
*****************************/

/*** https://www.mwsug.org/proceedings/2010/stats/MWSUG-2010-75.pdf
"Lifereg doesn't handle time-dependent covariates"***/

**exponential AIC = 6264.047;
proc lifereg data = final;
      class location gender revision bmi_cat race_num teaching;
```

```
        model new_time*event(0) = location gender race_num revision
bmi_cat teaching agestd / dist=exponential;
        title "Model 6: Exponential Survival Model";
        format location locationF. race_num raceF. bmi_cat bmiF. revision
revisionF.;
run;


**Weibull AIC = 5960.668 ;
proc lifereg data = final;
        class location gender revision bmi_cat race_num teaching;
        model new_time*event(0) = location gender race_num revision
bmi_cat teaching agestd / dist=weibull;
        title "Model 7: Weibull Survival Model";
        format location locationF. race_num raceF. bmi_cat bmiF. revision
revisionF.;
run;


**Log Logistic AIC = 5918.416 THIS IS THE LOWEST ;
proc lifereg data = final;
        class location gender revision bmi_cat race_num teaching;
        model new_time*event(0) = location gender race_num revision
bmi_cat teaching agestd / dist=llogistic;
        title "Model 8: Log Logistic Survival Model";
        format location locationF. race_num raceF. bmi_cat bmiF. revision
revisionF.;
run;



/*********************** FRAILTY************************/


/*

proc print data=final (obs=5); run;

*ods output ModelBuildingSummary=Summary1;
ods output FitStatistics=Fit1;
proc phreg data = final;
        class site location (ref="Knee") gender (ref="M") revision
(ref="First") bmi_cat (ref="Underweight") race_num (ref="Other")
teaching (ref="0")/ param = ref;
        model new_time*event(0) = location gender race_num revision
bmi_cat teaching agestd tlocation trace trev/ rl covb;
        tlocation = location*new_time;
        trace = race_num*new_time;
        trev = revision*new_time;
        random site; *frailty by site, not individual;
        title "Model 3: Full Model with Interaction for Location, Race,
and Revision plus FRAILTY";
        format location locationF. race_num raceF. bmi_cat bmiF. revision
revisionF.;
run; *NO AIC PRODUCED;

*proc print data=Summary1;run;
proc print data=fit1; run;
```

```
*ods output ModelBuildingSummary=Summary2;
ods output FitStatistics=Fit2;
proc phreg data = final;
      class site location (ref="Knee") gender (ref="M") revision
(ref="First") bmi_cat (ref="Underweight") race_num (ref="Other")
teaching (ref="0")/ param = ref;
      model new_time*event(0) = location gender race_num revision
bmi_cat teaching agestd/ rl covb;
      random site; *frailty by site, not individual;
      title "Model 3: Full Model FRAILTY";
      format location locationF. race_num raceF. bmi_cat bmiF. revision
revisionF.;
run; *NO AIC PRODUCED;
*proc print data=Summary2;run;
proc print data=Fit2; run;



*/


*Log logistic MODEL WITH FRAILTY?;



/*
*****
https://uhdspace.uhasselt.be/dspace/bitstream/1942/15714/1/113172320120
09.pdf *****;

example code

proc nlmixed data=efficacy1;
      bounds gamma > 0;
      parms b0=8 b1=1 gamma=1;
      linp = b0 + b1*LOGN;
      alpha = exp(-linp);
      G_t = 1/(1+(alpha*tte)**gamma);
      g = (gamma*((alpha)**gamma)*(tte)**(gamma-1)
/(1+(alpha*tte)**gamma))*G_t;
      ll = (vevent=1)*log(g) + (vevent=0)*log(G_t);
      model tte ~ general(ll);
run;
*/

/*

**Log Logistic AIC = 5918.416 THIS IS THE LOWEST ;
proc lifereg data = final;
      class location gender revision bmi_cat race_num teaching;
      model new_time*event(0) = location gender race_num revision
bmi_cat teaching agestd / dist=llogistic;
      title "Model 8: Log Logistic Survival Model";
      format location locationF. race_num raceF. bmi_cat bmiF. revision
revisionF.;
run;

*/
/*
```

```
*WITHOUT Frailty;
   proc nlmixed data=final;
    bounds gamma > 0;
    linp =
b0+b1*(location=0)+b2*(gender="F")+b3*(race_num=0)+b4*(revision=0);*+b5
*(bmi_cat=0)+b6*(bmi_cat=1)+b7*(bmi_cat=2)+b8*(teaching=0)+b9*agestd;
    alpha = exp(-linp);
    G_t  = exp(-(alpha*new_time)**gamma);
    g    = gamma*alpha*((alpha*new_time)**(gamma-1))*G_t;
    ll   = (event=1)*log(g) + (event=0)*log(G_t);
    model new_time ~ general(ll);
    predict 1-G_t out=cdf;
       title "AFT model via NLMIXED for a Weibull without a shared
frailty";
  run;

  proc lifereg data=final;
     class location gender race_num revision ;*bmi_cat teaching;
   model new_time*event(0) = location gender race_num revision bmi_cat
teaching / dist=weibull;
    *output out=new cdf=prob;
       title "Identical results via LIFEREG";
  run;




proc sort data=final;
     by site;
run;

*WITH Frailty;
  ods output ParameterEstimates=est;
  proc nlmixed data=final;
    bounds gamma > 0;
    linp = b0 + b1*(location) + z;
    alpha = exp(-linp);
    G_t  = exp(-(alpha*new_time)**gamma);
    g    = gamma*alpha*((alpha*new_time)**(gamma-1))*G_t;
    ll = (event=1)*log(g) + (event=0)*log(G_t);
    model new_time ~ general(ll);
    random z ~ normal(0,exp(2*logsig)) subject=site out=EB;
    predict 1-G_t out=cdf;
       title "AFT model via NLMIXED for a Weibull with a shared
frailty";
run;

*/


/*

**Log Logistic AIC = 5918.416 THIS IS THE LOWEST ;
proc lifereg data = final;
     class location gender revision bmi_cat race_num teaching;
```

```
      model new_time*event(0) = location gender race_num revision
bmi_cat teaching agestd / dist=llogistic;
      title "Model 8: Log Logistic Survival Model";
      format location locationF. race_num raceF. bmi_cat bmiF. revision
revisionF.;
run;



proc nlmixed data=final;
      bounds gamma > 0; *shape parameter;
      *parms b0=1.2521 b1=0.4361 b2=0.5020 b3=-0.1499 b4=2.2847
b5=0.0451 b6=0.4982 b7=0.8857 b8=0.8054 b9=-0.6480 gamma=1.4303;
      linp =
b0+b1*(location=0)+b2*(gender="F")+b3*(race_num=0)+b4*(revision=0)+b5*(
bmi_cat=0)+b6*(bmi_cat=1)+b7*(bmi_cat=2)+b8*(teaching=0)+b9*agestd;
      alpha = exp(-linp);
      G_t = 1/(1+(alpha*(new_time**gamma))); *distribution of survival
probabilities beyond time t;
      g = ((alpha*gamma*(new_time*alpha)**(gamma-
1))/(1+(alpha*(new_time*alpha)**gamma)))*G_t; *density of failure time;
      *g = (gamma*((alpha)**gamma)*(new_time)**(gamma-1)
/(1+(alpha*new_time)**gamma))*G_t;
      ll = (event=1)*log(g) + (event=0)*log(G_t);
      model new_time ~ general(ll);
      *random z ~ normal(0,exp(2*logsig)) subject=site;
      title "Log Logistic Parametric Model";
run;

*/



proc lifetest data = final method = km outsurv = one;
time new_time * event (0);
strata location;
run;

data work.one_new;
set work.one;
lls = log((1-survival)/(survival));
logwks = log(new_time);
run;

proc gplot data = work.one_new;
plot lls * logwks = location;
title "Log Odds of Failure for Implant Location";
run;



proc sort data=final; by site; run;


*****************AIC = 4592.5 BEST MODEL TO
USE**************************;
proc nlmixed data=final;
      bounds gamma > 0; *shape parameter;
```

```
      linp =
b0+b1*(location=0)+b2*(gender="F")+b3*(race_num=0)+b4*(revision=1)+b5*(
bmi_cat=1)+b6*(bmi_cat=2)+b7*(bmi_cat=3)+b8*(teaching=0)+b9*agestd+z;
      alpha = exp(-linp);
      G_t = 1/(1+(alpha*(new_time**gamma))); *distribution of survival
probabilities beyond time t;
      g = ((alpha*gamma*(new_time*alpha)**(gamma-
1))/(1+(alpha*(new_time*alpha)**gamma)))*G_t; *density of failure time;
      *g = (gamma*((alpha)**gamma)*(new_time)**(gamma-1)
/(1+(alpha*new_time)**gamma))*G_t;
      ll = (event=1)*log(g) + (event=0)*log(G_t);
      model new_time ~ general(ll);
      random z ~ normal(0,exp(2*logsig)) subject=site;
      title "Log Logistic Parametric Model with Frailty";
run;


*/
******************** SUMMARY STATISTICS TABLES
*************************************************;



proc sort data=final;
      by revision;
run;

proc means data=final mean std maxdec=2 n;
      title "MEANS BY revision";
      by revision;
      var age ;
      format location locationF. race_num raceF. bmi_cat bmiF. revision
revisionF.;
run;

proc freq data=final;
      title "FREQUENCIES BY revision";
      tables revision gender*revision race_new*revision
location*revision bmi_cat*revision / nocum norow nopercent;
      format location locationF. race_num raceF. bmi_cat bmiF. revision
revisionF.;
run;

proc freq data=final;
      tables revision;
      format revision revisionF.;
run;


proc contents data=final; run;

data test;
      set final;

      if Implantation_Time >= 10 then checkvar = 0;
            else if Implantation_Time = . then checkvar = .;
            else checkvar = 1;
```

```
run;

proc freq data=test;
      tables checkvar;
run;

proc means data=test n mean median min max p25 p50 p75 p90 p95 p99
maxdec=2;
      var Implantation_Time;
run;

proc univariate data=test;
  var Implantation_Time;
  histogram / endpoints = 0 to 45 by 1;
  title "Distribution of Implant Survival Time Overall";
run;

proc sort data = test; by location; run;

proc univariate data=test;
  var Implantation_Time;
  by location;
  histogram / endpoints = 0 to 45 by 1;
  title "Distribution of Implant Survival Time Overall";
  format location locationF.;
run;
```

Appendix B: PJI and Taper Corrosion Analysis SAS Script

```
ods graphics on;

*libname survival "C:\Users\ghiggs\Desktop\Data\4.14.17 Datasets\";
/************************ANALYSING HIPS AND KNEES DATA
SETS****************************/

/*
proc format;
value locationF
0 = "Hip"
1 = "Knee";

value sexF
0 = "Male"
1 = "Female";

value bmiF
0 = "Underweight"
1 = "Normal Weight"
2 = "Overweight"
3 = "Obese";

value revisionF
0 = "First"
1 = "Repeat";

value raceF
0 = "Other"
1 = "White";

run;
*/

*import datasets;
proc import datafile =
'C:\Users\ghiggs\Desktop\Genymphas\Research\Infection\JOA
Paper\Infection Datasets 10.12.17\Hips.xlsx'
     dbms = xlsx out=fhips replace;
run;

proc import datafile =
'C:\Users\ghiggs\Desktop\Genymphas\Research\Infection\JOA
Paper\Infection Datasets 10.12.17\Knees.xlsx'
     dbms = xlsx out=fknees replace;
run;

*look at data;
proc contents data=fhips varnum; run;

proc contents data=fknees varnum; run;

*data steps for cleaning data;
data hipsnew (drop = Age_at_Insertion);
      *ensure proper matching lengths of variables;
```

```
      length site $10 race_new $10;
      format Standardized_Reason $55. Study__ $25.;
  informat Standardized_Reason $55. Study__ $25.;

      set fhips;
      *convert age from character to numeric;
      if Age_at_Insertion = "?" then age = .;
      else age = input(Age_at_Insertion, 10.);
      *recode abnormal age/height/weight as missing;
      if age = 0 then age = .;
      if Height__in_ = 0 then Height__in_ = .;
      if Weight__lbs_ = 0 then Weight__lbs_ = .;
      *generate new variable of site ID from the patient ID - extract
substring before hyphen;
      if find(Study__,"-",'i') ge 1 then site =
substr(Study__,1,(index(Study__,"-")-1));
            *else if find(Study__,'HUMC','i') ge 1 then site = "HUMC";
            else if Study__ = "" then site = " ";
      bmi = (Weight__lbs_/(Height__in_**2))*703;
      *create variable defining PJI of interest as PJI and all others
(including missing) are censored;
      if find(Standardized_Reason,'infection','i') ge 1 then PJI = 1;
            else PJI = 0;
      *limit decimals on implantation time;
      format Implantation_Time 10.2;
      *recode race;
      if race = "A" then race_new = "Other";
            else if race = "AL" then race_new = "Other";
            else if race = "Blk" then race_new = "Other";
            else if race = "H" then race_new = "Other";
            else if race = "Other" then race_new = "Other";
            else if race = "Other/Blank" then race_new = "Other";
            else if race = "Pac" then race_new = "Other";
            else if race = "W" then race_new = "White";
      if Study__ = "HUMC 0667" then site = "HUMC";
            else if Study__ = "HUMC 623" then site = "HUMC";
      *Only select individuals with a reasonable age value;
      if age < 200;
run;

proc freq data=hipsnew;
      tables Standardized_Reason*PJI / list missing;
run;

proc print data=hipsnew (obs=5); run;

data kneesnew (drop = Age_at_Insertion);
      *ensure proper matching lengths of variables;
      length site $10 race_new $10;
      format Standardized_Reason $55. Study__ $25.;
  informat Standardized_Reason $55. Study__ $25.;

      *remove blank rows;
      set fknees (where=(Study__ ne " "));
      *rename revision number so names match;
      rename Number_of_Previous_Revision =
Number_of_Previous_Revisions;
```

```
      *convert age from character to numeric;
      if Age_at_Insertion = "?" then age = .;
      else age = input(Age_at_Insertion, 10.);
      *recode abnormal age/height/weight as missing;
      if age = 0 then age = .;
      if Height__in_ = 0 then Height__in_ = .;
      if Weight__lbs_ = 0 then Weight__lbs_ = .;
      *generate new variable of site ID from the patient ID - extract
substring before hyphen;
      if find(Study__,"-",'i') ge 1 then site =
substr(Study__,1,(index(Study__,"-")-1));
            else if anydigit(Study__) ge 1 then site =
substr(Study__,1,anydigit(Study__)-1);
            else if Study__ = "" then site = " ";
      bmi = (Weight__lbs_/(Height__in_**2))*703;
      *create variable defining PJI of interest as PJI and all others
(including missing) are censored;
      if find(Standardized_Reason,'PJI','i') ge 1 then PJI = 1;
            else PJI = 0;
      *limit decimals on implantation time;
      format Implantation_Time 10.2;
      *recode race;
      if race = "A" then race_new = "Other";
            else if race = "AL" then race_new = "Other";
            else if race = "Blk" then race_new = "Other";
            else if race = "H" then race_new = "Other";
            else if race = "Other" then race_new = "Other";
            else if race = "Other/Blank" then race_new = "Other";
            else if race = "Pac" then race_new = "Other";
            else if race = "W" then race_new = "White";
      *Only select individuals with a reasonable age value;
      if age < 200;
run;


proc freq data=kneesnew;
      tables Standardized_Reason*PJI / list missing;
run;

*look at data;
proc contents data=hipsnew varnum;
      title "hipsnew";
run;

proc contents data=kneesnew varnum;
      title "kneesnew";
run;

proc print data=hipsnew (obs=10);
      title "hipsnew";
run;

proc print data=kneesnew (obs=10);
      title "kneesnew";
run;

*frequencies by site;
proc freq data=hipsnew;
```

```
        tables site;
run;
proc freq data=kneesnew;
        tables site;
run;

*look at missing sites;
proc print data=hipsnew;
        title "hipsnew";
        where site = "";
run;

proc print data=kneesnew;
        title "kneesnew";
        where site = "";
run;


proc print data=hipsnew (obs=5); title "hipsnew"; run;

proc print data=kneesnew (obs=5); title "kneesnew";run;
/**********************************************************************
************************/
/*      Is having an PJI associated with greater corrosion?
*/
/**********************************************************************
***********************/

proc freq data = hipsnew;
tables PJI;
run;

proc freq data = kneesnew;
tables PJI;
run;

/***Part 2 Corrosion***/

ods rtf file="C:\Users\ghiggs\Desktop\Genymphas\Research\Infection\JOA
Paper\SAS Files\Infection Manuscript - Corrosion Output.rtf"
fontscale=85 style=rtf;

/*A: Read in data*/

data hips_cor;
        set hipsnew;
        length it_term $30 liner_mat $50;
        if Corrosion_Scoring__Internal_Slee ne . then head_cor =
Corrosion_Scoring__Internal_Slee;
              else headcor = Corrosion_Scoring__Femoral_Head;
        if headcor <2 then bin_headcor = 0;
        else bin_headcor = 1;
        stemcor = Corrosion_Scoring__Stem_Trunnion;
        if stemcor <2 then bin_stemcor = 0;
        else bin_stemcor = 1;
        maxcor = max(of headcor stemcor);
        if maxcor <2 then bin_maxcor = 0;
```

```
      else bin_maxcor = 1;
      maxoi = max(of FTIR_Chemical_Properties__Superi
FTIR_Chemical_Properties__Inferi FTIR_Chemical_Properties__Infer1
FTIR_Chemical_Properties__Infer2 FTIR_Chemical_Properties__Infer3
FTIR_Chemical_Properties__Maximu FTIR_Chemical_Properties__Maxim1
FTIR_Chemical_Properties__Maxim2);
      if maxoi <1 then oi_cat = "1";
      else if maxoi >3 then oi_cat = "2";
      else oi_cat = "3";
      if maxoi <1 then bin_oi = 0;
      else bin_oi = 1;
      if Implantation_Time <1 then it_term = "A: Less than 1 year";
      else if Implantation_Time <5 then it_term = "B: 1-5 years" ;
      else it_term = "C: 5+ years";
      if Implantation_Time <1 then it_cat = 0;
      else if Implantation_Time <5 then it_cat = 1;
      else it_cat = 3;
      if Triage_Information__Liner_Materi in ("A-Class", "Durasul",
"Longevity", "Marathon", "Marathon?", "Marathon 4150", "XLPE") then
liner_mat = "Remelted HXLPE";
      *if Triage_Information__Liner_Materi in ("E1", "Vivacit-E") then
liner_mat = "Vitamin E HXLPE";
      if Triage_Information__Liner_Materi in ("Gamma Inert", "Enduron",
"EtO", "Unknown") then liner_mat = "Other";
      if Triage_Information__Liner_Materi in ("Gamma Inert", "Enduron",
"EtO", "Unknown", "E1", "Vivacit-E") then liner_mat = "Other";
      if Triage_Information__Liner_Materi = "Crossfire" then liner_mat
= "Annealed HXLPE";
      if Triage_Information__Liner_Materi = "X3" then liner_mat =
"Sequentially Annealed HXLPE";
      if Number_of_Previous_Revisions = 0 then revision = 0;
      else if Number_of_Previous_Revisions > 0 then revision = 1;
      if site in ("STA","UTHSA","C-
UT","DRLU","UPMC","CW","HUMC","UP","RI") then teaching = 1;
            else teaching = 0;
      *if maxoi ne .;
      if maxcor ne .;
run;

      /*Take a look at the data
      proc contents data=hips_cor varnum; run;

      proc freq data=hips_cor; tables liner_mat;run;
      */

proc export
      data=hips_cor
      dbms=xlsx
      outfile='C:\Users\ghiggs\Desktop\Genymphas\Research\Infection\JOA
Paper\Infection Datasets 10.12.17\Datasets from
SAS\hips_analysis_cor.xlsx'
      replace;
run;

proc sort data = hips_cor;
      by PJI;
run;
```

```
proc means data = hips_cor;* n mean median min p25 p50 p75 max
maxdec=2;
      var Implantation_Time age bmi maxcor headcor stemcor;
      *implantation time is prior to cutting of at 10 years follow-up;
      title "Continuous Variables Summary Statistics by PJI";
      by PJI; /*
      format location locationF.;*/
run;

proc sort data = hips_cor;
by it_cat;
run;

proc means data = hips_cor;* n mean median min p25 p50 p75 max
maxdec=2;
      var Implantation_Time bmi;
      *implantation time is prior to cutting of at 10 years follow-up;
      title "Continuous Variables Summary Statistics by (Categorical)
Implantation Time";
      by it_cat; /*
      format location locationF.;*/
run;

proc sort data = hips_cor;
by PJI;
run;

proc freq data = hips_cor;
tables PJI;
run;

proc freq data=hips_cor;
      title "Categorical Variables Summary Statistics by PJI";
      tables bin_oi race_new gender PJI teaching revision/ missing;
      /*format location locationF.;*/
      by PJI;
run;

/*B: Cross-Sectional Analysis of Oxidation Index*/
proc npar1way wilcoxon correct=no data=hips_cor;
      class PJI;
      var maxcor;
      *exact wilcoxon;
      title 'Cross-Sectional Comparison (Wilocoxon) of Max Corrosion by
PJI';
run;

proc boxplot data = hips_cor;
      plot maxcor*PJI;
run;

proc npar1way wilcoxon correct=no data=hips_cor;
      class PJI;
      var headcor;
      *exact wilcoxon;
```

```
      title 'Cross-Sectional Comparison (Wilocoxon) of Head Corrosion
by PJI';
run;


proc boxplot data = hips_cor;
      plot headcor*PJI;
run;


proc npar1way wilcoxon correct=no data=hips_cor;
      class PJI;
      var stemcor;
      *exact wilcoxon;
      title 'Cross-Sectional Comparison (Wilocoxon) of Stem Corrosion
by PJI';
run;


proc boxplot data = hips_cor;
      plot stemcor*PJI;
run;


proc npar1way wilcoxon correct=no data=hips_cor;
      class PJI;
      var implantation_time;
      *exact wilcoxon;
      title 'Cross-Sectional Comparison (Wilocoxon) of Hip IT by PJI';
run;


proc npar1way wilcoxon correct=no data=hips_cor;
      class PJI;
      var age;
      *exact wilcoxon;
      title 'Cross-Sectional Comparison (Wilocoxon) of Age at Insertion
by PJI';
run;


proc npar1way wilcoxon correct=no data=hips_cor;
      class PJI;
      var bmi;
      *exact wilcoxon;
      title 'Cross-Sectional Comparison (Wilocoxon) of BMI by PJI';
run;


proc freq data=hips_cor;
      tables PJI*bin_cor / chisq expected norow nocol nopercent;
      title 'Cross-Sectional Comparison (Wilocoxon) of Binary Max
Corrosion by PJI';
run;


proc freq data=hips_cor;
      tables PJI*bin_headcor / chisq expected norow nocol nopercent;
      title 'Cross-Sectional Comparison (Wilocoxon) of Binary Head
Corrosion by PJI';
run;


proc freq data=hips_cor;
      tables PJI*bin_stemcor / chisq expected norow nocol nopercent;
```

```
          title 'Cross-Sectional Comparison (Wilocoxon) of Binary Stem
Corrosion by PJI';
     run;


proc freq data=hips_cor;
          tables PJI*gender / chisq expected norow nocol nopercent;
          title 'Cross-Sectional Comparison (Wilocoxon) of Gender by PJI';
     run;


proc freq data=hips_cor;
          tables PJI*race_new / chisq expected norow nocol nopercent;
          title 'Cross-Sectional Comparison (Wilocoxon) of Race by PJI';
     run;


proc freq data=hips_cor;
          tables PJI*revision / chisq expected norow nocol nopercent;
          title 'Cross-Sectional Comparison (Wilocoxon) of Revision by
PJI';
     run;


proc freq data=hips_cor;
          tables PJI*teaching / chisq expected norow nocol nopercent;
          title 'Cross-Sectional Comparison (Wilocoxon) of Teaching
Hospital by PJI';
     run;


options nobyline;
/*Stratified by Implantation Time Category*/
proc sort data =hips_cor;
          by it_term;
     run;
proc npar1way wilcoxon correct=no data=hips_cor;
          class PJI;
          var maxcor;
          by it_term;* descending;
          *exact wilcoxon;
          title1 'Stratified Cross-Sectional Comparison (Wilocoxon) of Max
Corrosion by PJI';
          title2 'Implantation Time Category #byval(it_term)';
     run;
proc npar1way wilcoxon correct=no data=hips_cor;
          class PJI;
          var headcor;
          by it_term;* descending;
          *exact wilcoxon;
          title1 'Stratified Cross-Sectional Comparison (Wilocoxon) of Head
Corrosion by PJI';
          title2 'Implantation Time Category #byval(it_term)';
     run;
proc npar1way wilcoxon correct=no data=hips_cor;
          class PJI;
          var stemcor;
          by it_term;* descending;
          *exact wilcoxon;
          title1 'Stratified Cross-Sectional Comparison (Wilocoxon) of Stem
Corrosion by PJI';
          title2 'Implantation Time Category #byval(it_term)';
```

```
run;
/*Check if implantation time is different between PJI and no PJI even
within the it_category*/

proc npar1way wilcoxon correct=no data=hips_cor;
      class PJI;
      var implantation_time;
      by it_term;* descending;
      *exact wilcoxon;
      title1 'Stratified Cross-Sectional Comparison (Wilocoxon) of
Implantation Time by PJI';
      title2 'Implantation Time Category #byval(it_term)';
run;

/*Stratified by Head Material Category
proc sort data =hips_cor;
      by liner_mat;
run;
proc npar1way wilcoxon correct=no data=hips_oi;
      class PJI;
      var maxoi;
      by liner_mat;* descending;
      *exact wilcoxon;
      title1 'Stratified Cross-Sectional Comparison (Wilocoxon) of
MaxOI Hips by PJI';
      title2 'Liner Material Category #byval(liner_mat)';
run;


/*complete the code below:

      if Head_Material = "Zirconia-Toughened Alumina" then delete;
      if Head_Material = "Titanium" then delete;
      Stem_Material = upcase(Stem_Material);
      *Stem_Material = strip(Stem_Material);
      if find(Stem_Material,'TMZF','i') ge 1 then Stem_Material=
'TMZF';
      if find(Stem_Material,'COCR','i') ge 1 then Stem_Material=
'COCR';

*/

/*Stratified by Previous Revision Status*/
proc sort data =hips_cor;
      by revision;
run;
proc npar1way wilcoxon correct=no data=hips_cor;
      class PJI;
      var maxcor;
      by revision;* descending;
      *exact wilcoxon;
      title1 'Stratified Cross-Sectional Comparison (Wilocoxon) of Max
Corrosion by PJI';
      title2 'Previous Revision Status #byval(revision)';
run;

proc npar1way wilcoxon correct=no data=hips_cor;
```

```
        class PJI;
        var headcor;
        by revision;* descending;
        *exact wilcoxon;
        title1 'Stratified Cross-Sectional Comparison (Wilocoxon) of Head
Corrosion by PJI';
        title2 'Previous Revision Status #byval(revision)';
run;


proc npar1way wilcoxon correct=no data=hips_cor;
        class PJI;
        var stemcor;
        by revision;* descending;
        *exact wilcoxon;
        title1 'Stratified Cross-Sectional Comparison (Wilocoxon) of Stem
Corrosion by PJI';
        title2 'Previous Revision Status #byval(revision)';
run;


/*repeat for IT*/
proc npar1way wilcoxon correct=no data=hips_cor;
        class PJI;
        var implantation_time;
        by revision;* descending;
        *exact wilcoxon;
        title1 'Stratified Cross-Sectional Comparison (Wilocoxon) of IT
Hips by PJI';
        title2 'Previous Revision Status #byval(revision)';
run;


/*Stratified by Hospital Teaching Status*/
proc sort data =hips_cor;
        by teaching;
run;
proc npar1way wilcoxon correct=no data=hips_cor;
        class PJI;
        var maxcor;
        by teaching;* descending;
        *exact wilcoxon;
        title1 'Stratified Cross-Sectional Comparison (Wilocoxon) of Max
Corrosion by PJI';
        title2 'Teaching Hospital Status #byval(teaching)';
run;
proc npar1way wilcoxon correct=no data=hips_cor;
        class PJI;
        var headcor;
        by teaching;* descending;
        *exact wilcoxon;
        title1 'Stratified Cross-Sectional Comparison (Wilocoxon) of Head
Corrosion by PJI';
        title2 'Teaching Hospital Status #byval(teaching)';
run;
proc npar1way wilcoxon correct=no data=hips_cor;
        class PJI;
        var stemcor;
        by teaching;* descending;
        *exact wilcoxon;
```

```
      title1 'Stratified Cross-Sectional Comparison (Wilocoxon) of Stem
Corrosion by PJI';
      title2 'Teaching Hospital Status #byval(teaching)';
run;


/*Stratified by Gender*/
proc sort data =hips_cor;
      by gender;
run;
proc npar1way wilcoxon correct=no data=hips_cor;
      class PJI;
      var maxcor;
      by gender;* descending;
      *exact wilcoxon;
      title1 'Stratified Cross-Sectional Comparison (Wilocoxon) of Max
Corrosion by PJI';
      title2 'Gender #byval(gender)';
run;


proc npar1way wilcoxon correct=no data=hips_cor;
      class PJI;
      var headcor;
      by gender;* descending;
      *exact wilcoxon;
      title1 'Stratified Cross-Sectional Comparison (Wilocoxon) of Head
Corrosion by PJI';
      title2 'Gender #byval(gender)';
run;


proc npar1way wilcoxon correct=no data=hips_cor;
      class PJI;
      var stemcor;
      by gender;* descending;
      *exact wilcoxon;
      title1 'Stratified Cross-Sectional Comparison (Wilocoxon) of Stem
Corrosion by PJI';
      title2 'Gender #byval(gender)';
run;


/*Stratified by Race*/
proc sort data =hips_cor;
      by race_new;
run;
proc npar1way wilcoxon correct=no data=hips_cor;
      class PJI;
      var maxcor;
      by race_new;* descending;
      where race_new ne "";
      *exact wilcoxon;
      title1 'Stratified Cross-Sectional Comparison (Wilocoxon) of Max
Corrosion by PJI';
      title2 'Race #byval(Race_new)';
run;
proc npar1way wilcoxon correct=no data=hips_cor;
      class PJI;
      var headcor;
      by race_new;* descending;
```

```
        where race_new ne "";
        *exact wilcoxon;
        title1 'Stratified Cross-Sectional Comparison (Wilocoxon) of Head
Corrosion by PJI';
        title2 'Race #byval(Race_new)';
run;
proc npar1way wilcoxon correct=no data=hips_cor;
        class PJI;
        var stemcor;
        by race_new;* descending;
        where race_new ne "";
        *exact wilcoxon;
        title1 'Stratified Cross-Sectional Comparison (Wilocoxon) of Stem
Corrosion by PJI';
        title2 'Race #byval(Race_new)';
run;


options byline;

/*C: Univariate Analysis of Corrosion*/

proc logistic data=hips_cor outest=betas covout
plots(only)=(effect(polybar) oddsratio(range=clip));
        class PJI (param=ref ref='0') it_cat(ref=first);
        model bin_maxcor (event=last) = PJI;
        *oddsratio Additive;
        title 'Logistic Regression for Max Corrosion by PJI';
run;

proc logistic data=hips_cor outest=betas covout
plots(only)=(effect(polybar) oddsratio(range=clip));
        class PJI (param=ref ref='0') it_cat(ref=first);
        model bin_headcor (event=last) = PJI;
        *oddsratio Additive;
        title 'Logistic Regression for Head Corrosion by PJI';
run;

proc logistic data=hips_cor outest=betas covout
plots(only)=(effect(polybar) oddsratio(range=clip));
        class PJI (param=ref ref='0') it_cat(ref=first);
        model bin_stemcor (event=last) = PJI;
        *oddsratio Additive;
        title 'Logistic Regression for Stem Corrosion by PJI';
run;


proc logistic data=hips_cor outest=betas covout
plots(only)=(effect(polybar) oddsratio(range=clip));
        class PJI (param=ref ref='0') it_cat(ref=first) liner_mat;
        model bin_maxcor (event=last) = implantation_time;
        *oddsratio Additive;
        title 'Logistic Regression for Max Corrosion by Implantation
Time';
run;

proc logistic data=hips_cor outest=betas covout
plots(only)=(effect(polybar) oddsratio(range=clip));
```

```
      class PJI (param=ref ref='0') it_cat(ref=first) liner_mat;
      model bin_headcor (event=last) = implantation_time;
      *oddsratio Additive;
      title 'Logistic Regression for Head Corrosion by Implantation
Time';
run;

proc logistic data=hips_cor outest=betas covout
plots(only)=(effect(polybar) oddsratio(range=clip));
      class PJI (param=ref ref='0') it_cat(ref=first) liner_mat;
      model bin_stemcor (event=last) = implantation_time;
      *oddsratio Additive;
      title 'Logistic Regression for Stem Corrosion by Implantation
Time';
run;

proc logistic data=hips_cor outest=betas covout
plots(only)=(effect(polybar) oddsratio(range=clip));
      class PJI (param=ref ref='0') it_cat(ref=first) liner_mat;
      model bin_maxcor (event=last) = age;
      *oddsratio Additive;
      title 'Logistic Regression for Max Corrosion by Age at
Implantation';
run;

proc logistic data=hips_cor outest=betas covout
plots(only)=(effect(polybar) oddsratio(range=clip));
      class PJI (param=ref ref='0') it_cat(ref=first) liner_mat;
      model bin_maxcor (event=last) = bmi;
      *oddsratio Additive;
      title 'Logistic Regression for Max Corrosion by BMI';
run;

      proc logistic data=hips_cor outest=betas covout
plots(only)=(effect(polybar) oddsratio(range=clip));
            class PJI (param=ref ref='0') it_cat(ref=first) liner_mat;
            model bin_maxcor (event=last) = Height__in_;
            *oddsratio Additive;
            title 'Logistic Regression for Max Corrosion by Height';
      run;

      proc logistic data=hips_cor outest=betas covout
plots(only)=(effect(polybar) oddsratio(range=clip));
            class PJI (param=ref ref='0') it_cat(ref=first) liner_mat;
            model bin_maxcor (event=last) = Weight__lbs_;
            *oddsratio Additive;
            title 'Logistic Regression for Max Corrosion by Weight';
      run;

proc logistic data=hips_cor outest=betas covout
plots(only)=(effect(polybar) oddsratio(range=clip));
      class PJI (param=ref ref='0') it_cat(ref=first) gender;
      model bin_maxcor (event=last) = gender;
      *oddsratio Additive;
      title 'Logistic Regression for Max Corrosion by Gender';
run;
```

```
proc logistic data=hips_cor outest=betas covout
plots(only)=(effect(polybar) oddsratio(range=clip));
     class PJI (param=ref ref='0') it_cat(ref=first) race_new;
     model bin_maxcor (event=last) = race_new;
     *oddsratio Additive;
     title 'Logistic Regression for Max Corrosion by race';
run;

proc logistic data=hips_cor outest=betas covout
plots(only)=(effect(polybar) oddsratio(range=clip));
     class PJI (param=ref ref='0') it_cat(ref=first)
revision(ref="0");
     model bin_maxcor (event=last) = revision;
     *oddsratio Additive;
     title 'Logistic Regression for Max Corrosion by History of
Previous Revision';
run;

proc logistic data=hips_cor outest=betas covout
plots(only)=(effect(polybar) oddsratio(range=clip));
     class PJI (param=ref ref='0') it_cat(ref=first) teaching
(ref=first);
     model bin_maxcor (event=last) = teaching;
     *oddsratio Additive;
     title 'Logistic Regression for Max Corrosion by teaching';
run;



/*Mulitvariate Analysis of Oxidation Index*/

proc logistic data=hips_cor outest=betas covout
plots(only)=(effect(polybar) oddsratio(range=clip));
     class PJI (param=ref ref='0') gender;
     model bin_maxcor (event=last) = PJI Gender;
     *oddsratio Additive;
     title 'Logistic Regression for Max Corrosion by PJI Controlling
for Gender';
run;

proc logistic data=hips_cor outest=betas covout
plots(only)=(effect(polybar) oddsratio(range=clip));
     class PJI (param=ref ref='0') revision(ref="0");
     model bin_maxcor (event=last) = PJI revision;
     *oddsratio Additive;
     title 'Logistic Regression for Max Corrosion by PJI Controlling
for History of Previous Revision';
run;

proc logistic data=hips_cor outest=betas covout
plots(only)=(effect(polybar) oddsratio(range=clip));
     class PJI (param=ref ref='0') revision(ref="0") gender;
     model bin_maxcor (event=last) = PJI revision gender;
     *oddsratio Additive;
     title 'Logistic Regression for Max Corrosion by PJI Controlling
for History of Previous Revision and Gender';
run;
```

```
ods rtf close;


/***************For AAHKS Poster**************/
/***************For AAHKS Poster**************/
/***************For AAHKS Poster**************/
/***************For AAHKS Poster**************/
/***************For AAHKS Poster**************/

ods rtf file="C:\Users\ghiggs\Desktop\Genymphas\Research\Infection\JOA
Paper\SAS Files\Infection Manuscript - Corrosion Output-AAHKS.rtf"
fontscale=85 style=rtf;


/*Univariate Analysis of Corrosion*/

proc logistic data=hips_cor outest=betas covout
plots(only)=(effect(polybar) oddsratio(range=clip));
     class PJI (param=ref ref='0') it_cat(ref=first);
     model bin_maxcor (event=last) = PJI;
     *oddsratio Additive;
     title 'Logistic Regression for Max Corrosion by PJI';
run;


proc logistic data=hips_cor outest=betas covout
plots(only)=(effect(polybar) oddsratio(range=clip));
     class PJI (param=ref ref='0') it_cat(ref=first) liner_mat;
     model bin_maxcor (event=last) = implantation_time;
     *oddsratio Additive;
     title 'Logistic Regression for Max Corrosion by Implantation
Time';
run;

proc logistic data=hips_cor outest=betas covout
plots(only)=(effect(polybar) oddsratio(range=clip));
     class PJI (param=ref ref='0') it_cat(ref=first) liner_mat;
     model bin_maxcor (event=last) = age;
     *oddsratio Additive;
     title 'Logistic Regression for Max Corrosion by Age at
Implantation';
run;

proc logistic data=hips_cor outest=betas covout
plots(only)=(effect(polybar) oddsratio(range=clip));
     class PJI (param=ref ref='0') it_cat(ref=first) liner_mat;
     model bin_maxcor (event=last) = bmi;
     *oddsratio Additive;
     title 'Logistic Regression for Max Corrosion by BMI';
run;

     proc logistic data=hips_cor outest=betas covout
plots(only)=(effect(polybar) oddsratio(range=clip));
         class PJI (param=ref ref='0') it_cat(ref=first) liner_mat;
         model bin_maxcor (event=last) = Height__in_;
         *oddsratio Additive;
```

```
            title 'Logistic Regression for Max Corrosion by Height';
     run;


     proc logistic data=hips_cor outest=betas covout
plots(only)=(effect(polybar) oddsratio(range=clip));
            class PJI (param=ref ref='0') it_cat(ref=first) liner_mat;
            model bin_maxcor (event=last) = Weight__lbs_;
            *oddsratio Additive;
            title 'Logistic Regression for Max Corrosion by Weight';
     run;

proc logistic data=hips_cor outest=betas covout
plots(only)=(effect(polybar) oddsratio(range=clip));
     class PJI (param=ref ref='0') it_cat(ref=first) gender;
     model bin_maxcor (event=last) = gender;
     *oddsratio Additive;
     title 'Logistic Regression for Max Corrosion by Gender';
run;

proc logistic data=hips_cor outest=betas covout
plots(only)=(effect(polybar) oddsratio(range=clip));
     class PJI (param=ref ref='0') it_cat(ref=first) gender;
     model bin_maxcor (event=last) = bmi;
     *oddsratio Additive;
     title 'Logistic Regression for Max Corrosion from BMI';
run;

proc logistic data=hips_cor outest=betas covout
plots(only)=(effect(polybar) oddsratio(range=clip));
     class PJI (param=ref ref='0') it_cat(ref=first) gender;
     model bin_maxcor (event=last) = gender bmi;
     *oddsratio Additive;
     title 'Logistic Regression for Max Corrosion by Gender and BMI';
run;

proc logistic data=hips_cor outest=betas covout
plots(only)=(effect(polybar) oddsratio(range=clip));
     class PJI (param=ref ref='0') it_cat(ref=first) race_new;
     model bin_maxcor (event=last) = race_new;
     *oddsratio Additive;
     title 'Logistic Regression for Max Corrosion by race';
run;

proc logistic data=hips_cor outest=betas covout
plots(only)=(effect(polybar) oddsratio(range=clip));
     class PJI (param=ref ref='0') it_cat(ref=first)
revision(ref="0");
     model bin_maxcor (event=last) = revision;
     *oddsratio Additive;
     title 'Logistic Regression for Max Corrosion by History of
Previous Revision';
run;

proc logistic data=hips_cor outest=betas covout
plots(only)=(effect(polybar) oddsratio(range=clip));
     class PJI (param=ref ref='0') it_cat(ref=first) teaching
(ref=first);
```

```
        model bin_maxcor (event=last) = teaching;
        *oddsratio Additive;
        title 'Logistic Regression for Max Corrosion by teaching';
run;

ods rtf close;

proc freq data=hips_cor;
tables Weight__lbs_;
run;

/*Mulitvariate Analysis of Oxidation Index*/

proc logistic data=hips_cor outest=betas covout
plots(only)=(effect(polybar) oddsratio(range=clip));
        class PJI (param=ref ref='0') gender;
        model bin_maxcor (event=last) = PJI Gender;
        *oddsratio Additive;
        title 'Logistic Regression for Max Corrosion by PJI Controlling
for Gender';
run;

proc logistic data=hips_cor outest=betas covout
plots(only)=(effect(polybar) oddsratio(range=clip));
        class PJI (param=ref ref='0') revision(ref="0");
        model bin_maxcor (event=last) = PJI revision;
        *oddsratio Additive;
        title 'Logistic Regression for Max Corrosion by PJI Controlling
for History of Previous Revision';
run;

proc logistic data=hips_cor outest=betas covout
plots(only)=(effect(polybar) oddsratio(range=clip));
        class PJI (param=ref ref='0') revision(ref="0") gender;
        model bin_maxcor (event=last) = PJI revision gender;
        *oddsratio Additive;
        title 'Logistic Regression for Max Corrosion by PJI Controlling
for History of Previous Revision and Gender';
run;

ods rtf close;

proc contents data=hips_cor;
run;

proc freq data=hips_cor;
tables bmi*Weight__lbs_;
run;
```

Appendix C: Taper Interface Strength and Corrosion Analysis SAS Script

```
ods graphics on;
ods html sge=on;

*libname biocorr
"C:\Users\ghiggs\Desktop\Genymphas\Research\Disassembly\Disassembly
Datasheets";
/************************ANALYSING HIPS AND KNEES DATA
SETS***************************/

*import datasets;
/*
proc import datafile =
"C:\Users\ghiggs\Desktop\Genymphas\Research\Disassembly\Disassembly
Datasheets\Final\Taper Evaluation.xlsx"
     dbms = xlsx out=tapereval replace;
     getnames=yes;
run;

proc import datafile =
"C:\Users\ghiggs\Desktop\Genymphas\Research\Disassembly\Disassembly
Datasheets\Final\Measurements Update.xlsx"
     dbms = xlsx out=tapermeasure replace;
     getnames=yes;
run;

proc import datafile =
"C:\Users\ghiggs\Desktop\Genymphas\Research\Disassembly\Disassembly
Datasheets\Final\Disassembly Export 8.9.17.xlsx"
     dbms = xlsx out=export replace;
     getnames=yes;
run;

proc sort data=tapereval;
     by Study__;
run;

proc sort data=tapermeasure;
     by Study__;
run;

data tapereval2;
     merge tapereval tapermeasure;
     by Study__;
run;

proc sort data=export;
     by Study__;
run;

data tapereval3;
     merge export tapereval2;
     by Study__;
run;
```

```
proc export
      data=tapereval3
      dbms=xlsx
      outfile='C:\Users\ghiggs\Desktop\Genymphas\Research\Disassembly\D
isassembly Datasheets\Final\tapereval3.xlsx'
      replace;
run;
*/

proc import datafile =
"C:\Users\ghiggs\Desktop\Genymphas\Research\Disassembly\Disassembly
Datasheets\Final\Disassembly Export Final.xlsx"
      dbms = xlsx out=raw_data replace;
      getnames=yes;
run;

*look at data;
proc contents data=raw_data varnum; run;

*data step for renaming variables;
data hips (drop = Clinical_Information_Converted12
Clinical_Information_Converted13 Head_Size);
      set raw_data;
      rename Study__ = Study_ID;
      rename Clinical_Information_Converted__ = Gender;
      rename Clinical_Information_Converted_1 = Race;
      rename Clinical_Information_Converted_2 = Height;
      rename Clinical_Information_Converted_3 = Weight;
      rename Clinical_Information_Converted_4 = Primary_Reason;
      rename Clinical_Information_Converted_6 = Implantation_Date;
      rename Clinical_Information_Converted_9 = Implantation_Surgeon;
      rename Clinical_Information_Converted14 = Date_Recd;
      rename Clinical_Information_Converted_7 = Revision_Date;
      rename Clinical_Information_Converted_8 = Age;
      rename Clinical_Information_Converted_9 = Implantation_Time;
      rename Clinical_Information_Converted_5 =
Number_of_Previous_Revisions;
      rename Clinical_Information_Converted10 = Revision_Reason;
      rename Clinical_Information_Converted11 = Standardized_Reason;
      rename Corrosion_Scoring__Femoral_Head = Final_Female;
      rename Corrosion_Scoring__Stem_Trunnion = Final_Male;
      rename Taper_Characterization__Taper_Di = Disassembly_Force;
      rename Taper_Characterization__Stem_Len = app_LOE;
      rename Taper_Characterization__Stem_Tap = width;
      rename Taper_Characterization__Stem_Ta1 = LOE;
      if Head_Size = "--" then Head_Size_New = .;
            else Head_Size_New = input(Head_Size,10.);
      if Clinical_Information_Converted12 = "N/A" then UCLA_Score1 = .;
            else UCLA_Score1 =
input(Clinical_Information_Converted12,10.);
      if Clinical_Information_Converted13 = "N/A" then UCLA_Score2 = .;
            else UCLA_Score2 =
input(Clinical_Information_Converted13,10.);
run;

proc contents data=hips varnum;
run;
```

```
/*
proc freq data=hips;
tables num_head_offset char_head_offset head_offset stem_taper_size
taper_type/missing;
run;
*/


*data step for creating new variables and correcting erroneous
observations;
data hipsnew;
      set hips;
      if Height = 0 then Height = .;
      if Weight = 0 then Weight = .;
      if Height > . and Weight >. then BMI = (Weight/Height**2)*703;
      if Implantation_Date = . or Revision_Date = . then
Implantation_Time = .;
      if age < 18 then age = .;
      if race = "A" then race_new = "Other";
            else if race = "AL" then race_new = "Other";
            else if race = "Blk" then race_new = "Other";
            else if race = "H" then race_new = "Other";
            else if race = "Other" then race_new = "Other";
            else if race = "Other/Blank" then race_new = "Other";
            else if race = "Pac" then race_new = "Other";
            else if race = "W" then race_new = "White";
      if Final_Female = . then delete;
      if Head_Material = "Zirconia-Toughened Alumina" then delete;
      if Head_Material = "Titanium" then delete;
      Stem_Material = upcase(Stem_Material);
      *Stem_Material = strip(Stem_Material);
      if find(Stem_Material,'TMZF','i') ge 1 then Stem_Material=
'TMZF';
      if find(Stem_Material,'COCR','i') ge 1 then Stem_Material=
'COCR';
      if Retrieval = "Retrieval" then Retrieval = "Revision";
      if find(Standardized_Reason,'Fracture','i') ge 1 then
Standardized_Reason= 'Fracture';
      if Standardized_Reason in("Loosening", "Infection", "Fracture",
"") then Standardized_Reason = Standardized_Reason;
            else Standardized_Reason = "Other";
      if Standardized_Reason = "Loosening" then Loosening = "Yes";
            else if Standardized_Reason = "" then Loosening = "";
            else Loosening = "No";
      if Disassembly_Force ne .;
      UCLA_max = max(of UCLA_Score1 UCLA_Score2);
      *width = mean(of Trunnion_Width_1 Trunnion_Width_2
Trunnion_Width_3);
      *LOE = mean(of Trunnion_Length_1 Trunnion_Length_2
Trunnion_Length_3);
      *app_LOE = mean(of Apparent_Length_of_Engagement_1
Apparent_Length_of_Engagement_2 Apparent_Length_of_Engagement_3);
      *disassembly_force = final_disassembly_force;
      pi=constant("pi");
      I = (pi/4)*((width/2)*0.001)**4;
      if Stem_Material = "TMZF" then E = 80;
      if Stem_Material = "TI ALLOY" then E = 110;
      if Stem_Material = "COCR" then E = 200;
```

```
      Flex_Rigid = I*E*1000000000;
      char_head_offset = head_offset;
      if find(Head_Offset,'--','i') ge 1 then char_head_offset = "";
      else char_head_offset = compress(head_offset,' -.','kd');
      if char_head_offset = '-' then char_head_offset = '';
      num_head_offset = input(char_head_offset, 8.);
      taper_type = stem_taper_size;
      if find(stem_taper_size,'--','i') ge 1 then taper_type = "";
      if find(stem_taper_size,'12/14','i') ge 1 then taper_type =
'12/14';
      if find(stem_taper_size,'38','i') ge 1 then taper_type = 'C-
Taper';
      if find(stem_taper_size,'C','i') ge 1 then taper_type = 'C-
Taper';
      if find(stem_taper_size,'6','i') ge 1 then taper_type = '6°';
      if find(stem_taper_size,'52','i') ge 1 then taper_type = '2°52';
      if find(stem_taper_size,'40','i') ge 1 then taper_type = '5°40';
      if find(stem_taper_size,'type 1','i') ge 1 then taper_type =
'Type 1';
      if taper_type = "12/14" then bin_taper_type = "12/14";
      else if taper_type = "" then bin_taper_type = "";
      else bin_taper_type = "other";
      if taper_type = '5°40' then taper_angle = 5.6667;
      if taper_type = 'C-Taper' then taper_angle = 5.6436;
      if taper_type = '6°' then taper_angle = 6;
      if taper_type = '2°52' then taper_angle = 2.8667;
      if taper_type = 'Type 1' then taper_angle = 4.0;
      if taper_type = '12/14' then taper_angle = 5.6;
      if find(Study_ID,'C-UT','i') ge 1 then retrieval = "Cadaver";
      else if find(Study_ID,'RLU','i') ge 1 then retrieval = "Cadaver";
      else retrieval = "Revision";
run;


proc contents data=hipsnew varnum;
run;


proc export
      data=hipsnew
      dbms=xlsx
      outfile='C:\Users\ghiggs\Desktop\Genymphas\Research\Disassembly\D
isassembly Datasheets\Final\Disassembly_SAS_Export_Final.xlsx'
      replace;
run;

ods rtf
file="C:\Users\ghiggs\Desktop\Genymphas\Research\Disassembly\Biocorrosi
on_Disassembly_Output_Stratified.rtf" fontscale=85 style=rtf;



data hipsnew;
set hipsnew;
if Disassembly_Force < 3400 then Disassembly_Force_Cat = 1;
else if Disassembly_Force > 3400 then Disassembly_Force_Cat = 2;
run;

/*Clinical and Implant Summaries*/
proc tabulate data=hipsnew;
```

```
      var Implantation_Date Revision_Date;
      table Implantation_Date Revision_Date,
            n nmiss (min max)*f=mmddyy10.;
      title "Implantation and Revision Dates";
run;


proc freq data=hipsnew;
      tables Retrieval Stem_Manufacturer Gender Standardized_Reason
Loosening Head_Material*Stem_Material head_taper_angle stem_taper_size
taper_type trunnion_finish head_size_new /missing;
      title "Clinical and Implant Summaries";
run;


proc means data=hipsnew;
      var Implantation_Time Age flex_rigid;
run;


proc capability data=hipsnew normaltest; *also a check for normality;
      var Disassembly_Force;
      title "Disassembly Force Distribution and Summary";
run;


proc freq data=hipsnew;
      tables Final_Female Final_Male;
      title "Taper Damage Summaries";
run;


/*Correlation Computation*/
proc corr data=hipsnew spearman; * pearson kendall polyserial;
      var Disassembly_Force;
      with Final_Male Final_Female;
      where disassembly_force_cat=1;
      title "Correlations Between Disassembly Force and Taper Damage";
run;


proc corr data=hipsnew spearman; * pearson kendall polyserial;
      var Disassembly_Force;
      with Final_Male Final_Female;
      where disassembly_force_cat=1;
      title "Stratified Correlations Between Disassembly Force and
Taper Damage (<3.4kN)";
run;


proc corr data=hipsnew spearman; * pearson kendall polyserial;
      var Disassembly_Force;
      with Final_Male Final_Female;
      where disassembly_force_cat=2;
      title "Stratified Correlations Between Disassembly Force and
Taper Damage (>3.4kN)";
run;



                              /*proc corr data=hipsnew spearman; *
pearson kendall polyserial;*/
                              /*    var Disassembly_Force;*/
                              /*    with LOE app_LOE;*/
```

```
                                         /*     title "Correlation: Disassembly
Force with Apparent Length of Engagement, Length of Engagement";*/
                                         /*run;*/
                                         /**/
                                         /*proc corr data=hipsnew spearman; *
pearson kendall polyserial;*/
                                         /*     var LOE;*/
                                         /*     with Final_Male Final_Female;*/
                                         /*     title "Correlations Between Length
of Engagement and Taper Damage";*/
                                         /*run; */
                                         /**/
                                         /*proc corr data=hipsnew spearman; *
pearson kendall polyserial;*/
                                         /*     var app_LOE;*/
                                         /*     with Final_Male Final_Female;*/
                                         /*     title "Correlations Between
Apparent Length of Engagement and Taper Damage";*/
                                         /*run; */

                                         /*Check Linear Regression Model
Assumptions*/

                                         /*
                                         proc insight data=hipsnew;
                                          scatter disassembly_force
implantation_time age*
                                                 disassembly_force implantation_time
age;
                                         run;
                                         quit;

                                         proc corr data=hipsnew
plots=matrix(histogram);
                                                 var disassembly_force
implantation_time age;
                                         run;
                                         */

/*Model Clinical and Device Variables Relating to Disassembly Force*/
proc glm data=hipsnew;
     model Disassembly_Force = age;
     title "Disassembly Force and Age";
run;
proc glm data=hipsnew;
     class gender;
     model Disassembly_Force = gender/solution;
     title "Disassembly Force and gender";
run;
proc glm data=hipsnew;
     model Disassembly_Force = bmi;
     title "Disassembly Force and BMI";
run;
proc glm data=hipsnew;
     model Disassembly_Force = Implantation_Time;
     title "Disassembly Force and Implantation Time";
run;
```

```
proc glm data=hipsnew;
     class Loosening (ref=first);
     model Disassembly_Force = Loosening/solution ;
     title "Disassembly Force and Loosening";
run;
proc glm data=hipsnew;
     class stem_material (ref=first);
     model Disassembly_Force = Stem_Material/solution ;
     title "Disassembly Force and Stem Material";
run;
proc glm data=hipsnew;
     model Disassembly_Force = flex_rigid;
     title "Disassembly Force and Flexural Rigidity";
run;
proc glm data=hipsnew;
     *class stem_material;
     model Disassembly_Force = Head_Size_New/solution ;
     title "Disassembly Force and Head Size";
run;
proc glm data=hipsnew;
     model Disassembly_Force = Num_Head_Offset/solution ;
     title "Disassembly Force and Head Offset";
run;
                    /*proc glm data=hipsnew;*/
                    /*    class taper_type (ref="12/14");*/
                    /*    model Disassembly_Force = taper_type/solution
;*/
                    /*    title "Disassembly Force and Taper Type";*/
                    /*run;*/
                    /*proc glm data=hipsnew;*/
                    /*    class bin_taper_type (ref="12/14");*/
                    /*    model Disassembly_Force =
bin_taper_type/solution ;*/
                    /*    title "Disassembly Force and 12/14 Tapers vs
Other";*/
                    /*run;*/
                    /*    proc glm data=hipsnew;*/
                    /*        class bin_taper_type (ref="12/14");*/
                    /*        model implantation_time =
bin_taper_type/solution ;*/
                    /*        title "Implantation_time and 12/14 Tapers
vs Other";*/
                    /*    run;*/
proc glm data=hipsnew;
     model Disassembly_Force = taper_angle/solution ;
     title "Disassembly Force and Taper Angle";
run;
proc glm data=hipsnew;
     model Disassembly_Force = LOE/solution ;
     title "Disassembly Force and LOE";
run;
                    /*proc glm data=hipsnew;*/
                    /*    model Disassembly_Force = app_LOE/solution ;*/
                    /*    title "Disassembly Force and Apparent Length of
Engagement";*/
                    /*run;*/
proc glm data=hipsnew;
```

```
        class Trunnion_Finish (ref=first);
        model Disassembly_Force = Trunnion_Finish/solution ;
        title "Disassembly Force and Trunnion Finish";
run;
                /*              /*Assess the effect of taper type, as per
reviewer's request*/*/
                /*          proc sort data=hipsnew;*/
                /*              by taper_type;*/
                /*          run;*/
                /**/
                /*          proc capability data=hipsnew; */
                /*              var Disassembly_Force;*/
                /*              by Taper_Type;*/
                /*              title 'Disassembly Force Summary
Statistics by Taper Type';*/
                /*          run;*/
                /**/
                /*          proc npar1way wilcoxon correct=no
data=hipsnew PLOTS=wilcoxon;*/
                /*              class Taper_Type;*/
                /*              var Disassembly_Force;*/
                /*              title 'Cross-Sectional Comparison
(Wilcoxon) of Disassembly Force by Taper Type';*/
                /*          run;*/
                /**/
                /*          proc corr data=hipsnew spearman; *
pearson kendall polyserial;*/
                /*          var Disassembly_Force;*/
                /*          with Final_Male Final_Female;*/
                /*          by taper_type;*/
                /*          title "Correlations Between Disassembly
Force and Taper Damage, by Taper Type";*/
                /*          run;

proc sort data=hipsnew;
     by trunnion_finish;
run;

proc capability data=hipsnew;
     var disassembly_force;
     by trunnion_finish;
     title 'Disassembly Force by Trunnion Finish';
run;

proc npar1way wilcoxon correct=no data=hipsnew;
     class Trunnion_Finish;
     var Disassembly_Force;
     title 'Cross-Sectional Comparison (Wilcoxon) of Disassembly Force
by Trunnion Finish';
run;


/*Model Clinical and Device Variables Relating to Head Corrosion*/

proc logistic data=hipsnew;
     model Final_Female = age;
     title "Head Taper Damage and Age";
```

```
run;

proc logistic data=hipsnew;
     class gender;
     model Final_Female = gender;
     title "Head Taper Damage and Gender";
run;

proc logistic data=hipsnew;
     model Final_Female = BMI;
     title "Head Taper Damage and BMI";
run;

proc logistic data=hipsnew;
     model Final_Female = Implantation_Time;
     title "Head Taper Damage and Implantation Time";
run;

proc logistic data=hipsnew;
     class Stem_Material (ref=first);
     model Final_Female = Stem_Material;
     title "Head Taper Damage and Stem Material";
run;

proc logistic data=hipsnew;
     model Final_Female = Flex_Rigid;
     title "Head Taper Damage and Flexural Rigidity";
run;

proc logistic data=hipsnew;
     model Final_Female = Head_Size_New;
     title "Head Taper Damage and Head Size";
run;

proc logistic data=hipsnew;
     model Final_Female = num_head_offset;
     title "Head Taper Damage and Head Offset";
run;

proc logistic data=hipsnew;
     model Final_Female = taper_angle;
     title "Head Taper Damage and Taper Angle";
run;

proc logistic data=hipsnew;
     model Final_Female = LOE;
     title "Head Taper Damage and Taper Length";
run;

proc logistic data=hipsnew;
     class trunnion_finish (ref="Micro-Grooved");
     model Final_Female = trunnion_finish;
     title "Head Taper Damage and Trunnion Finish";
run;

               /*proc glm data=hipsnew;*/
               /*    class Trunnion_Finish;*/
```

```
                         /*    model Final_Female = Trunnion_Finish/solution
;*/
                         /*    title "Head Taper Damage and Trunnion
Finish";*/
                         /*run;*/


proc logistic data=hipsnew;
      class Loosening (ref=first);
      model Final_Female = Loosening;
      title "Head Taper Damage and Loosening";
run;



/*Model Clinical and Device Variables Relating to Stem Corrosion*/

proc logistic data=hipsnew;
      model Final_Male = age;
      title "Stem Taper Damage and Age";
run;

proc logistic data=hipsnew;
      class gender;
      model Final_Male = gender;
      title "Stem Taper Damage and Gender";
run;

proc logistic data=hipsnew;
      model Final_Male = BMI;
      title "Stem Taper Damage and BMI";
run;

proc logistic data=hipsnew;
      model Final_Male = Implantation_Time;
      title "Stem Taper Damage and Implantation Time";
run;

proc logistic data=hipsnew;
      class Loosening (ref="No");
      model Final_Male = Loosening;
      title "Stem Taper Damage and Loosening";
run;

proc logistic data=hipsnew;
      model Final_Male = Head_Size_New;
      title "Stem Taper Damage and Head Size";
run;

proc logistic data=hipsnew;
      model Final_male = num_head_offset;
      title "Stem Taper Damage and Head Offset";
run;

proc logistic data=hipsnew;
      class Stem_Material (ref=first);
      model Final_Male = Stem_Material;
      title "Stem Taper Damage and Stem Material";
```

```
run;

proc logistic data=hipsnew;
      class Stem_Material;
      model Final_Male = Flex_Rigid;
      title "Stem Taper Damage and Flexural Rigidity";
run;

proc logistic data=hipsnew;
      model Final_male = taper_angle;
      title "Stem Taper Damage and Taper Angle";
run;

proc logistic data=hipsnew;
      model Final_male = LOE;
      title "Stem Taper Damage and Taper Length";
run;
proc logistic data=hipsnew;
      class trunnion_finish (ref="Micro-Grooved");
      model Final_male = trunnion_finish;
      title "Stem Taper Damage and Trunnion Finish";
run;

/*Adjust for Confounding Factors and Effect Modifiers*/

*Head Damage - Trunnion Finish;

proc sort data=hipsnew;
by trunnion_finish;
run;

proc glm data=hipsnew;
      class Trunnion_Finish;
      model Disassembly_Force = Final_female/solution ;
      title "Disassembly Force and Head Damage";
run;

proc glm data=hipsnew;
      class Trunnion_Finish;
      model Disassembly_Force = Final_female/solution ;
      by trunnion_finish; *Identify Effect Modification;
      title "Disassembly Force and Head Damage by Trunnion Finish";
run;

proc glm data=hipsnew;
      class Trunnion_Finish;
      model Disassembly_Force = final_female trunnion_finish
Final_female*trunnion_finish/solution ;
      title "Disassembly Force and Head Damage controlling for Trunnion
Finish with Interaction";
run;

*Stem Damage - Head Size, Taper Length and Trunnion Finish;

proc glm data=hipsnew;
      class Trunnion_Finish;
      model Disassembly_Force = Final_male/solution ;
```

```
      title "Disassembly Force and Stem Damage";
run;


proc glm data=hipsnew;
      class Trunnion_Finish;
      model Disassembly_Force = Final_male/solution ;
      by trunnion_finish; *Identify Effect Modification;
      title "Disassembly Force and Stem Damage by Trunnion Finish";
run;


proc glm data=hipsnew;
      class Trunnion_Finish;
      model Disassembly_Force = Final_male head_size_new LOE/solution ;
      by trunnion_finish;
      title "Disassembly Force and Stem Damage controlling for Head
Size and Taper Length by Trunnion Finish";
run;


proc glm data=hipsnew;
      class Trunnion_Finish;
      model Disassembly_Force = Final_male Trunnion_Finish
final_male*trunnion_finish/solution ;
      title "Disassembly Force and Stem Damage controlling for Trunnion
Finish with Interaction";
run;


proc glm data=hipsnew;
      class Trunnion_Finish;
      model Disassembly_Force = Final_male head_size_new LOE
trunnion_finish trunnion_finish*final_male/solution ;
      title "Disassembly Force and Stem Damage controlling for Head
Size, Taper Length and Trunnion Finish with Interaction";
run;
                        /*              proc glmselect data=hipsnew;*/
                        /*                  class Trunnion_Finish;*/
                        /*                  model Disassembly_Force =
Final_male Trunnion_Finish; *final_male*trunnion_finish; * /solution
;*/
                        /*                  title "Disassembly Force and
Stem Damage controlling for Trunnion Finish";*/
                        /*              run;*/
                        /**/
                        /*              proc glmselect data=hipsnew;*/
                        /*                  class Trunnion_Finish;*/
                        /*                  model Disassembly_Force =
Final_male Trunnion_Finish final_male*trunnion_finish; * /solution ;*/
                        /*                  title "Disassembly Force and
Stem Damage controlling for Trunnion Finish";*/
                        /*              run;*/


                        *Taper Type with Interaction;


                        /*proc glm data=hipsnew;*/
                        /*   class taper_type (ref="12/14");*/
                        /*   model Disassembly_Force = Final_male
taper_type/solution; * final_male*trunnion_finish/solution ;*/
```

```
                /*     title "Disassembly Force and Stem Damage
controlling for Trunnion Finish"; * with Interaction";*/
                /*run;*/
                /**/
                /*proc glm data=hipsnew;*/
                /*     class Trunnion_Finish;*/
                /*     model Disassembly_Force = Final_female
Trunnion_Finish final_female*trunnion_finish/solution ;*/
                /*     title "Disassembly Force and Head Damage
controlling for Trunnion Finish with Interaction";*/
                /*run;        */
                /**/
                /*proc glm data=hipsnew;*/
                /*     class bin_taper_type;*/
                /*     model Disassembly_Force = Final_female
bin_taper_type final_female*bin_taper_type/solution ;*/
                /*     title "Disassembly Force and Head Damage
controlling for Binary Taper Type";*/
                /*run;        */
                /**/
                /*proc glm data=hipsnew;*/
                /*     class bin_taper_type;*/
                /*     model Disassembly_Force = Final_male
bin_taper_type /solution ;*/
                /*     title "Disassembly Force and Stem Damage
controlling for Binary Taper Type";*/
                /*run;        */
                /**/
                /*proc glm data=hipsnew;*/
                /*     class bin_taper_type;*/
                /*     model Disassembly_Force = Final_male
bin_taper_type final_male*bin_taper_type/solution ;*/
                /*     title "Disassembly Force and Stem Damage
controlling for Binary Taper Type with Interaction";*/
                /*run;        */


/*Compare Disassembly Force Between Revision and Cadaver Retrievals*/
proc sort data=hipsnew;
     by Retrieval;
run;

proc capability data=hipsnew;
     var Disassembly_Force;
     by Retrieval;
     title 'Disassembly Force Summary Statistics by Retrieval Type';
run;

proc npar1way wilcoxon correct=no data=hipsnew;
     class Retrieval;
     var Disassembly_Force;
     title 'Cross-Sectional Comparison (Wilcoxon) of Disassembly Force
by Retrieval Type';
run;


/*Compare Head Taper Damage Between Revision and Cadaver Retrievals*/
proc sort data=hipsnew;
```

```
      by Retrieval;
run;

proc capability data=hipsnew;
      var Final_Female;
      by Retrieval;
      title 'Head Taper Damage Summary Statistics by Retrieval Type';
run;

proc npar1way wilcoxon correct=no data=hipsnew;
      class Retrieval;
      var Final_Female;
      title 'Cross-Sectional Comparison (Wilcoxon) of Head Taper Damage
by Retrieval Type';
run;

proc logistic data=hipsnew;
      class retrieval (ref="Cadaver");
      model Final_Female = Retrieval;
      title "Head Taper Damage by Retrieval Type";
run;

/*Compare Stem Taper Damage Between Revision and Cadaver Retrievals*/
proc sort data=hipsnew;
      by Retrieval;
run;

proc capability data=hipsnew;
      var Final_Male;
      by Retrieval;
      title 'Stem Taper Damage Summary Statistics by Retrieval Type';
run;

proc npar1way wilcoxon correct=no data=hipsnew;
      class Retrieval;
      var Final_Male;
      title 'Cross-Sectional Comparison (Wilcoxon) of Stem Taper Damage
by Retrieval Type';
run;

proc logistic data=hipsnew;
      class retrieval (ref="Cadaver");
      model Final_Male = Retrieval;
      title "Stem Taper Damage by Retrieval Type";
run;

ods rtf close;

                  /*/*Additional Analysis Looking at the Effect of
Loosening*/*/
                  /**/
                  /*proc freq data=hipsnew;*/
                  /*    tables Retrieval Stem_Manufacturer Gender
Standardized_Reason Loosening Head_Material*Stem_Material
loosening*stem_material;*/
                  /*    title "Clinical and Implant Summaries";*/
                  /*run;*/
```

```
                              /**/
                              /**/
                              /*proc glm data=hipsnew;*/
                              /*    class Final_Male;*/
                              /*    model Disassembly_Force = Final_Male/solution
;*/
                              /*    title "Disassembly Force and Stem Taper
Damage";*/
                              /*run;*/
                              /**/
                              /*ods graphics off;*/
                              /*proc plot data=hipsnew;*/
                              /*plot disassembly_force*final_male;*/
                              /*run;*/
                              /*quit;*/
                              /**/
                              /*proc sort data=hipsnew;*/
                              /*by final_male;*/
                              /*run;*/
                              /**/
                              /*proc capability data=hipsnew normaltest; *also a
check for normality;*/
                              /*    var Disassembly_Force;*/
                              /*    by final_male;*/
                              /*    title "Disassembly Force Distribution by Stem
Score";*/
                              /*run;*/
```

Vita

Genymphas B. Higgs

EDUCATION

(in progress)	**Drexel University, Philadelphia, Pennsylvania**
	School of Biomedical Engineering, Science, and Health Systems
	Ph.D. in Biomedical Engineering
	In vivo Performance of Modular Taper Connections and Development of an Electrochemical Framework for Quantitative Corrosion Investigations
June 2017	**Drexel University, Philadelphia, Pennsylvania**
	School of Public Health
	M.S. in Epidemiology
June 2013	**Drexel University, Philadelphia, Pennsylvania**
	School of Biomedical Engineering, Science, and Health Systems
	M.S. in Biomedical Engineering
	B.S. in Biomedical Engineering
	Dean's Award, Distinction, Summa Cum Laude

PROFESSIONAL EXPERIENCE

2017-Present	**Exponent**
	Biomedical Engineering Practice	Philadelphia, Pennsylvania
	Engineering Assistant

- Assessed medical device safety and functionality in accordance with national and international testing standards within an American Association Lab Accreditation (A2LA) certified laboratory
- Examined the economics, utilization and comparative effectiveness of medical technologies using national healthcare databases and hospital records

2013-2019	**Implant Research Center**
	Drexel University	Philadelphia, Pennsylvania
	Graduate Research Student

- Developed mechanical, electrochemical and 3-D imaging methodologies to quantitatively assess modular tapers in total hip devices
- Demonstrated the feasibility of using interdisciplinary analytical methods to study untested links between clinical factors and *in vivo* changes to hip and knee devices

2018	**CeramTec**
	Medical Products	Plochingen, Germany
	Regulatory Affairs and Product Development Fellow, German Academic Exchange Service (DAAD)

- Provided technical and regulatory guidance for navigating the FDA approval pathways for novel medical devices
- Identified opportunities for strategic investments to achieve continued growth and development within the evolving regulatory landscape of the European Union and United States

2015-2017   **U.S. Food and Drug Administration (FDA)**

Center for Devices and Radiological Health | Silver Spring, Maryland

<u>Research Fellow, Oak Ridge Institute for Science and Education</u>
- Advanced a multidisciplinary initiative to expand orthopedic implant registries with device evaluation as an engineering consultant
- Coordinated an institutional partnership between regulatory, clinical, and academic stakeholders within the Medical Device Epidemiology Network (MDEpiNet)

2010-2013   **Implant Research Center**

Drexel University | Philadelphia, Pennsylvania

<u>Engineering Research Assistant</u>
- Published a novel protocol for the analysis of polyetheretherketone (PEEK) spinal stabilization systems
- Characterized mechanical and chemical properties of ultra-high molecular weight polyethylene (UHMWPE) and PEEK components
- Investigated metal-on-metal total hip arthroplasty devices to characterize corrosion and fretting mechanisms

2009   **Wheatley Research Lab**

Drexel University | Philadelphia, Pennsylvania

<u>Research Assistant</u>
- Explored the performance of laminin-modified alginate as a permissive substrate for neural cell regeneration research
- Established the efficacy of a new peptide for further studies involving neuroblastoma cell adhesion

FELLOWSHIPS AND AWARDS

2019   Three Minute Thesis (3MT®) People's Choice Award, Drexel University

2019   Top 3 Finalist, Johnson and Johnson Engineering Showcase

2018   Young Investigator Award, International Society for Technology in Arthroplasty

2018   German Academic Exchange Service (DAAD) Fellowship

2017   Charles E. Etting Award for Excellence and Character, Drexel University Student Life

2015   Oak Ridge Institute for Science and Education (ORISE) Fellowship

2013   Dean's Award for Most Outstanding Graduate, Drexel University Pennoni Honors College

2012   Most Outstanding Paper in Arthroplasty Surgery, American Association of Hip & Knee Surgeons

2012   Best Student Paper, American Society for Testing and Materials (ASTM)

PUBLICATIONS

MacDonald DW, **Higgs GB**, Chen AF, Malkani AL, Mont MA, Kurtz SM. Oxidation, Damage Mechanisms, and Reasons for Revision of Sequentially Annealed Highly Crosslinked Polyethylene in Total Knee Arthroplasty. The Journal of arthroplasty. 2018 Apr 1;33(4):1235-41.

Higgs GB, MacDonald DW, Lowell J, Padayatil A, Mihalko WM, Siskey RL, Gilbert JL, Rimnac CM, Kurtz SM. Is Corrosion a Threat to the Strength of the Taper Connection in Femoral Components of Total Hip Replacements?. Corrosion. 2017 Oct 5;73(12):1538-43.

Urish KL, Hamlin BR, Plakseychuk AY, Levison TJ, **Higgs GB**, Kurtz SM, DiGioia AM. Trunnion failure of the recalled low friction ion treatment cobalt chromium alloy femoral head. The Journal of arthroplasty. 2017 Sep 1;32(9):2857-63.

Higgs GB, MacDonald DW, Gilbert JL, Rimnac CM, Kurtz SM, Chen AF, Klein GR, Hamlin BR, Lee GC, Mont MA, Cates HE. Does taper size have an effect on taper damage in retrieved metal-on-polyethylene total hip devices?. The Journal of arthroplasty. 2016 Sep 1;31(9):277-81.

Mihalko WM, Lowell J, **Higgs GB**, Kurtz S. Total knee post-cam design variations and their effects on kinematics and wear patterns. Orthopedics. 2016 May 26;39(3):S45-9.

Kurtz SM, Lanman TH, **Higgs GB**, MacDonald DW, Berven SH, Isaza JE, Phillips E, Steinbeck MJ. Retrieval analysis of PEEK rods for posterior fusion and motion preservation. European Spine Journal. 2013 Dec 1;22(12):2752-9.

Higgs GB, Hanzlik JA, MacDonald DW, Gilbert JL, Rimnac CM, Kurtz SM, Implant Research Center Writing Committee. Is increased modularity associated with increased fretting and corrosion damage in metal-on-metal total hip arthroplasty devices?: a retrieval study. The Journal of arthroplasty. 2013 Sep 1;28(8):2-6.

MacDonald DW, **Higgs GB**, Parvizi J, Klein G, Hartzband M, Levine H, Kraay M, Rimnac CM, Kurtz SM. Oxidative properties and surface damage mechanisms of remelted highly crosslinked polyethylenes in total knee arthroplasty. International orthopaedics. 2013 Apr 1;37(4):611-5.

BOOK CHAPTERS

Arnholt CM, Underwood RJ, MacDonald DW, **Higgs GB**, Chen A, Klein GR, Hamlin B, Lee GC, Mont MA, Cates H, Malkani A, Rimnac CM, Kurtz SM. Microgrooved surface topography does not influence fretting corrosion of tapers in total hip arthroplasty: classification and retrieval analysis. In: Modularity and Tapers in Total Joint Replacement Devices, STP 1591. Conshohocken, PA: ASTM; 2015.

Higgs GB, Hanzlik JA, MacDonald DW, Kane WM, Day JS, Klein GR, Parviz iJ, Mont MA, Kraay MJ, Martell JM, Gilbert JL, Rimnac CM, Kurtz SM. Method of characterizing fretting and corrosion at the various taper connections of retrieved modular components from metal-on-metal total hip arthroplasty. In: Metal-on-Metal Total Hip Replacement Devices, STP 1560. Conshohocken, PA: ASTM; 2013.

PRESENTATIONS

Higgs GB, Lewis TD, Darville LL, Brown SR. Shelter from the Storm: Climatic Adaptations for the Future. Sustainable Grand Bahama Conference. University of the Bahamas, Grand Bahama, Bahamas. March 5-6, 2020.

Higgs GB, Lin J, Khullar P, Kurtz SM, Gilbert JL. A Quantitative Method to Assess Corrosion Severity. Talk 8, Workshop on Accelerated Aging Methods and Testing Techniques for Medical Devices. ASTM International, Denver, CO, May 14, 2019.

Higgs GB, Sullivan M, Shenoy A, Kane W, Siskey RL, Gilbert JL, Kurtz SM. Nondestructive Identification of Subsurface Corrosion Features in Orthopedic Alloys Talk 7, Workshop on Accelerated Aging Methods and Testing Techniques for Medical Devices. ASTM International, Denver, CO, May 14, 2019.

Evans L, **Higgs GB**, Siskey RL. In Vitro Evaluation of Fretting Corrosion in a Modular Acetabular Taper. Poster No. 2220, 65th Annual Meeting of the Orthopaedic Research Society, Austin, TX, February 2-5, 2019.

Higgs GB, Siskey RL, Mihalko WM, Rimnac CM, Gilbert JL, Kurtz SM. Electrochemical Impedance Spectroscopy as a Method to Distinguish Corrosion Severity and Damage Modes in Retrieved Femoral Heads? 25th Annual Congress of the International Society for Technology in Arthroplasty, London, UK, October 10-13, 2018.

Higgs GB, Gerveshi C, Evans A, Tabb L, Kurtz SM. Incorporating Retrieval Analysis into Database Research to Understand the Role of Periprosthetic Joint Infection on Taper Corrosion in Total Hip Replacements. Paper No. 123, 7th Annual International Congress of Arthroplasty Registries, Reykjavik, Iceland, June 9-11, 2018.

Higgs GB, MacDonald DW, Lowell J, Padayatil A, Mihalko WM, Siskey RL, Gilbert JL, Rimnac CM, Kurtz SM. Does Corrosion Loosen the Taper Connection of Femoral Components in Total Hip Replacements? Paper No. 0276, 64th Annual Meeting of the Orthopaedic Research Society, New Orleans, LA, March 10-13, 2018.

Higgs GB, Gerveshi C, Evans A, Tabb L, Kurtz SM. Can an Infection Cause Corrosion of a Hip Replacement? Bridging the Gap Between Epidemiology and Engineering. Poster No. 1807, 64th Annual Meeting of the Orthopaedic Research Society, New Orleans, LA, March 10-13, 2018.

Arnholt CM, White JB, **Higgs GB**, MacDonald DW, Lowell JA, Perkins MR, Mihalko WM, Kurtz SM. Associations Between Metallosis and Tissue Metal Concentration in Autopsy Retrieved TKA. Paper No. 207, 64th Annual Meeting of the Orthopaedic Research Society, New Orleans, LA, March 10-13, 2018.

Higgs GB, Gervishi C, Tabb L, Evans A, Kurtz SM. Bridging the Gap Between Implant Retrieval Research and Epidemiological Studies using Survival Analysis. Poster No. 6, 27th Annual Meeting of the American Association of Hip and Knee Surgeons, Dallas, TX, November 2-5, 2017.

Higgs GB, Macdonald DW, Paxton L, Marinac-Dabic M, Kurtz SM, Combining Retrieval Research with Epidemiology to Understand the Role of Periprosthetic Joint Infection on the Oxidative Degradation of Total Hip Replacements. Poster No. 2, 8th International UHMWPE Meeting, Torino, Italy, October 19, 2017.

Higgs GB, Macdonald DW, Padayatil A, Spece H, Siskey RL, Callander S, Kurtz SM. Method of Estimating Material Loss for Retrieved Femoral Stems with Gross Trunnion Failure. Symposium on Beyond the Implant Retrieval Analysis Methods for Implant Surveillance. ASTM International, Toronto, Canada, May 9, 2017.

Higgs GB, Siskey RL, Mejia L, Burke D, Mahr A, Kurtz SM. Mechano-Electrochemical Testing for Clinically Relevant Evaluation of Total Hip Arthroplasty Device Performance. 21st Congress of the European Society of Biomechanics. Lyon, France, July 10–16, 2016.

Higgs GB, MacDonald DW, Gilbert JL, Rimnac CM, Kurtz SM. Does Taper Size Have an Effect on Taper Damage in Retrieved Metal-on-Polyethylene Total Hip Devices? 25th Annual Meeting of

the American Association of Hip and Knee Surgeons, Dallas, TX, November 5-8, 2015.

Higgs GB, Siskey RL, Gilbert JL, Mihalko WM, Rimnac CM, Kurtz SM. What Effect Does the Strength of the Taper Connection Have on Taper Damage in Retrieved Total Hip Devices? 61st Annual Meeting of the Orthopaedic Research Society. Las Vegas, NV, March 28–31, 2015.

Higgs GB, MacDonald DW, Chen AF, Klein GR, Hamlin BR, Lee G-C, Mont MA, Cates HE, Malkani AL, Kraay MJ, Gilbert JL, Rimnac CR, Kurtz SM. Does Taper Size Have an Effect on Taper Damage in Retrieved Total Hip Devices? 61st Annual Meeting of the Orthopaedic Research Society. Las Vegas, NV, March 28–31, 2015.

Arnholt CM, Underwood RJ, MacDonald DW, **Higgs GB**, Chen A, Klein GR, Hamlin B, Lee GC, Mont MA, Cates H, Malkani A, Rimnac CM, Kurtz SM. Micro-grooved Surface Topography Does Not Influence Fretting Corrosion of Tapers in THA: Classification and Retrieval Analysis. Symposium on Modularity and Tapers in Total Joint Replacement Devices. ASTM International, New Orleans, LA, November 10, 2014.

Higgs GB, MacDonald DW, Mihalko WM, Siskey RL, Gilbert JL, Rimnac CM, Kurtz SM. A Pilot Study Characterizing Taper Interface Integrity and Its Relationship with Taper Damage in Retrieved Femoral Components of Total Hip Replacement Devices. Symposium on Modularity and Tapers in Total Joint Replacement Devices. ASTM International, New Orleans, LA, November 10, 2014.

Higgs GB, Hanzlik J, MacDonald D, Klein G, Parvizi J, Mont MA, Kraay M, Rimnac CM, Kurtz SM. Does Fretting and Corrosion Occur at Modular Interfaces other than the Head-Stem Junction in Metal-on-Metal Total Hip Arthroplasty Devices? Poster No. 1759, 59th Annual Meeting of the Orthopaedic Research Society, San Antonio, TX, January 26–29, 2013.

Underwood RJ, MacDonald D, **Higgs GB**, Day J, Siskey RL, Kurtz SM. Tribocorrosion in Taper Junctions: Measurements and Observations from Explanted MoM Hips. Poster No. 1763, 59th Annual Meeting of the Orthopaedic Research Society, San Antonio, TX, January 26–29, 2013.

Kurtz SM, MacDonald DW, **Higgs GB**, Gilbert JL, Parvizi J, Klein G, Mont MA, Marshall A, Kraay M, Stulberg B, Cates H, Malkani A, Rimnac CM. Are 36+ MM Diameter HXLPE Bearings at Risk of Increased Wear from Modular Taper Corrosion with Ceramic and CoCr Heads? Poster No. 1768, 59th Annual Meeting of the Orthopaedic Research Society, San Antonio, TX, January 26–29, 2013.

Underwood RJ, MacDonald D, **Higgs GB**, Day J, Siskey RL, Kurtz SM. Does Visual Inspection of the Taper Head / Stem Junctions in Metal-on-Metal Hips Accurately Characterize the Corrosion and Wear? Poster No. 1797, 59th Annual Meeting of the Orthopaedic Research Society, San Antonio, TX, January 26–29, 2013.

Higgs GB, Kurtz SM. Hanzlik JA, MacDonald DW, Klein G, Parvizi J, Mont M, Kraay M, Martell J, Gilbert J, Rimnac CM. Is increased modularity associated with increased wear debris in metal-on-metal total hip arthroplasty devices? James A. Rand Award, 22nd Annual Meeting of the American Association of Hip and Knee Surgeons, Dallas, TX, November 1-3, 2012.

Higgs GB, Kurtz SM. Hanzlik JA, MacDonald DW, Kane WM, Day JS, Klein G, Parvizi J, Mont M, Kraay M, Martell J, Gilbert J, Rimnac CM. Retrieval analysis of metal-on-metal total hip prostheses: Characterizing fretting and corrosion at modular interfaces. 25th Annual Congress of the International Society for Technology in Arthroplasty, Sydney, Australia, October 3-6, 2012.

Higgs GB, Kurtz SM, Berven S, Isaza J, Lanman T, MacDonald D, Jaekel D, Penmatsa M, Ho C, Steinbeck M. Characterization of *in vivo* change and histological response of retrieved PEEK rod systems for posterior lumbar stabilization and fusion. 9th World Biomaterials Congress, Chengdu, China, June 1–5, 2012.

Ho CM, MacDonald D, Penmatsa MK, **Higgs GB**, Isaza J, Kurtz SM, Steinbeck M. Histological and retrieval analysis of PEEK spherical nucleus pulposus replacements, 9th World Biomaterials Congress, Chengdu, China, June 1–5, 2012.

MacDonald D, **Higgs GB**, Parvizi J, Klein G, Hartzband M, Lee GC, Levine H, Kraay M, Rimnac C,

Kurtz S. Oxidative stability, reasons for revision, and damage mechanisms of remelted highly crosslinked polyethylenes in TKA. 9th World Biomaterials Congress, Chengdu, China, June 1–5, 2012.

Higgs GB, Hanzlik JA, MacDonald DW, Kane WM, Day JS, Klein G, Parvizi J, Mont M, Kurtz SM. Fretting and corrosion at the taper connections of retrieved modular components from metal-on-metal total hip arthroplasty. Talk 13, Symposium on Metal-on-Metal Total Hip Replacement Devices, Phoenix, AZ, May 8, 2012.

MacDonald D, **Higgs GB,** Parvizi J, Klein G, Hartzband M, Levine H, Kraay MJ, Rimnac C, Kurtz SM. Surface damage and oxidative properties of remelted highly crosslinked polyethylenes in total knee arthroplasty. Poster No. 143, 79th Annual Meeting of the American Academy of Orthopaedic Surgeons, San Francisco, CA, February 7–11, 2012.

Higgs GB, MacDonald, DM, Jaekel DJ, Penmatsa MK, Ho CM, Lanman TH, Berven SH, Isaza JE, Steinbeck MJ, Kurtz SM. Retrieval Analysis of PEEK Rods for Posterior Lumbar Stabilization and Fusion. Poster No. 1117, 58th Annual Meeting of the Orthopaedic Research Society, San Francisco, CA, February 4–7, 2012.

Ho CM, Penmatsa MK, MacDonald DW, **Higgs GB**, Isaza J, Kurtz SM, Steinbeck MJ. Histology of Periprosthetic Tissues and Analysis of Retrieved PEEK Spherical Nucleus Pulposus Replacements. Poster No. 1118, 58th Annual Meeting of the Orthopaedic Research Society, San Francisco, CA, February 4–7, 2012.

MacDonald DW, **Higgs GB**, Parvizi J, Klein G, Hartzband M, Levine H, Kraay M, Rimnac C, Kurtz SM. Material and Clinical Performance of Remelted Highly Crosslinked Polyethylene Used in Total Knee Arthroplasty. Poster No. 1999, 58th Annual Meeting of the Orthopaedic Research Society, San Francisco, CA, February 4–7, 2012.

MacDonald D, **Higgs GB**, Parvizi J, Klein G, Hartzband M, Levine H, Kraay MJ, Rimnac C, Kurtz SM. Oxidative properties of remelted highly crosslinked polyethylenes in total knee arthroplasty. Paper No. 34, 21st Annual Meeting of the American Association of Hip and Knee Surgeons, Dallas, TX, November 4-6, 2011.

MacDonald D, Hanzlik J, Day J, Heffernan J, **Higgs GB**, Klein G, Kraay K, Rimnac CM, Parvizi J, Kurtz SM. Bone ongrowth in retrieved porous tantalum monoblock tibial plates. Poster 1036, 57th Annual Meeting of the Orthopaedic Research Society, Vol. 36, Long Beach, CA, January 13–16, 2011.